Regulation of WNT pathway specification by DUB-E3 interactions

By

Casey Paulasue Nielsen

Dissertation

Submitted to the Faculty of the

Graduate School of Vanderbilt University

in partial fulfillment of the requirements

for the degree of

DOCTOR OF PHILOSOPHY

in

Cell and Developmental Biology

September 30, 2019

Nashville, Tennessee

Approved:

Andrea Page-McCaw, Ph.D.

Barbara Fingleton, Ph.D.

Ian Macara, Ph.D.

Jason MacGurn, Ph.D.

This work is dedicated to my Scottie

Acknowledgements

I am very grateful to my thesis advisor, Jason MacGurn, who served as an exceptional mentor and support throughout my graduate career. As an advisor, Jason has done an outstanding job of guiding me through the graduate process by always offering an abundance of ideas, enthusiasm, and patience. He has spent countless hours training and advising me and has shaped the scientist that I am today. He has also been incredibly kind and understanding throughout personal struggles and I have deeply valued his support during those times. His dedication and personal investment in my success helped carry me through even the lowest points of graduate school and for that I will be forever grateful. I am also so thankful for my lab mates that made conducting this research every day an absolute joy. Additionally, I thank my thesis committee members, Dr. Andrea Page-McCaw, Dr. Barbara Fingleton, and Dr. Ian Macara, for their feedback, guidance, and support over the years. Their insight and encouragement was vital to my success in graduate school.

I am also extremely grateful to all of the collaborators at Vanderbilt that I have worked with over the years. Specifically, I thank Dr. Donna Webb and Dr. Nicole Diggins for their eager participation in studying cell migration in breast cancer cells. I learned so much from this collaboration and it was instrumental for the completion of my research.

I thank my parents, Mike and Sandy, for being my unwavering support through every journey of my life. Without their love, strength, and encouragement, finishing this degree would not have been possible. They have made many sacrifices so that I could achieve my dreams; my appreciation, admiration, and love for them knows no bounds. I

also want to thank my siblings Alexis, Trevor, and Dan for cheering me on, making me laugh, and believing in me every step of the way. They are my greatest source of inspiration and creativity. My family has shared in this journey with me from the very beginning, through every up and down. They have always been my greatest advocates and I could have never accomplished this without them.

Finally, I thank my precious Scottie. She has been by my side for every long night of homework, she has listened to me practice countless presentations, she has waited up for me after every late night in the lab, and she has given me endless, unconditional love. She is my partner crime, the light of my life, and the real MVP of this PhD.

Table of Contents

Page

List of Tables

Table **Page**

List of Figures

Figure **Page**

CHAPTER 1

Introduction

In order to adapt to changing environmental conditions, cells must be able to adjust the contents of their proteome with a high degree of efficiency and specificity. Cells have evolved several ways to regulate protein expression at the levels of transcription, translation, and post-translation and disruption of these regulatory nodes can have drastic consequences. The ubiquitin system is a key contributor to the protein homeostasis network. As such, it is not surprising that mutations in many components of the UPS have been found to drive various human diseases including neurodegenerative diseases, chronic inflammatory diseases, and cancer (Reinstein and Ciechanover, 2006). There have been increasing efforts to develop therapeutics that target ubiquitin proteasome system (UPS) effectors and activity, several of which have already made it to market (Huang and Dixit, 2016). While there is great potential in the UPS for development of therapeutics to treat various disease pathologies, there is still much to be learned. Of note, the dynamic interplay occurring within the UPS dictates the complexity of the ubiquitin code but is not well understood. The work presented in this thesis characterizes an interaction between a deubiquitylating enzyme (DUB), USP9X, with an E3 ubiquitin ligase that regulate the WNT signaling pathway in complex ways to modify cell behavior. In **Chapter 3** I present evidence that this DUB-E3 complex functions to regulate a ubiquitin rheostat on DVL2, a cytoplasmic transducer of WNT signaling, to influence WNT pathway specification. In **Chapter 4** I present a biochemical

characterization of this molecular rheostat on DVL2 and the activities associated with this DUB-E3 complex. In **Chapter 5** I provide preliminary investigation of the cellular function and interaction profiles of USP9X and the E3 ubiquitin ligase NEDD4L. As a whole, the information provided in this thesis sheds light on the regulatory logic behind DUB-E3 interactions. Importantly, this data also reveals important considerations that should be taken into account when developing therapeutics that targeting dynamic enzymes of the ubiquitin proteasome (UPS) system such as a deubiquitylase or an E3 ubiquitin ligase.

1.1 Ubiquitin modification is a complex, dynamic code

Ubiquitin can be conjugated to other proteins by the formation of an isopeptide bond between the C-terminal glycine carboxyl group of ubiquitin and the ε–amino group of a lysine residue on the recipient protein. The process of ubiquitin conjugation, or ubiquitylation, is carried out by an enzymatic cascade through which the activity of a ubiquitin activating enzyme (E1) activates ubiquitin in an ATP-dependent manner (**FIGURE 1.1**, step 1). This activated ubiquitin is then transferred to a ubiquitin conjugating enzyme (E2) through a transthiolation reaction (**FIGURE 1.1**, step 2). Finally, a ubiquitin ligase (E3) (**FIGURE 1.1**, step 3) which can bind both the E2-Ub conjugate and the substrate protein, facilitates the transfer of ubiquitin onto the ε-amino group of a lysine in the substrate protein (Komander and Rape, 2012; Vucic et al., 2011). It is important to note that this process is reversible by the activity of DUBs. The regulatory function of protein ubiquitylation ultimately is determined by the interactions it facilitates with ubiquitin-binding domains (UBDs), which function to decipher

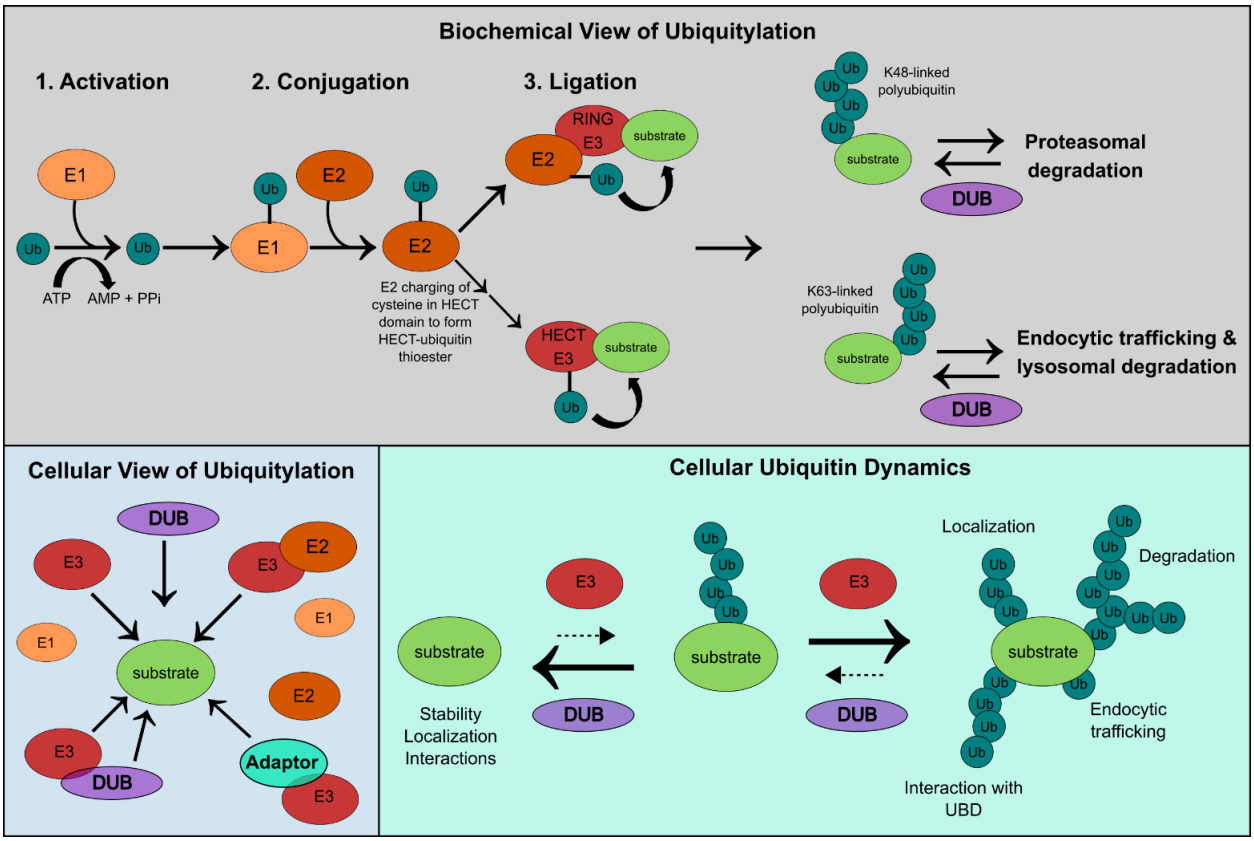

FIGURE 1.1: The ubiquitin conjugation pathway and cellular dynamics. **Top Panel**, *Biochemical view of ubiquitylation*: (1) The E1 ubiquitin activating enzyme activates ubiquitin in an ATP-dependent manner, (2) Subsequently, the activated ubiquitin is transferred to the E2 ubiquitin conjugating enzyme, (3) For RING E3 ubiquitin ligases (top arrow) the E2 transfers the activated ubiquitin directly to the protein substrate that is bound to the RING E3 ubiquitin ligase; For HECT E3 ubiquitin ligases (bottom arrow) the E2 first transfers the active ubiquitin to the HECT E3 ligase via an additional thiol-ester intermediate on the ligase before transferring the ubiquitin onto the protein substrate. **Bottom left panel**, *Cellular view of ubiquitylation*: In the cell multiple components of the ubiquitin system simultaneously contribute to the ubiquitylation state of substrates. **Bottom right panel**, *Cellular Ubiquitin Dynamics*: Dynamic ubiquitylation of substrates controlled by DUBs and E3s can dictate a variety of different outcomes.

ubiquitylation target signals. UBDs have diverse structural and functional features which allow recognition of many different ubiquitin topologies and convert ubiquitin signals into specific outcomes (**FIGURE 1.1**) (Husnjak and Dikic, 2012).

1.1.1 Discovery of the ubiquitin proteasome system

The UPS was originally discovered and characterized in the early 1980s by Aaron Ciechanover, Avram Hershko, and Irwin Rose and for their efforts they were awarded the Nobel Prize in Chemistry in 2004 (Ciechanover et al., 1980b; Hershko et al., 1980; Hershko et al., 1979; Hershko et al., 1983). Their studies began in the late 1970s with the intent to understand the ATP-dependence of intracellular proteolysis, which was originally observed by Melvin Simpson in 1953 (SIMPSON, 1953). By biochemically fractionating reticulocyte lysates, they were able to separate this system into two fractions that had to be recombined in order for ATP-dependent proteolysis to occur (Ciechanover et al., 2012). In fraction I they identified a small, heat-stable protein they named APF-1 (ATP-dependent proteolysis factor 1), which turned out to be ubiquitin. In fraction II they found a high molecular weight protein that was required for reconstitution of proteolysis, which was later found to be the 26S proteasome. They soon found that, upon recombination of fraction I and fraction II, ubiquitin shifts to a high molecular weight through covalent association with proteins in fraction II (Ciechanover et al., 1980a). Interestingly, they also found that the association between ubiquitin and target proteins was reversible. Altogether, their results revealed ubiquitin to be the major driver of ATP-dependent proteolysis by the proteasome, a concept that was not previously understood. Their studies provided the framework for our understanding of

targeted protein degradation and paved the way for future studies uncovering the major players in the ubiquitin proteasome system (Wilkinson, 2005). This early enzymatic analysis established the foundations of the classical cascade of the ubiquitin conjugation pathway (**FIG 1.1**, top panel).

In the decades following its discovery, we have come to appreciate the complexity of the UPS and the roles it plays in regulating dynamic cellular processes (**FIG 1.1**, bottom panel). In addition to proteolysis, the UPS regulates processes such as endocytic trafficking and cell signaling by affecting substrate localization and interactions. The diversity of functions for ubiquitin is largely facilitated by the complexity of the ubiquitin code itself. The complexity of the ubiquitin code is established by the myriad of enzymatic activities that are balanced and regulated. In the sections that follow I will describe the molecular features that contribute to cellular ubiquitin dynamics

1.1.2 Structural and functional diversity of polyubiquitin chains

Ubiquitin can form polymeric chains through conjugation of ubiquitin moieties through any one of the seven lysine residues (K6, K11, K27, K29, K33, K48, K63) or the N terminus of ubiquitin, facilitating diversity of polyubiquitin chain length and topology (Akutsu et al., 2016). This diversity adds an important layer of specificity within the ubiquitin system for targeting substrate proteins to different fates. Of these linkage types, the function of K48- and K63-linked polyubiquitin has been the most extensively studied.

K48-linked polyubiquitin chains are the most abundant linkage in cells representing over 50% of the polyubiquitin in HEK293 cells and 25% in *S. cerevisiae*

(Heride et al., 2014). K48-linked ubiquitin targets for proteasomal degradation of substrate proteins (Clague and Urbé, 2010). K48-linked polyubiquitin has been shown to bind the 26S proteasome through interactions with UBDs in the proteasome subunits Rpn10 and Rpn13 (Peth et al., 2010). This interaction brings substrate proteins in close proximity with the proteolytic activity of the proteasome and stimulates protein degradation (Chau et al., 1989; Thrower et al., 2000). While the classical view is that K48-linked polyubiquitin targets proteins for degradation by the proteasome, there is also evidence that K48-linked modifications can elicit non-degradative outcomes (McIntosh et al., 2018).

K63-linked polyubiquitin chains are also very abundant in cells, making up approximately 35% of polyubiquitin linkages in HEK293 cells and approximately 10% in *S. cerevisiae* (Heride et al., 2014). K63 largely regulates substrate interactions and localization and is not involved in proteasomal targeting. K63-linked polyubiquitin is known to regulate DNA repair pathways, intracellular signaling, and endocytic trafficking events (Grice and Nathan, 2016). Of note, integral membrane proteins are often modified with K63-linked chains for endocytic sorting or trafficking events that result in lysosomal delivery and degradation (Clague and Urbé, 2010). Similarly, monoubiquitin modifications can also function to direct endocytic trafficking and sorting of membrane proteins (Clague and Urbé, 2010). Mono-ubiquitin also plays a well-established role in histone modification and transcriptional regulation (Nakagawa and Nakayama, 2015).

K48- and K63-linked polyubiquitin represent the majority of polyubiquitin in most cells and less is known about other linkage types. K11–linked polyubiquitin has been shown to function as a powerful degradative signal during mitosis (Matsumoto et al.,

2010). These studies showed that the anaphase-promoting complex (APC/C) conjugates K11-linked ubiquitin chains to substrates to drive proteasomal degradation and subsequent mitotic exit (Akutsu et al., 2016). As a result, the abundance of K11-linkages peaks upon APC/C activation during mitosis. On the other hand, K27–linked polyubiquitin chains have been reported to be involved in the DNA damage response. In these reports K27-linkages represent the most abundant ubiquitin chain type on chromatin upon DNA damage (Gatti et al., 2015). Another report suggested K27-linked polyubiquitin plays a role in the innate immune response triggered by microbial DNA, whereby K27-linked polyubiquitin is conjugated to STING (stimulator of interferon genes) and serves as a scaffold for interactions with TBK1, a critical kinase in the innate immune response (Akutsu et al., 2016; Wang et al., 2014a). Interestingly, K29–linked polyubiquitin has been found to function as an inhibitor of WNT signaling in a report showing that the NEDD4 family E3 ubiquitin ligase SMURF1 modifies Axin, a critical scaffold protein of the β-catenin destruction complex, resulting in disruption of interactions between Axin and the WNT receptor LRP5/6 (Fei et al., 2013). K33-linked polyubiquitin has been found to play a role in post-Golgi protein trafficking through a mechanism in which K33-linked ubiquitylation of the protein coronin7 (Crn7) results in recruitment of the clathrin adaptor protein Eps15 (Yuan et al., 2014). This causes the eventual assembly and elongation of Trans Golgi Network (TGN)-derived carrier tubules (Yuan et al., 2014). M1-linked or linear polyubiquitin has been reported to play key regulatory roles in NFκB signaling (Akutsu et al., 2016). Based on the results of several biochemical studies it is thought that the functions of the less abundant polyubiquitin linkage types, with the exception of linear ubiquitin, are likely degradative in nature

(Ikeda and Dikic, 2008).

The functions of polyubiquitin chains are coupled to recognition by linkage-specific UBDs. There are two categories of linkage-specific UBDs: (1) domains that detect the linker region between two ubiquitin moieties, and (2) domains recognizing the positioning and spatial distribution of the individual components of the polyubiquitin chain (Dikic et al., 2009). In addition to the linkage-specific components of the ubiquitin system that function in the recognition of ubiquitin, there is also enzymatic specificity with DUBs and E3s for the generation and reversal of ubiquitylation events. Establishing the linkage-specificity of components of the ubiquitin system can provide important information about function.

1.1.3 The growing complexity of the ubiquitin code

The variety of ubiquitin chains found in cells is further expanded by the fact that ubiquitin can generate heterotypic chains and/or branched chains – in this case one ubiquitin molecule is ubiquitylated at two or more lysines (Meyer and Rape, 2014). It has been reported that branched linkages through K27, K29, and K33 of ubiquitin interfere with proteasomal recognition *in vitro* (Kim et al., 2007). Interestingly, it has also been reported that the anaphase promoting complex (APC/C) can synthesize branched chains on substrate proteins that enhance substrate recognition by the proteasome and ultimately drive turnover of cell-cycle regulators during mitosis (Meyer and Rape, 2014). Thus, branching has the potential to modify the strength of proteasomal targeting. There is still much to learn about the physiological function of branched chains but the tools available to study them in a cellular/physiological context are limited.

The ubiquitin code was expanded even further by the finding that ubiquitin itself can be regulated by post-translational modifications such as phosphorylation and acetylation (Herhaus and Dikic, 2015). Of note, phosphorylation of ubiquitin at the Serine 57 residue has been shown to play a critical role in regulator of ubiquitin turnover and endocytic trafficking (Lee et al., 2017). Additionally, phosphorylation of the Serine 65 residue of ubiquitin has been reported to play a critical role in mitophagy (Koyano et al., 2014; Wauer et al., 2015). While there is still much to be learned about post-translational modifications of ubiquitin, these modifications clearly contribute to cellular ubiquitin dynamics. Altogether, the role of known ubiquitin PTMs suggest that the ubiquitin code is even more complex and dynamic than currently appreciated.

1.2 Structural and functional features of DUBs

The balance of ubiquitylation and deubiquitylation is critical for maintaining many cellular functions. Thus, DUBs represent a major regulator of the complex, dynamic ubiquitin code. To date, 99 DUBs have been identified in the human genome and those that have been characterized have been found to play roles in regulating diverse cellular functions including signaling modulation, ubiquitin biogenesis and recycling, and substrate stabilization (Komander et al., 2009). Here I provide an overview of the biochemistry of DUBs and their role as regulators of diverse cellular processes.

1.2.1 Families of DUBs

Deubiquitylating enzymes can be subdivided into five well-defined families based on the structure of their catalytic domains: ubiquitin C-terminal hydrolases (UCHs),

ubiquitin-specific proteases (USPs), ovarian tumour proteases (OTUs), Josephins (MJDs), and JAMM metalloproteases (Clague et al., 2019; Komander et al., 2009). In recent years, additional DUB families - MINDY and ZUP1 - have also been identified (Abdul Rehman et al., 2016; Hermanns et al., 2018). While the majority of DUBs fall within the USP family, their domain structures are largely uncharacterized outside of the catalytic USP domain (Komander et al., 2009). However, the information we do have regarding the structures of DUB catalytic domains provides great insight into their activity and specificity. For instance, while all of the cysteine protease DUB families (UCH, USP, OTU, MJD, MINDY, and ZUP1) have divergent folds, their catalytic residues show high degrees of structural similarity when bound to ubiquitin (Komander and Barford, 2008).

The cellular function of many DUBs is not well understood, perhaps owing to the difficulty associated with characterizing these complex enzymes. This is exemplified by USP9X - a DUB at the center of my thesis research – which is a large protein (2570 amino acids) that has been linked to several different cellular processes but its precise mechanism of action remains unknown (Murtaza et al., 2015). The USP catalytic domain of USP9X, the structure of which has only recently been reported (**FIGURE 1.2**) (Paudel et al., 2019), contains a critical catalytic cysteine residue (C1556) that functions as part of a catalytic triad that enables this cysteine residue to perform a nucleophilic attack on isopeptide linkages to remove ubiquitin from substrate proteins (Komander et al., 2009). The structure of the USP catalytic domain has often been likened to that of a hand whereby the catalytic center lies at the interface between the “palm” and “thumb” subdomains and the “fingers” grip the distal ubiquitin (**FIGURE 1.2**) (Hu et al., 2002). In

Chapter 3 of this thesis, I perform detailed biochemical analysis of USP9X - including the functional effects of mutating this catalytic cysteine to valine (C1556V), rendering the deubiquitylase inactive. USP9X is also similar to many other DUBs in that it possesses a ubiquitin-like fold (UBL) (reported by SGC, PDB:5VBD) which adopts a three-dimensional structure that is highly similar to that of ubiquitin and presumably functions to associate with the catalytic domain in order to regulate DUB activity. It is important to note that the catalytic domain of USP9X, like most DUBs, only represents a small portion of the overall structure (**FIGURE 1.2**). It is likely that USP9X (and other DUBs) may contain additional domains within these uncharacterized regions that contribute to their function and activity in cells.

While the structural features of DUB catalytic domains are well understood, there are major knowledge gaps in our understanding of: (1) how DUBs are regulated, (2) the contributions of the non-catalytic domains of DUBs, (3) how their interactors or other regulatory factors influence their activity, and (4) the substrate specificity of DUBs. Furthermore, characterizing the function of DUBs in cells is complicated by redundancy. For example, in genetic studies it was found that knockout of individual DUBs did not cause growth defects or lethality in *S. cerevisiae* whereas combined knockout of multiple DUBs had detrimental effects (Amerik et al., 2000). Thus our appreciation for the cellular functions of DUBs has lagged behind biochemical characterization.

1.2.2 Cellular functions of DUBs

Although there are far fewer DUBs than E3s encoded in the human genome, there is still great functional diversity among DUBs. Some DUBs, such as USP14,

UCH37, RPN11, and USP8/UBPY play critical house-keeping roles in the cell by regulating ubiquitin recycling prior to degradation (Finley, 2009). USP14, UCH37, and RPN11 associate with the proteasome and cleave ubiquitin modifications from substrate proteins prior to proteasomal degradation, thus facilitating ubiquitin recycling. Similarly, USP8/UBPY functions to recycle ubiquitin from endosomal substrates prior to lysosomal degradation (Mizuno et al., 2006; Row et al., 2006). Other DUBs facilitate the generation of free ubiquitin for use by the cell. This process requires several DUBs that function to breakdown free polyubiquitin chains or newly synthesized ubiquitin which is translated as linear ubiquitin fusions containing multiple ubiquitin molecules (Komander et al., 2009).

There are multiple DUBs with known functions in endocytic trafficking events. For example, the DUB complex BRISC has been shown to regulate the internalization and lysosomal degradation of the type 1 interferon receptor chain 1 (IFNAR1) receptor and thereby regulates interferon responses (Zheng et al., 2013). Additionally, the DUB AMSH is a key regulator of receptor fate determination through its regulation of endocytic machinery including the endosomal sorting complex required for transport (ESCRT) 0 component STAM1 (Sierra et al., 2010).

Additionally, some DUBs function to regulate cell signaling pathways. One example of this is the DUB OTULIN which opposes linear polyubiquitin chain formation by the E3 ubiquitin ligase LUBAC and in turn antagonizes cytokine signaling (Keusekotten et al., 2013). The DUBs USP9X and CYLD are both known to regulate

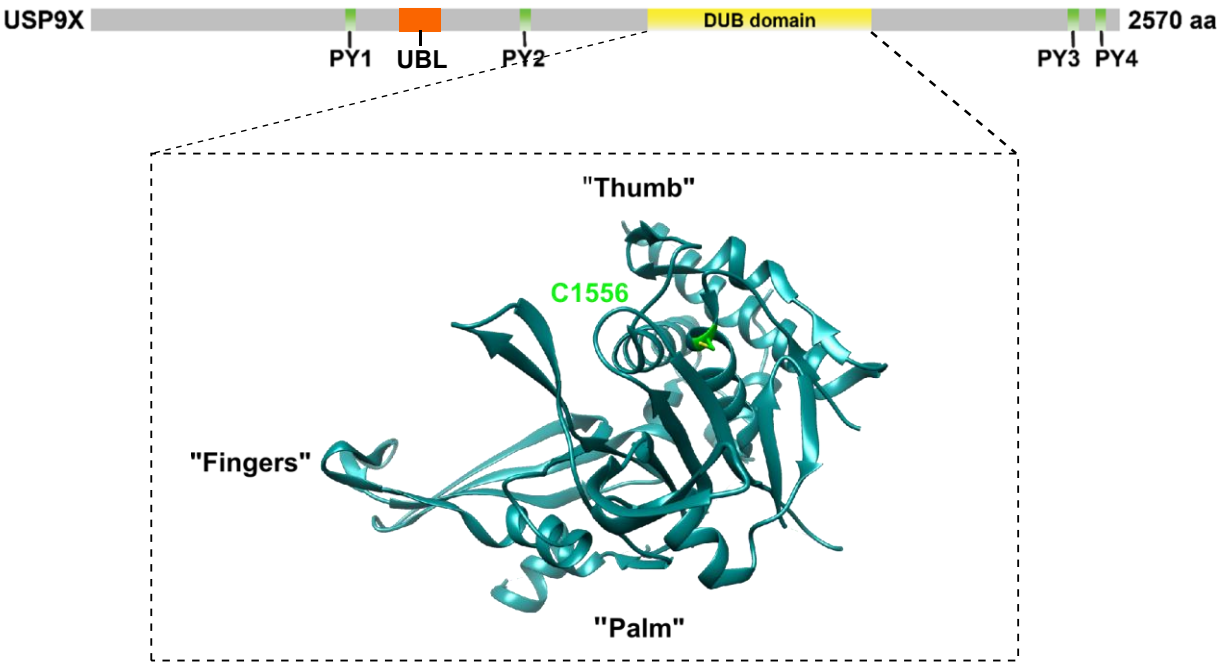

FIGURE 1.2 USP9X catalytic domain structure. Top: Domain structure of USP9X with PY motifs labeled in green, UBL labeled in orange, and the USP deubiquitylase (DUB) domain labeled in yellow; **Bottom**: Crystal structure of the catalytic domain of USP9X (PDB 5WCH) with catalytic residue (C1556) labeled in green.

WNT signaling via the shared substrate protein, DVL2 (Tauriello et al., 2010) (Nielsen et al., 2019). Interestingly, these DUBs have opposite roles in regulating the WNT pathway. CYLD is reported to remove ubiquitylation events critical for DVL2 head-to-tail polymerization and subsequent WNT activation (Tauriello et al., 2010) (Madrzak et al., 2015). On the other hand, the results outlined in **Chapter 3** of this thesis indicate that USP9X deubiquitylates DVL2 to promote canonical WNT activation. These examples underscore the diverse roles DUBs can play in cells.

USP9X, the DUB of focus in this thesis, has several proposed cellular functions. Importantly, USP9X has been implicated in the regulation of several protein trafficking pathways. Of note, USP9X is known to regulate the endocytic adaptor Epsin to regulate the surface stability of the Notch receptor and EGFR (Cadavid et al., 2000; Chen et al., 2002; Overstreet et al., 2004). There is also evidence that USP9X plays a role in regulating cell polarity pathways (Théard et al., 2010)(Nielsen et al., 2019). USP9X has also been found to regulate cellular apoptotic mechanisms by deubiquitylating and stabilizing the anti-apoptotic protein MCL1 (Schwickart et al., 2010). While it is apparent that USP9X is involved in several important physiological pathways, the mechanistic details of these activities are not clear.

Although the structural aspects of the catalytic domains of many DUBs have been determined, detailed understanding of DUB function and specificity is lacking. This may be because there have been many challenges in characterizing the regions outside of the catalytic domains of DUBs due to their large size. Additionally, many DUBs have a tendency to associate in large protein complexes in which adaptor proteins or other interactors may contribute to DUB activity and specificity. For example, the DUB

BRCC36 has been found to be a component of at least two different complexes with distinct localization (one complex existing in the cytosol and one existing only in the nucleus) and unique functions (Cooper et al., 2009; Dong et al., 2003; Shao et al., 2009; Wang and Elledge, 2007). I speculate that contributions of these uncharacterized domains as well as interacting proteins may contribute to substrate selection or regulation of DUB activity, adding to the complexity of DUB activity in cells.

1.2.3 DUBs as drug targets

Over the past few decades there have been increasing efforts to utilize components of the ubiquitin machinery as therapeutic targets (Cohen and Tcherpakov, 2010). Great progress has been made toward development of small molecule inhibitors of E1 ubiquitin activating enzymes (Huang and Dixit, 2016). However, the pleiotropic nature of E1s limits these drugs to use for acute treatment of aggressive cancers. The increased number and diversity of E3s and DUBs provides the potential to develop drugs with more specific effects. As such, the focus for therapeutically targeting components of the ubiquitin system have shifted toward DUBs and E3s. The well-defined catalytic structure of DUBs makes them desirable as potential drug targets however, the lack of understanding of DUB cellular function has limited these pursuits (Cohen and Tcherpakov, 2010).

There has only been one small-molecule DUB inhibitor that has reached the clinical trial phase of development (Wang et al., 2016). This compound, named VLX1570, targets the proteasome-associated DUBs USP14 and UCHL5 and has indications in oncology – specifically multiple myeloma and solid tumors (D'Arcy et al.,

2011; Wang et al., 2015). The major advantage of targeting proteasome-associated DUBs as an alternative to directly targeting proteasome activity is an increased selectivity and decreased toxicity. While such drugs represent a promising avenue for the development of novel therapeutics, VLX1570 failed at phase 1 of clinical trial.

Additionally, inhibitors targeting USP1, a DUB known to play an integral role in the Fanconi anemia pathway of DNA crosslink repair, are being developed at the pre-clinical stage (Castella et al., 2015; Nijman et al., 2005). This inhibitor blocks complex formation between USP1 and USP1-associated factor 1 (UAF1), a USP1-interacting protein that stimulates USP1 activity. Treatment with this inhibitor to USP1 ultimately results in the attenuation of DNA damage repair pathways and subsequent cell death (Dexheimer et al., 2014).

USP7, a DUB known to negatively regulate the stability of the tumor suppressor p53 through interactions with the E3 ubiquitin ligase MDM2, is also being pursued by multiple pharmaceutical companies for its potential as a disease therapeutic (Colland et al., 2009; Gavory et al., 2018; Reverdy et al., 2012; Weinstock et al., 2012). While several inhibitors of USP7 have been shown to inhibit tumor growth and prolong survival in animal models, these chemicals are relatively non-specific and little is known about how they bind USP7.

USP9X, the DUB at the center of my thesis research, has also emerged as a potential drug target in recent years as a result of its function in several physiological pathways. To date, the best described inhibitor of USP9X activity is the compound WP1130 (Kapuria et al., 2010), a compound that is being actively pursued in pre-clinical studies. One study demonstrated that combined treatment of cisplatin with WP1130

could increase estrogen receptor-negative breast cancer cell sensitivity to cisplatin, a common chemotherapy drug (Fu et al., 2017). Other groups suggest that WP1130 has potential for treatment of multiple myeloma or other hematologic malignancies owing to the oncogenic function of USP9X in these contexts (Peterson et al., 2015; Sun et al., 2011).

While there are multiple examples of chemical modulators of DUBs in clinical or pre-clinical studies, the clinical development of selective DUB inhibitors has been a major challenge due to the lack of understanding of the physiological functions of DUBs. Additionally, since many DUBs have very similar catalytic structures, it is difficult to develop compounds targeting DUB catalytic activity that are specific. In order to improve the specificity of compounds targeting DUBs, it will be important to explore the areas outside of the catalytic domain. Detailed characterization of DUB functions in cells will be critical for development of specific and selective DUB inhibitors.

1.3 NEDD4 family E3 ubiquitin ligases regulate receptor signaling and trafficking

There are two classes of E3 ubiquitin ligases – RING and HECT - that utilize distinct mechanisms to modify substrates with ubiquitin (**FIGURE 1.1 Step 3**). RING E3s are characterized by their catalytic domain which facilitates direct transfer of ubiquitin from the E2 to a substrate protein (Zheng and Shabek, 2017). In contrast, HECT E3 ubiquitin ligases are defined by their catalytic domains which form a thioester-linked intermediate with ubiquitin before transferring the ubiquitin modification to the substrate (Pickart, 2001). It is important to note that, despite the common HECT E3 ligase catalytic domains, there is great functional diversity among the HECT E3 ligases.

This is exemplified by the NEDD4 family of E3 ubiquitin ligases – the E3s at the center of my thesis research.

1.3.1 Biochemical characteristics of NEDD4 family members

The NEDD4 family of E3 ubiquitin ligases is conserved from yeast to humans and has been broadly implicated in the ubiquitin-mediated endocytosis of many membrane proteins including surface receptors, ion channels, and nutrient transporters (He et al., 2008; Hryciw et al., 2004; Lin et al., 2011; MacGurn et al., 2012). There are nine NEDD4 family E3 ligases encoded in the human genome and each has distinct physiological functions (Rotin and Kumar, 2009). While not all of the NEDD4 family E3 ligases have been characterized, several NEDD4 family members have a strong preference for catalyzing K63-linked polyubiquitin chains *in vitro* (Ingham et al., 2004; Kim and Huibregtse, 2009), but others have been reported to deviate from this trend. For example, NEDD4L has been reported to generate K6-, K27-, and K29-linked polyubiquitin modifications on DVL2, although the results I present in **Chapter 4** are not consistent with these findings (Ding et al., 2013). It is possible that linkage preference could be dictated by many factors including structural contributions or interacting proteins, which could vary significantly depending on the cellular context.

NEDD4 family ligases have a conserved domain structure that includes an N-terminal C2 domain that can bind to lipids, a C-terminal HECT ubiquitin ligase domain, and 2-4 internal WW domains, a 40 amino acid domain with 2 conserved tryptophan (W) residues (**FIGURE 1.3**). The WW domains have a high affinity for PY motifs (Pro-Pro-x-Tyr) and mediate interactions with substrates, adaptors, and regulatory factors

(Ingham et al., 2004).

1.3.2 Cellular functions of NEDD4 family members

NEDD4s are known regulators of receptor signaling and trafficking events in cells. NEDD4-mediated regulation of cell surface receptors in response to changing environmental conditions has been well characterized for the yeast NEDD4 ubiquitin ligase called RSP5. Of note, RSP5 regulates the stability of the amino acid permeases STE2, GAP1, and FUR4 at the membrane and selectively targets these receptors for internalization and eventual lysosomal degradation in response to certain environmental stimuli (Dunn and Hicke, 2001; Galan et al., 1996; Hein et al., 1995).

NEDD4 family members also play an important role in regulation of fluid and electrolyte homeostasis through regulation of the epithelial sodium channel (ENaC) (Garty and Palmer, 1997; Rossier et al., 2002). The C-terminal tails of each of the subunits of the ENaC complex contain PY motifs that have been shown to engage several NEDD4 family members including NEDD4, WWP2, and NEDD4L (Debonneville et al., 2001; Harvey et al., 2001; McDonald et al., 2002; Staub et al., 1996). These studies showed that individual WW domains of these NEDD4 family members provided specificity for ENaC binding whereas the remaining NEDD4 WW domains were dispensable for interaction with ENaC. Their results suggest that NEDD4s interact with and ubiquitylate the C-terminus of the ENaC subunits in order to downregulate ENaC at the cell surface (Staub et al., 1996). Interestingly, the importance of this regulation is evident from common mutations that occur in the C-terminal tails of ENaC subunits

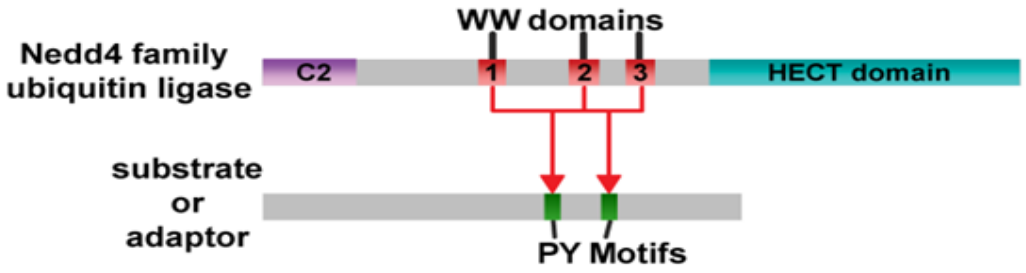

FIGURE 1.3 NEDD4 family E3 ubiquitin ligases engage substrates or adaptors via WW-PY interactions. TOP: Characteristic domain structure of NEDD4 family members. Bottom: Characteristic motif structure of NEDD4 substrate or adaptor proteins

which results in a hypertension disorder known as Liddle's Syndrome, a disease initially characterized by Dr. Grant W. Liddle at Vanderbilt University (Botero-Velez et al., 1994; Staub et al., 1996). These mutations have been shown to result in partial or complete loss of the C-terminal PY motifs of ENaC and in turn interferes with binding by the NEDD4 WW domains. This inability of ENaC to engage NEDD4s causes increased stability of ENaC at the plasma membrane and, as a result, increased sodium ion uptake (Abriel et al., 1999; Goulet et al., 1998; Schild et al., 1996; Snyder et al., 1995).

The NEDD4s are also important regulators of receptor signaling pathways. For example, SMURF1 and SMURF2 have been shown to play distinct roles in the regulation of TGFβ signaling pathways through degradation of specific pathway components (Kavsak et al., 2000; Lin et al., 2000; Zhang et al., 2001; Zhu et al., 1999). Additionally, NEDD4s have been implicated as key regulators of WNT signaling pathways. Of note, the WNT signaling component DVL2, which is of central focus in **Chapter 3** and **Chapter 4** of this thesis, contains 2 PY motifs through which NEDD4L, ITCH, WWP1, and potentially other NEDD4s are able to interact (Ding et al., 2013; Wei et al., 2012). These reports indicate that ITCH and NEDD4L promote degradation of DVL2 and function as negative regulators of the WNT pathway. While previous work implicated that the function of NEDD4s in the regulation of WNT signaling was purely degradative, the results presented in this thesis suggest that NEDD4-mediated ubiquitylation events on DVL2 can drive non-degradative outcomes as well.

1.4 Regulatory logic of DUB-E3 interactions

Almost 50% of all DUBs have been reported to interact with at least one E3

ubiquitin ligase (**FIG 1.4**), many interacting with multiple E3 ubiquitin ligases. To date, 193 DUB-E3 interactions have been reported (**APPENDIX A**) but only 48 of these interactions have a known cellular or biochemical function. Each of the characterized DUB-E3 interactions can be grouped into one of three categories based on the functional significance of the association: (i) the DUB directly antagonizes E3 substrate ubiquitylation (**FIG 1.5,** Model 1), (ii) the DUB stabilizes the E3 by removal of autoubiquitylation events or vice versa (**FIG 1.5,** Model 2), or (iii) the DUB contributes to a ubiquitin chain editing event to redirect the fate of the E3 ligase's substrate (**FIG 1.5,** Model 3). Several examples of each model can be found in the literature that highlight the complex layers of regulation that DUB-E3 complexes can exhibit (**TABLE 1.1**).

1.4.1 DUB-E3 interactions can be antagonistic

Since the core enzymatic function of DUBs and E3s are directly opposing, it is not surprising that many DUB-E3 interactions result in antagonism (**FIG 1.5**, Model 1). Of the 48 characterized DUB-E3 interactions, 15 interactions appear to be antagonistic (**TABLE 1.1**). One interesting example of this mechanism can be found in the WNT signaling pathway in which, in an inactive state, the E3 ubiquitin ligase β-TrCP functions to keep levels of cytoplasmic β-catenin low by targeting β-catenin for proteasomal degradation (Marikawa and Elinson, 1998). USP15, a deubiquitylating enzyme known to interact with β-TrCP, has been reported to prevent basal turnover of β-catenin by reversing β-TrCP-mediated ubiquitylation of β-catenin (Greenblatt et al., 2016). E3 antagonization has the potential to result in a futile cycle, but coordinated regulation of

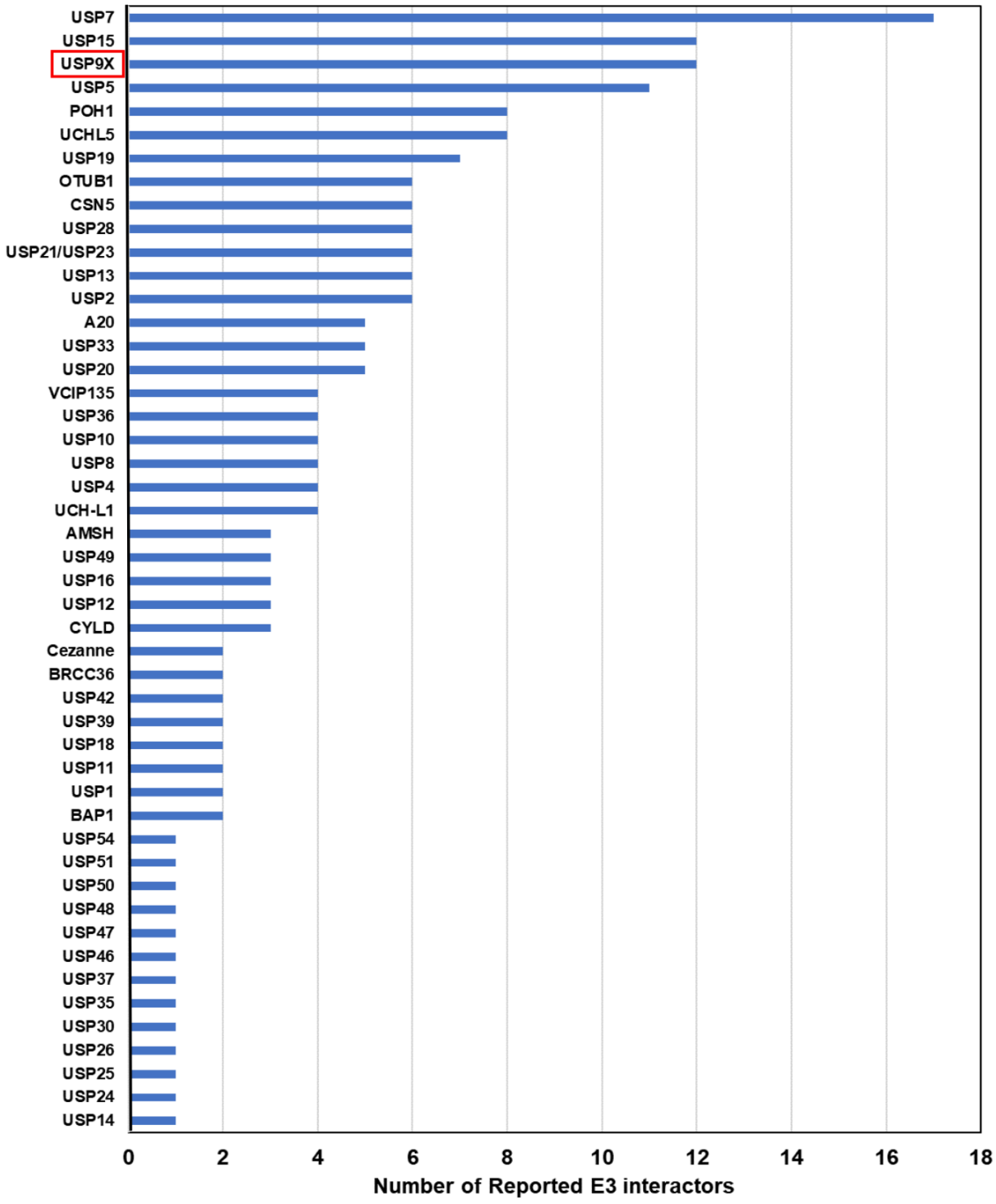

FIGURE 1.4 Reported DUB-E3 interactions. Of the 99 DUBs encoded in the human genome, 48 have reported interactions with E3s, the remaining 51 have no reported interactions with E3s. Plot of all known DUBs with E3 interactions (y-axis) and corresponding number of interacting E3 ubiquitin ligases (x-axis).
not surprising that many DUB-E3 interactions result in antagonism (**FIG 1.5,** Model 1).

ligase and DUB activities in the dynamic environment of the cell could also establish something more complex such as a ubiquitin rheostat on a shared substrate. In this case, a ubiquitin rheostat would function as a tunable signal in which the extent of ubiquitylation would determine the strength of the output signal.

1.4.2 Reciprocal regulation of DUB/E3 ubiquitylation

One of the major mechanisms for regulating E3 activity is autoubiquitylation events that dictate E3 stability (Zheng and Shabek, 2017). Since this activity is very common for E3s, it is not surprising that there are at least 20 known DUB-E3 complexes in which the DUB functions to reverse this autoubiquitylation activity when an E3 needs to be in an "on" state (**FIG 1.5**, Model 2; **TABLE 1.1**). For example, USP9X – the DUB that is of central focus in Chapter 3 of this thesis – is known to reverse autoubiquitylation events of at least 3 E3 ubiquitin ligases, SMURF1, ITCH, and MARCH7 (Mouchantaf et al., 2006; Nathan et al., 2008; Xie et al., 2013).

Typically, DUBs are thought to associate with E3s in order to fine-tune the stability and activity of the E3. However, the reverse model can also occur in which the E3 functions to regulate the stability or activity of the DUB (**FIG 1.5**, Model 2, **TABLE 1.1**). For example, the DUB USP5, which is known to be play a key role in Tumor Necrosis Factor-alpha (TNF-α) production during inflammatory responses, is regulated by the E3 ubiquitin ligase SMURF1 (Yoshioka et al., 2013). In this DUB-E3 complex, SMURF1 has been reported to regulate USP5 stability and consequently USP5-mediated TNF-α production by targeting USP5 for proteasomal degradation (Qian et al., 2016). The potential for auto-deubiquitylation activity is not well understood, but

presumably E3 regulation of a DUB would require ubiquitylation of a site that is inaccessible to the catalytic domain of the DUB.

1.4.3 Ubiquitin chain-editing

While there are far fewer examples of DUB-E3 complexes functioning in ubiquitin chain-editing mechanisms (**FIG 1.5**, Model 3, **TABLE 1.1**), these mechanisms have been shown to provide fine-tuned spatial and temporal regulation to critical cell signaling pathways. To date, the clearest example of this is the NFκB regulator A20 which contains both a DUB and E3 ligase domain within the same protein. The DUB domain of A20 removes K63-linked polyubiquitin chains from receptor interacting protein (RIP), a critical mediator of the proximal Tumor Necrosis Factor (TNF) receptor 1 (TNFR1) signaling complex, and the E3 ligase domain of A20 subsequently conjugates K48-linked polyubiquitin chains to RIP and targets it for proteasomal degradation thus inhibiting NFκB signaling (Wertz et al., 2004). Another DUB-E3 complex that exemplifies the ubiquitin chain-editing model (**FIG 1.5**, Model 3) is the E3 ubiquitin ligase ITCH in complex with the DUB CYLD. Here, ITCH and CYLD employ sequential activities toward the kinase TAK1 to perform ubiquitin chain-editing which ultimately serves an important regulatory function in innate inflammatory cells (Ahmed et al., 2011). Upon TNF activation, TAK1 undergoes K63-linked polyubiquitylation via the activity of TRAF2/TRAF6 to potentiate the NFκB signaling pathway (Fan et al., 2011; Fan et al., 2010). In order to attenuate inflammatory signaling, CYLD then cleaves K63-linked polyubiquitin chains from TAK1 which allows ITCH to catalyze K48-linked polyubiquitin onto TAK1 and target TAK1 for degradation by the proteasome (Ahmed et al., 2011).

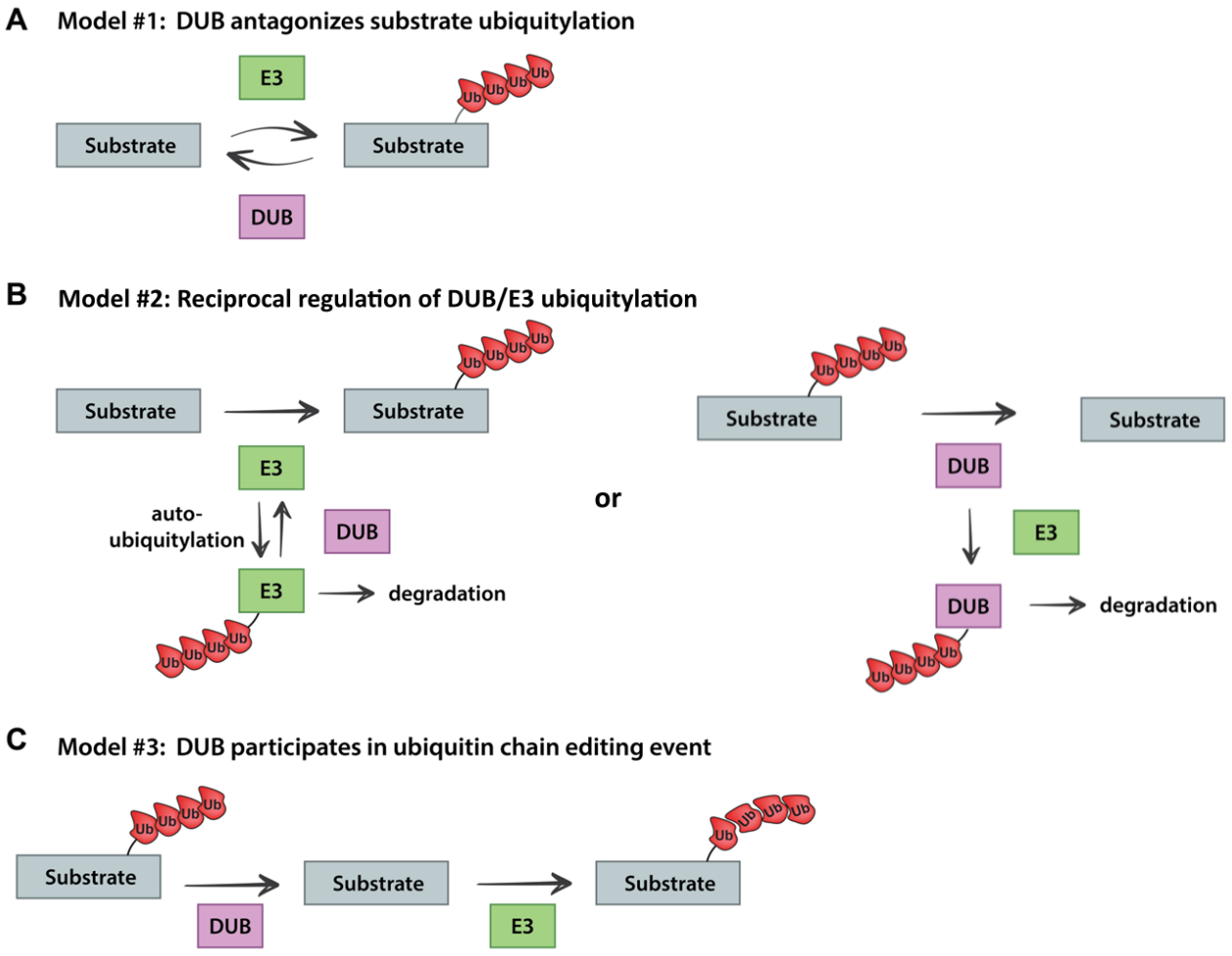

FIGURE 1.5 Models for DUB-E3 ubiquitin ligase interactions. **A.** DUB antagonizes E3 activity by removing ubiquitylation events from an E3 substrate. **B.** E3 ubiquitin ligases that undergo autoubiquitylation can be stabilized through interactions with DUBs. **C.** DUB-E3 complexes can allow for editing of the type of ubiquitylation conjugated to a substrate to change the fate of a substrate

Model	DUB	E3	Functional significance of DUB-E3 interaction	Reference
Model # 1 DUB antagonizes E3 activity	USP4	TRAF2	USP4 deubiquitylates TRAF2 and TRAF6 and inhibits TNFalpha-induced cancer cell migration	Xiao N (2011) Zhou F (2012)
	USP4	TRAF6	USP4 deubiquitylates TRAF2 and TRAF6 and inhibits TNFalpha-induced cancer cell migration	Xiao N (2011) Zhou F (2012)
	USP36	FBXW7	USP36 reverses FBXW7-mediated ubiquitylation of MYC to stabilize MYC and promote cancer progression	Sun XX (2015)
	USP28	FBXW7	USP28 is required for MYC stability. USP28 binds MYC through an interaction with FBXW7, an F-box protein that is part of an SCF-type E3 ubiquitin ligase. USP28 stabilizes MYC in the nucleus. In the nucleolus FBXW7 ubiquitylates MYC and targets it for degradation	Popov N (2007)
	USP28	RCHY1/PIRH2	USP28 interacts in a complex with PIRH2 and the DNA damage checkpoint protein CHK2. USP28 antagonizes PIRH2-mediated polyubiquitylation and proteasomal degradation of CHK2	Bohgaki M (2013)
	USP20	TRAF6	USP20 interacts with and deubiquitylates TRAF6 in a β-arrestin2-dependent manner. USP20 functions as a negative regulator of TLR4-mediated activation of NFκB signaling by reversing ubiquitylation of β-arrestin2	Jean-Charles PY (2016) Yasunaga J (2011)
	USP15	β-TrCP	USP15 antagonizes β-TrCP-mediated ubiquitylation of β-catenin, preventing its proteasomal degradation	Greenblatt MB (2016)
	USP13	gp78/AMFR	USP13 reverses gp78-mediated ubiquitylation of UBL4A to promote ERAD	Liu Y (2014)
	USP12	ITCH	USP12 acts as a negative regulator of the Notch pathway by reversing ITCH-mediated ubiquitylation of Notch ligand	Moretti J (2012) Jahan AS (2016)
	USP10	RNF168	USP10 interacts with RNF168 and opposes RNF168-mediated ubiquitylation of TOP2α and restricts TOP2α binding to chromatin	Guturi KK (2016)
	UCH-L1	TRAF6	UCH-L1 antagonizes TRAF6-mediated ubiquitylation of TRAF3	Karim R (2013)
	UCH-L1	MDM2	UCH-L1 antagonizes MDM2-mediated ubiquitylation of p53	Li L (2010)
	OTUB1	TRAF6	OTUB1 and OTUB2 negatively regulate virus-triggered type I IFN induction and cellular antiviral response by deubiquitinating TRAF3 and -6	Li S (2010) Bremm A (2010)
	USP13	SKP2	nuclear Ufd1 recruits the deubiquitinating enzyme USP13 to counteract APC/C(Cdh1)-mediated ubiquitination of Skp2	Chen M (2011)
	USP10	MDM2	After DNA damage USP10 translocates into the nucleus and reverses the activity of MDM2 to stabilize p53	Yuan J (2010)

Model	DUB	E3	Functional significance of DUB-E3 interaction	Reference
Model # 2 Reciprocal regulation of DUB/E3 ubiquitylation	USP9X	SMURF1	USP9X stabilizes SMURF by removing autoubiquitylation events	Xie Y (2013)
	USP9X	ITCH	USP9X stabilizes ITCH by removing autoubiquitylation events	O'Connor HF (2015) Mouchantaf R (2006) Azakir BA (2009)
	USP7	RNF169	USP7 deubiquitylates and stabilizes RNF169 to promote double-strand break repair	Hein MY (2015) An L (2017)
	USP7	RNF168	USP7 deubiquitylates and stabilizes RNF168 to promote ubiquitin-dependent DNA damage signaling	Zhu Q (2015)
	USP7	RAD18	USP7 deubiquitylates and stabilizes RAD18 to promote ubiquitin-dependent DNA damage signaling	Zlatanou A (2016)
	USP48	MDM2	USP48 binds Mdm2 and promotes Mdm2 stability and enhances Mdm2-mediated p53 ubiquitination and degradation	Cetkovska K (2017)
	USP4	HUWE1	USP4 deubiquitylates and stabilizes HUWE1 resulting in decreased p53 levels	Zhang X (2011)
	USP33	TRAF6	USP33 negatively regulates NFκB activation by deubiquitylating TRAF6	Yasunaga J (2011)
	USP2	MDM2	USP2a regualtes the p53 pathway by deubiquitylating and stabilizing MDM2	Stevenson LF (2007)
	USP2	TRAF6	USP2a deSUMOylates TRAF6 and mediates TRAF6-MALT1 interactions to regulate NFKB signaling	Li Y (2013) Bremm A (2010) Li Y (2013) Rolland T (2014)
	USP26	MDM2	USP26 deubiquitylates and stabilizes MDM2 resulting in decreased stability of the tumor suppressor p53	Lahav-Baratz S (2017)
	USP19	XIAP	USP19 regulates the stability of XIAP and enhances TNFα-induced caspase activation and apoptosis	Mei Y (2011)
	USP15	TRAF6	USP15 interacts with TRAF6 and removes K63-linked polyubiquitylation of TRAF6	Bremm A (2010)
	USP15	SMURF2	USP15 deubiquitylates SMURF2 which results in enhanced stability of TGFβ receptor and downstream pathway activation	Iyengar PV (2015) Eichhorn PJ (2012)
	USP12	MDM2	USP12 negatively regulates p53 stability by deubiquitylating MDM2	McClurg UL (2018)
	USP11	XIAP	USP11 exhibits pro-survival activity by stabilizing XIAP and promoting tumor initiation and progression	Sowa ME (2009) Zhou Z (2017)
	USP10	TRAF6	USP10 interacts in a complex with TANK and MCPIP1 in order to deubiquitylate TRAF6 and attenuate NFκB activation	Wang W (2015)

Model	DUB	E3	Functional significance of DUB-E3 interaction	Reference
Model # 2 Reciprocal regulation of DUB/E3 ubiquitylation	USP7	MARCH7-	MARCH7 undergoes compartment specific-deubiquitylation by USP9X in the cytosol and USP7 in the nucleus	Nathan JA (2008) Zhang L (2016) Lim J (2006) Hayes SD (2012)
	USP9X	MARCH7-	MARCH7 undergoes compartment specific-deubiquitylation by USP9X in the cytosol and USP7 in the nucleus	Agrawal P (2012) Nathan JA (2008)
	CSN5	MDM2	CSN5 stabilizes MDM2 through reducing MDM2 self-ubiquitination and decelerating turnover rate of MDM2 and thereby regulates p53 stability	Zhang XC (2008)
	USP33	β-TrCP	USP33 is negatively regulated by β-TrCP and ubiquitin-dependent proteolysis	Cheng Q (2017)
	USP20	VHL	USP20 can be ubiquitylated and degraded in a pVHL-dependent manner	Li Z (2002)
	USP5	SMURF1	Smurf1 interacts with and ubiquitylates USP5 to target for proteasomal degradation, and thereby inhibits the production of TNF-alpha	Qian G (2016) Andrews PS (2010)
	USP18	SKP2	SKP2 regulates the stability of USP18, an ISG15 isopeptidase	Tokarz S (2004) Zhang X (2014)
	USP19	SIAH1	SIAH1 and SIAH2 promote USP19 ubiquitylation and proteasomal degradation	Velasco K (2013) Zhang Q (2017) Altun M (2012)
	USP19	SIAH2	SIAH1 and SIAH2 promote USP19 ubiquitylation and proteasomal degradation	Altun M (2012) Velasco K (2013)
	UP37	β-TrCP	SCF-BTRCP regulates USP37 stability during G2-phase to promote mitotic entry	Huttlin EL (2017) Burrows AC (2012) Saxena N (2014) Yeh C (2015)
	AMSH	SMURF2	RNF11 recruits AMSH to Smurf2 for ubiquitination, leading to its degradation by the 26S proteasome	Li H (2004)
	USP33	VHL	pVHL ubiquitylates and destabilizes USP33	Li Z (2002) Yuasa-Kawada J (2009)
	USP30	PARK2	Parkin interacts with and ubiquitylates USP30 to target USP30 for degradation. USP30 antagonizes mitophagy by deubiquitylating mitochondrial proteins.	Gersch M (2017)
	UCH-L1	PARK2	PARK2 targets UCH-L1 for degradation	McKeon JE (2014)

Model	DUB	E3	Functional significance of DUB-E3 interaction	Reference
Model # 3 DUB-E3 complex perform ubiquitin chain editing	A20	TRAF6	The NFκB response to TLR activation is attenuated through a mechanism in which TRAF6 is deubiquitylated by A20	Heyninck K (1999) Evans PC (2001) Lin SC (2008) Xiong Y (2011) Kelly C (2012) Garg AV (2013) Bremm A (2010) Lin SC (2008) Boone DL (2004) Hayes SD (2012) Schimmack G (2017)
	CYLD	ITCH	Itch-CYLD complex first cleves K63-linked ubiquitin from Tak1 and then subsequently adds K48-linked ubiquitin to terminate inflammatory signaling via tumor necrosis factor	Ahmed N (2011)

TABLE 1.1 Function of known DUB-E3 complexes. Table of identified DUB-E3 complexes in humans with known functional significance, grouped by function.

Ubiquitin chain editing mechanisms often result from interactions of multiple DUBs and E3s and often contribute to intricate regulatory pathways. However, due to the contributions of multiple enzymatic activities, the biochemical determinants of these mechanisms can be difficult to reconstitute.

1.4.4 Regulation of DUB-E3 interactions

In some cases, the functional significance of a DUB-E3 complex can shift in a context-dependent manner. A clear example that highlights this phenomenon is the DUB USP7 which is known to interact with and regulate multiple E3 ubiquitin ligases. One well-characterized regulatory interactor of USP7 is the E3 ubiquitin ligase MDM2. Under normal conditions MDM2 functions to regulate levels of the transcription factor p53 (Prives, 1998). In these conditions, USP7 was found to interact in a complex with MDM2 and p53 to reverse autoubiquitylation events on MDM2 and ultimately drive p53 degradation (**FIG 1.5**, Model 2). However, under stress conditions USP7 preferentially deubiquitylates and stabilizes p53 in order to activate an apoptotic pathway (**FIG 1.5**, model 1) (Kim and Sixma, 2017). This switch in USP7 function has been shown to result from altered associations with regulatory proteins under stress conditions (Tavana and Gu, 2017). USP7 has also been reported to display similar substrate-switching behavior through regulation of the E3 UHRF-1 and its substrate, DNA methyltransferase-1 (DNMT1). USP7 interacts with UHRF1 in a trimeric complex with DNMT1 whereby USP7 functions to deubiquitylate and stabilize UHRF1 or DNMT1 in a cell-cycle dependent manner (**FIG 1.5,** Model 2) (Felle et al., 2011).

While DUB-E3 complexes already lend themselves to intricate regulation of

substrate proteins, the complexity of these associations is further expanded when multiple E3s or multiple DUBs associate with each other or shared substrates. For instance, there are some cases in which multiple DUBs interact with the same substrate yet exhibit different activities to ultimately elicit different outcomes for the substrate/signaling pathway. For example, the DUB USP2a interacts with and deubiquitylates MDM2 in order to promote MDM2 stability and p53 degradation (Stevenson et al., 2007). This differs from USP7, which can deubiquitylate both MDM2 and p53 in a context-dependent manner and can thus function to promote or antagonize p53 stability (Kim and Sixma, 2017).

Additionally, there are some E3 ubiquitin ligases that have promiscuous activity but can engage with DUBs to fine-tune their specificity. An important example highlighting this activity comes in the ER-associated degradation (ERAD) pathway where multiple E3 ubiquitin ligases and DUBs play critical regulatory roles. Largely, these DUBs function as negative regulators of the ERAD pathway by reversing the activity of E3s and inhibiting protein turnover of ERAD substrates. However, some DUBs have been reported to function as positive regulators of ERAD (Blount et al., 2012; Ernst et al., 2009; Wang et al., 2006; Zhong and Pittman, 2006). For example, the DUB USP13 is reported to be a positive regulator of the ERAD pathway by enhancing the substrate specificity of the critical ERAD E3 ubiquitin ligase gp78 (Liu et al., 2014b). During ERAD the E3 gp78 functions to ubiquitylate ERAD substrates but this E3 lacks substrate specificity and sometimes ubiquitylates ERAD machinery including UBL4A. UBL4A normally associates in a complex with BAG6 and TRC35 to exhibit chaperone activity by delivering substrates to gp78 for ubiquitylation and proteasomal degradation

(Chen et al., 2006). Upon ubiquitylation of UBL4A, BAG6 undergoes proteolytic cleavage and inactivation which ultimately diminishes ERAD functionality. USP13 has been shown to interact with gp78 and promote ERAD by fine-tuning gp78 substrate specificity via removal of ubiquitin modifications from ERAD machinery. This interaction highlights an instance when a DUB can essentially protect the activity of an associated E3.

DUB-E3 interactions can also establish a ubiquitin rheostat on substrate proteins to tune their function or the strength of the signal they transduce. Such a rheostat has been reported to occur in the context of ER quality control machinery, where DUB activities can sharpen the distinction between folded and misfolded membrane proteins (Zhang et al., 2013). In this case, the interactions between E3 ligases and substrates in the membrane directly influences the processivity of ubiquitin modifications and dictates extent of substrate polyubiquitylation. These E3-interacting DUBs can then alter polyubiquitin dwell times on substrates to tune the extent of net degradation. Another notable example involves the DUB USP7, which was shown to interact with the MAGE-L2-TRIM27 E3 ubiquitin ligase to regulate the ubiquitylation status of WASH, a shared substrate, on the endosome (Wu et al., 2014). These studies showed that K63-linked ubiquitylation regulates WASH function as an actin-nucleating protein during endosomal protein recycling and the USP7-TRIM27 rheostat functions to tune WASH ubiquitylation and consequently tunes endosomal protein recycling. Interestingly, USP7 has been reported to interact with multiple E3 ubiquitin ligases (**FIG 1.4**) (Kim and Sixma, 2017) but the functional significance of many of these interactions remain unclear.

While it is clear that DUB-E3 interactions have the potential to provide many

layers of regulation within the ubiquitin proteasome system, many reported DUB-E3 interactions are not well understood and remain to be characterized.

1.4.5 Association of NEDD4s with DUBs

Multiple NEDD4 family members have been reported to interact with and undergo regulation by DUBs (**TABLE 1.2**). The functional significance of these interactions can vary greatly – with some DUBs antagonizing the activity of the NEDD4, some DUBs functioning to stabilize the NEDD4, or others functioning in a ubiquitin chain editing event. Understanding the regulatory logic of these DUB-E3 interactions could provide critical information about the molecular functions of DUBs and E3s and give powerful insight into the role these components play in the progression of disease.

1.5 Summary of thesis

The work presented in this thesis outlines the functional significance of the interactions of the DUB USP9X with the NEDD4 family of E3 ubiquitin ligases and how these DUB-E3 associations contribute to complex regulatory mechanisms for both the canonical and non-canonical WNT signaling pathways. In **Chapter 3** I provide rigorous analysis of the USP9X and WWP1-mediated ubiquitin rheostat on DVL2 that regulates WNT pathway specification in breast cancer cells. In **Chapter 4** I summarize the biochemical analysis of this DUB-E3 complex to determine the molecular and enzymatic determinants of the ubiquitin rheostat on DVL2. In **Chapter 5** I provide insight and discussion into the cellular function of DUB-E3 complexes, the dysregulation of USP9X and NEDD4s in disease states, and how targeting these activities may or may not be

NEDD4	DUB	Functional significance of interaction	Reference
ITCH	CYLD	ITCH-CYLD complex first cleaves K63-linked ubiquitin from Tak1 and then subsequently adds K48-linked ubiquitin to terminate inflammatory signaling via tumor necrosis factor	Ahmed N (2011)
ITCH	USP5	unknown	O'Connor HF (2015)
ITCH	USP9X	USP9X stabilizes ITCH by removing autoubiquitylation events	O'Connor HF (2015) Mouchantaf R (2006) Azakir BA (2009)
ITCH	USP12	USP12 acts as a negative regulator of the Notch pathway by reversing ITCH-mediated ubiquitylation of Notch ligand	Moretti J (2012) Jahan AS (2016)
ITCH	USP13	unknown	Sowa ME (2009)
NEDD4L	USP36	USP36 regulates degradation of TrkA neurotrophin receptor by regulating NEDD4L interactions with TrKA	Anta B (2016)
NEDD4L	A20	unknown	Huttlin EL (2017)
SMURF1	USP5	SMURF1 interacts with and ubiquitylates USP5 to target for proteasomal degradation, and thereby inhibits the production of TNF-alpha	Qian G (2016) Andrews PS (2010)
SMURF1	USP9X	USP9X stabilizes SMURF by removing autoubiquitylation events	Xie Y (2013)
SMURF1	USP15	unknown	Xie Y (2013)
SMURF2	USP15	USP15 deubiquitylates SMURF2 which results in enhanced stability of TGFβ receptor and downstream pathway activation	Iyengar PV (2015) Eichhorn PJ (2012)
SMURF2	USP35	unknown	Hein MY (2015)
SMURF2	AMSH	RNF11 recruits AMSH to SMURF2 for ubiquitylation, leading to its degradation by the 26S proteasome	Li H (2004)

TABLE 1.2 NEDD4 family-interacting DUBs. Table of reported DUB-NEDD4 interactions with information on functional significance of indicated interactions

useful for developing therapeutics. Altogether, the information in this thesis provides a unique perspective to the dynamic interplay within the ubiquitin system and draws attention to important considerations to be made before pursuing disease therapeutics that modulate these components.

CHAPTER 2

Materials & Methods

2.1 Experimental model and subject details

HEK293 STF cells (Female) and MDA-MB-231 cells (Female) were purchased from the American Type Culture Collection (ATCC). HEK293 STF cells were cultured in DMEM with 10% FBS and 1% penicillin/streptomycin at 37ºC in 5% CO2. MDA-MB-231 cells were cultured in RPMI with 10% FBS and 1% penicillin/streptomycin at 37ºC in 5% CO2. MDA-MB-231 cells stably expressing FLAG-WWP1, FLAG-DVL2, FLAG-DUB-DVL2, or FLAG-DUB*-DVL2 were generated using the pQCXIP retroviral vector system. MDA-MB-231 *usp9x* knockout cells were generated using a CRISPR/Cas-9 genome editing system.

2.2 Method details

2.2.1 Assays for measuring WNT activation

Topflash reporter assays in HEK293 STF cells were performed as follows: HEK293 STF cells were seeded on 24-well plates at ~50% confluency. Cells were treated with 100ng/mL purified recombinant WNT3a (R&D Systems) and 100ng/mL purified recombinant R-spondin (R&D systems) 24 hours prior to lysis with 1X Passive Lysis buffer (Promega). Luciferase activity was measured using the Steady-Glo luciferase Assay (Promega). Luciferase signal was normalized to viable cell number using Cell-

Titer Glo Assay (Promega). For siRNA knockdown studies, cells were treated for 72 hours prior to lysis, for inhibitor studies cells were treated for 24 hours prior to lysis, and for overexpression studies cells were transfected with plasmid DNA for 48 hours prior to lysis.

Topflash reporter assays in MDA-MB-231 cells were performed as follows: Cells were plated, co-transfected with TOPflash and Renilla expression plasmids at 24 hours and lysed at 48 hours using the Dual-Glo Luciferase Assay system (Promega). Luciferase signal was normalized to co-transfected Renilla expression. Data were normalized to a positive control (set at 100% activation). Assays were performed in triplicate and repeated at least 3 times.

B-catenin stabilization assay: HEK293 STF cells were cultured in Dulbecco's modified Eagle's Medium (DMEM) and activated with WNT3A ligand or LiCl for 24 hours. Then cells were lysed and nuclear/cytoplasmic fractionation was performed as previously described (Thorne et al., 2010).

2.2.2 Transfections

Plasmid and siRNA transfections were performed using Lipojet (SignaGen, SL100468) and Lipofectamine LTX with PLUS reagent (Thermo Fisher, 15338100) according to manufacturer's protocol.

2.2.3 Immunoblots

Whole-cell lysates were generated by lysing cells in Laemmli Sample Buffer (Bio-Rad) with 5% βME and subsequently boiling samples at 95ºC for 5 minutes. Proteins were

analyzed by SDS-PAGE and immunoblotting using the LiCor Odyssey reagents and protocols. Fluorescence signaling was detected using an Odyssey CLx Infrared Scanner (LiCor).

2.2.4 Cell lines

HEK293 STF cells and MDA-MB-231 cells were purchased from the American Type Culture Collection (ATCC). HEK293 STF cells were cultured in DMEM with 10% FBS and 1% penicillin/streptomycin at 37ºC in 5% CO2. MDA-MB-231 cells were cultured in DMEM with 10% FBS and 1% penicillin/streptomycin at 37ºC in 5% CO2. MDA-MB-231 cells stably expressing FLAG-WWP1, FLAG-DVL2, FLAG-DUB-DVL2, or FLAG-DUB*-DVL2 were generated using the pQCXIP retroviral vector system. MDA-MB-231 *usp9x* knockout cells were generated using a CRISPR/Cas-9 genome editing system.

2.2.5 SILAC-based quantitative proteomic analysis

Quantitative mass spectrometry analysis by SILAC was performed on MDA-MB-231 cells stably expressing the indicated FLAG-tagged substrates. These cells were cultured in the presence of either heavy or light isotopes (lysine and arginine, Sigma-Aldrich) for at least 6 doublings to ensure incorporation of these isotopes into 100% of the proteome. Affinity purification was performed as previously described (Lee et al., 2017). Eluted proteins were digested with 1µg Trypsin Gold (Promega) at 37ºC overnight. Digested peptides were cleaned-up on a Sep-Pak C18 column. Purified peptides were then dried, reconstituted in 0.1% trifluoroacetic acid, and analyzed by LC-MS/MS using an Orbitrap XL mass spectrometer. Database search and SILAC

quantitation were performed using MaxQuant software.

2.2.6 Co-immunoprecipitation studies

For coimmunoprecipitation assays, cells were washed with cold PBS and lysed with a nondenaturing lysis buffer (NDLB): 50mM tris (pH 7.4), 300mM NaCl, 5mM EDTA, 1% Triton X-100, cOmplete protease inhibitor cocktail (Roche), Phosphatase inhibitor cocktail (Roche), 1mM PMSF, 1mM Phenanthroline, 10mM Iodoacetamide, and 20μM MG132. Lysates were diluted to 1mg/mL with NDLB and incubated with Sigma FLAG EZ-view beads for 2 hours with rotation at 4°C. Beads were washed 3 times with cold NDLB and once with cold PBS. Proteins were then eluted from beads using sample buffer and samples were processed for SDS-PAGE followed by immunoblotting.

2.2.7 Fluorescence microscopy

MDA-MB-231 cells were seeded on coverslips at 50% confluency. At 24 hours after seeding, cells were transfected with FLAG-Dvl2 using LipoJet Transfection Reagent (Signagen). 72 hours after seeding cells were fixed and permeabilized using 4% paraformaldehyde (PFA) and immunofluorescence block buffer (PBS + 0.1% Triton-x + 10% FBS). Cells were then labeled with primary antibodies for 1 hour followed by a 1 hour incubation with alexa-fluor conjugated secondary antibodies. Coverslips were mounted on slides using ProLong AntiFade mountant (Thermo). Microscopy images were acquired using a DeltaVision Elite system (GE Healthcare) and processed using SoftWoRx software (GE Healthcare, Chicago, IL).

2.2.8 In vitro ubiquitin conjugation and deubiquitylation assays

Due to the limited solubility of full-length DVL2 in solution, in all *in vitro* conjugation and deconjugation assays HA-DVL2 was purified from human HEK293 cells using magnetic anti-HA beads (Pierce #88836) and all conjugation/deconjugation reactions were performed on HA-DVL2 bound to anti-HA beads. Lysis and purification were performed as follows: 24 hours after seeding, HEK293 cells were transfected with HA-Dvl2 and 48 hours post-transfection cells were lysed in NDLB and clarified by centrifugation. Lysates bound anti-HA magnetic beads overnight at 4ºC with rotation. Beads were washed 3 times in NDLB and 1 time in cold 1X PBS before being resuspended in conjugation buffer (40 mM Tris pH 7.5, 10 mM MgCl2, and 0.6 mM DTT) for immediate use in conjugation/deconjugation reactions.

For the conjugation reactions, 56 nM GST-Ube1 (Boston Biochem, Cambridge, MA, E-300), 0.77 mM UBE2D3, 2.3 mM Ub, HA-DVL2, and 60 nM FLAG-WWP1 (Sigma, SRP0229) were incubated in conjugation buffer (40 mM Tris pH 7.5, 10 mM MgCl2, and 0.6 mM DTT) with 1 mM ATP, at 37°C. Reactions were initiated by the addition of FLAG-WWP1. Samples were removed at indicated time-points, boiled in 2x Laemmli sample buffer for 10 min, and analyzed by blotting for HA-DVL2 with DVL2 antibody (Cell Signaling Technology, #3216) using goat anti-rabbit secondary (IRDye 800 CW, LI-COR Biosciences, Lincoln, NE). Quantification was performed using ImageStudioLite software (LI-COR).

For deconjugation reactions, polyubiquitinated substrate (HA-DVL2) was generated using the conjugation assay described above within one exception in that 0.1 mM ATP was used. The conjugation reaction was stopped by incubation with 0.75 units Apyrase

in a 90 µl reaction at 30°C for 1 hr. For the deconjugation reaction, 100 nM His6-USP9X (Boston Biochem E-552), 100nM OTUB1, or 100nM AMSH was added to conjugated HA-DVL2 as well as 10X DUB buffer (0.5 M Tris pH 7.5, 500 mM NaCl, 50mM DTT) to 1X. Reactions were initiated by the addition of His6-USP9X protein. The reaction was incubated at 37ºC. Samples were removed at indicated time-points and boiled in 2x Laemmli sample buffer. HA-DVL2 levels were determined as described in the conjugation assay.

For Rheostat experiments, HA-DVL2 substrate was resuspended in conjugation buffer with 1mM ATP and treated with 56 nM GST-Ube1 , 0.77 mM UBE2D3, 2.3 mM Ub, and indicated concentrations of FLAG-WWP1 and His-USP9X for 60 minutes at 37°C. Samples were then boiled in 2x Lammli sample buffer for 10 minutes and analyzed by blotting for HA-DVL2 with DVL2 antibody (CST #3216). Line profile analysis was performed using ImageJ (NIH).

For linkage-restricted ubiquitylation experiments, conjugation reactions were performed as described above with the exception of the recombinant ubiquitin used. Here we use linkage-restricted ubiquitin variants (i.e. lacking every lysine except one) that can only form polyubiquitin chains of one linkage type (Boston Biochem).

2.2.9 Migration assays

Cell culture dishes were coated with 5 µg/ml rat tail ColI (Corning #354236) in PBS for 1 h at 37°C then cells were plated at low density and incubated at 37°C for 1 hour in cell culture medium. Cells were kept at 37°C in SFM4MAb medium (HyClone, Logan, UT) supplemented with 2% FBS at pH 7.4 during imaging using phase-contrast and fluorescence microscopy techniques. Images were acquired at 5 min intervals for 6 h,

using DeltaVision Elite system software (GE Healthcare) and cell speed was quantified using SoftWoRx software (GE Healthcare, Chicago, IL). Wind rose plots were generated by transposing x,y coordinates of cell tracks to a common origin.

2.2.10 Rho activation assays

Rho activation assays were performed using the Rho Activation Assay Kit (Millipore Sigma #17-924). MDA-MB-231 cells (WT and *usp9x* KO cells) were grown until confluent, washed in ice-cold 1XPBS, lysed in ice-cold 1X Mg^{2+} Lysis/Wash buffer (MLB) (Millipore Sigma #20-168), scraped and collected in microfuge tubes on ice, and incubated at 4°C for 15 minutes with agitation. Lysates were then cleared of cellular debris by centrifugation at 14,000xg for 5 minutes at 4°C. Clarified lysate was then bound to Rho Assay Reagent (Millipore Sigma #14-383) at 4°C for 45 minutes with gentle agitation. Agarose beads were then washed 3 times with 1X MLB and proteins were eluted in 2x Laemmli reducing sample buffer (BioRad #1610737) by boiling at 95°C for 5 minutes. Samples were fractionated by SDS-PAGE and analyzed by blotting using the Anti-Rho (-A, -B, -C) clone 55 antibody (Millipore Sigma #05-778). GTPγS/GDP loading for positive and negative controls were prepared as described above with an additional 30 minute incubation at 30°C with agitation of cell lysate in the presence of 10mM EDTA and either 100uM GTPγS (Millipore Sigma #20-176) or 1mM GDP (Millipore Sigma #20-177). This step was performed prior to binding the Rho Assay Reagent.

2.3 Quantification and statistical analysis

A Student's T-test was used to test for a statistically significant difference between the means of the two variables of interest. The alpha value for each experiment was set at 0.05 and a p-value was calculated using the Student's t-test function in Microsoft Excel to determine statistical significance. Each figure with statistical analysis represents $n \geq 3$ for all coIP and luciferase assay experiments, where n represents biological replicates. For quantitation of all microscopy-based data an $n \geq 25$ was used where n represents single cells. In all figures including statistics, error bars represent standard deviation of the mean. Details of statistical analysis can also be found in figure legends.

Where indicated, a one-way ANOVA was used to compare the means of more than two samples. This analysis was performed using GraphPad Prism software.

2.4 Key resources table

REAGENT or RESOURCE	SOURCE	IDENTIFIER
Antibodies		
Monoclonal ANTI-FLAG® M2 antibody produced in mouse	Millipore	Product #: F1804
USP9X/Y Antibody (E-12)	Santa Cruz	Cat #: sc-365353
WWP1 monoclonal antibody (M01), clone 1A7	Abnova	Catalog #: H00011059-M01
Dvl2 Antibody #3216	Cell Signaling Technology	Product # 3216S
GAPDH (14C10) Rabbit mAb #2118	Cell signaling technology	Product # 2118S
USP24 (S-18) antibody	Cell Signaling Technology	Catalog #: sc-82080
Anti-beta Catenin antibody [E247]	Abcam	ab32572
Tubulin antibody	Vanderbilt Antibody and Protein Resource Core	N/A
NEDD4L Antibody #4013	Cell Signaling Technology	Product # 4013S
WWP2 (AIP2) Antibody (A-3)	Santa Cruz	Catalog #: sc-398090
HA antibody	Vanderbilt Antibody and Protein Resource Core	N/A
Alpha adaptin antibody (AP2A1) AC1-M11	Thermo Fisher	Cat #: MA3-061
Anti-AP2M1 antibody [EP2695Y]	Abcam	ab75995
Anti-VANGL1	Sigma	Product #: HPA025235
Cofilin (D3F9) XP Rabbit mAb	Cell Signaling Technology	D3F9
Anti-Rho (-A, -B, -C) clone 55	Millipore Sigma	Catalog # 05-778
Anti-HA magnetic beads	Pierce	Catalog # 88836
Bacterial and Virus Strains		
Biological Samples		

Chemicals, Peptides, and Recombinant Proteins		
WP1130	UBPBio	Cat #: F2120
MG-132	APExBIO	Cat #: A2585
Phenanthroline	Sigma-Aldrich	Cat #: P9375
Iodoacetamide	Sigma-Aldrich	Cat #: I1149
LGK-974	Selleck Chem	Catalog No.S7143
Recombinant Human/mouse Wnt5a	R&D System	Cat #: 645-WN
WWP1 Active human recombinant, expressed in baculovirus infected insect cells	Sigma-Aldrich	Prod #: SRP0229
USP9x-His6, isoform 2, human recombinant	Boston Biochem	Cat. # E-552
Recombinant OTUB1	UBPBio	Catalog #: H3000
AMSH, human recombinant	Boston Biochem	Cat. # E-548B
GST-Ubiquitin E1 Enzyme (UBE1), S.cer. recombinant	Boston Biochem	Cat. # E-300
Recombinant Human UbcH5c/UBE2D3	Boston Biochem	Cat. # E2627
Recombinant Mouse Wnt-3a	R&D Systems	Cat #: 1324-WN
Recombinant Mouse R-spondin	R&D Systems	Cat #: 3474-RS
Corning® Collagen I, Rat Tail	Corning	Product #: 354236
Heavy Lysine: L-Lysine-13C6,15N2 hydrochloride	Sigma-Aldrich	Product #: 608041
Heavy Arginine: L-Arginine-13C6,15N4 hydrochloride	Sigma-Aldrich	Product #: 608033
Ubiquitin mutant with K33 only	Boston Biochem	Catalog #: UM-K330
Ubiquitin mutant with K63 only	Boston Biochem	Catalog #: UM-K630
Ubiquitin mutant with K6 only	Boston Biochem	Catalog #: UM-K60
Ubiquitin mutant with K11 only	Boston Biochem	Catalog #: UM-K110
Ubiquitin mutant with K27 only	Boston Biochem	Catalog #: UM-K270
Ubiquitin mutant with K29 only	Boston Biochem	Catalog #: UM-K290
Ubiquitin mutant with K48 only	Boston Biochem	Catalog #: UM-K480
Ubiquitin mutant with no K	Boston Biochem	Catalog #UM-NOK
Critical Commercial Assays		

Steady Glo Luciferase Assay System	Promega	Catalog #: E2510
Dual Glo Luciferase Assay System	Promega	Catalog #: E2920
Rho Activation Assay Kit	Millipore Sigma	Catalog #: 17-294
Deposited Data		
Experimental Models: Cell Lines		
Human cells: MDA-MB-231 cells	ATCC	Product #: MDA-MB-231 (ATCC® HTB-26™)
Human cells: HEK293 cells	ATCC	Product #: 293 [HEK-293] (ATCC® CRL-1573™
Human cells: HEK 293 STF	ATCC	Product #: HEK 293 STF (ATCC® CRL-3249)
Human cells: MDA-MB-231 cells stably expressing FLAG-DVL2, FLAG-DUB-DVL2, or FLAG-DUB*-DVL2	This paper	N/A
Human cells: MDA-MB-231 *usp9x* KO cells +/- FLAG-DVL2	This paper	N/A
Experimental Models: Organisms/Strains		
Oligonucleotides		
Control siRNA: orKKJ1-s, nonsilencing/pGL2 sense, CGUACGCGGAAUACUUCGAUU	This paper	N/A
Usp9x siRNA #1 sequence: AGAAAUCGCUGGUAUAAAUU	This paper	N/A
Usp9x siRNA #2 sequence: ACACGAUGCUUUAGAAUUUU	This paper	N/A
Nedd4L siRNA #1 sequence: GCUAGACUGUGGAUUGAGUUU	This paper	N/A
Nedd4L siRNA #2 sequence: UGAGGAUCAUUUGUCCUACUU	This paper	N/A
WWP1 siRNA #1 sequence: GAAGUCAUCUGUAACUAAA**UU**	This paper	N/A
WWP1 siRNA #2 sequence: GCAGAGAAAUACUGUUUAU**UU**	This paper	N/A

WWP2 siRNA #1 sequence: GGGAGAAGAGACAGGACAA**UU**	This paper	N/A
WWP2 siRNA #2 sequence: CAGGAUGGGAGAUGAAAUA**UU**	This paper	N/A
VANGL1 Silencer Select siRNA	Thermo Fisher	Catalog #: 4392420
Recombinant DNA		
Plasmid: FLAG-Wwp1	This paper	N/A
Plasmid: FLAG-Wwp1-ww1 (W377F, P380A)	This paper	N/A
Plasmid: FLAG-Wwp1-ww2 (W409F, P412A)	This paper	N/A
Plasmid: FLAG-Wwp1-ww3 (W484F, P487A)	This paper	N/A
Plasmid: FLAG-Wwp1-ww4 (F524A, P527A)	This paper	N/A
Plasmid: FLAG-Wwp1-4ww (W377F, P380A, W409F, P412A, W484F, P487A, F524A, P527A)	This paper	N/A
Plasmid: FLAG-Wwp1-WW1 (W409F, P412A, W484F, P487A, F524A, P527A)	This paper	N/A
Plasmid: FLAG-Wwp1-WW2 (W377F, P380A, W484F, P487A, F524A, P527A)	This paper	N/A
Plasmid: FLAG-Wwp1-WW3 (W377F, P380A, W409F, P412A, F524A, P527A)	This paper	N/A
Plasmid: FLAG-Wwpw-WW4 (W377F, P380A, W409F, P412A, W484F, P487A)	This paper	N/A
Plasmid: FLAG-DVL2 PY1: $FPAY_{393} \rightarrow FAAA_{393}$	This paper	N/A
Plasmid: FLAG-DVL2 PY2: $PPPY_{568} \rightarrow PAPA_{568}$	This paper	N/A
Plasmid: FLAG-DVL2 2PY: $FPAY_{393} \rightarrow FAAA_{393}$ and $PPPY_{568} \rightarrow PAPA_{568}$	This paper	N/A
Plasmid: $USP9X_{1\text{-}2433}$, or *usp9x-Δpy3-4* $NPQY_{2437} \rightarrow NAQA_{2437}$ (*py3*) and $APLY_{2515} \rightarrow AALA_{2515}$ (*py4*)	This paper	N/A
Plasmid: UL36-DVL2	Stringer & Piper (2011) doi: 10.1083/jcb.201008121 Kettenhorn et al. (2005) Doi: 10.1016/j.molcel.2005.07.003	N/A

Plasmid: UL36 (C65A) catalytic dead-DVL2	Stringer & Piper (2011) doi:10.1083/jcb.201008121 Kettenhorn et al. (2005) Doi: 10.1016/j.molcel.2005.07.003	N/A
Plasmid: FLAG-DVL2-K0 (all lysines K→R)	This paper	N/A
Plasmid: FLAG-USP9X	This paper	N/A
Plasmid: FLAG-USP9X (C1556V) catalytic dead	This paper	N/A
Plasmid: FLAG-WWP1 (C890S) catalytic dead	This paper	N/A
Plasmid: GFP-DVL2	This paper	N/A
Plasmid: GFP-DVL2-K0 (all lysines K→R)	This paper	N/A
Plasmid: GFP-WWP1	This paper	N/A
Plasmid: GFP-USP9X	This paper	N/A
Software and Algorithms		
SoftWorx	GE	
MaxQuant	Max Planck Institute of Biochemistry	
ImageJ	NIH	
ImageStudioLite software	LICORE	
Other		

CHAPTER 3

USP9X Deubiquitylates DVL2 to Regulate WNT Pathway Specification

A paper published in *Cell Reports* (2019)

Casey P. Nielsen,[1] Kristin K. Jernigan,[1] Nicole L. Diggins,[2] Donna J. Webb,[2] and Jason A. MacGurn[1,3,*]

[1] Department of Cell and Developmental Biology, Vanderbilt University, Nashville, TN, 37240, United States

[2] Department of Biological Sciences, Vanderbilt University, Nashville, TN, 37240, United States

[3] Lead Contact

*Address correspondence to Jason A. MacGurn; email: jason.a.macgurn@vanderbilt.edu

3.1 Summary

The WNT signaling network is comprised of multiple receptors that relay various input signals via distinct transduction pathways to execute multiple complex and context-specific output processes. Integrity of the WNT signaling network relies on proper specification between canonical and non-canonical pathways, which presents a regulatory challenge given that several signal transducing elements are shared between pathways. Here, we report that USP9X, a deubiquitylase, and WWP1, an E3 ubiquitin ligase, regulate a ubiquitin rheostat on DVL2, a WNT signaling protein. Our findings indicate that USP9X-mediated deubiquitylation of DVL2 is required for canonical WNT activation, while increased DVL2 ubiquitylation is associated with localization to actin-rich projections and activation of the planar cell polarity (PCP) pathway. We propose that a WWP1-USP9X axis regulates a ubiquitin rheostat on DVL2 that specifies its participation in either canonical WNT or WNT-PCP pathways. These findings have important implications for therapeutic targeting of USP9X in human cancer.

3.2 Introduction

The canonical WNT β-catenin signaling pathway is involved in regulating many cellular processes such as cell fate determination during embryonic development, cell proliferation, and adult tissue homeostasis. Thus, it is not surprising that aberrant activation of the canonical Wnt pathway is known to occur in many types of cancer (MacDonald et al., 2009; Saito-Diaz et al., 2013). There are also several noncanonical WNT signaling pathways including the WNT-Planar Cell Polarity (WNT-PCP) pathway

which controls cell migration and tissue polarity. Dysregulation of the WNT-PCP pathway has been linked to cancer invasion and metastasis (Katoh, 2005; Luga et al., 2012; Wang, 2009). While the canonical WNT β-catenin pathway and the noncanonical WNT-PCP pathway use divergent effector mechanisms to regulate distinct cellular functions, these pathways share membrane receptor components and the cytoplasmic WNT transducer protein dishevelled (DVL). Despite its key role in both pathways, the mechanisms dictating DVL participation in canonical or noncanonical WNT signaling are yet to be elucidated.

Initiation of the canonical WNT β-catenin pathway occurs when extracellular WNT ligand binds to the co-receptors Frizzled (FZD) and low-density lipoprotein receptor-related protein 5/6 (LRP5/6) leading to recruitment of DVL and AXIN to the WNT ligand receptor complex (MacDonald et al., 2009). This ultimately results in the inhibition of β-catenin ubiquitylation and degradation such that stabilized β-catenin can enter the nucleus to initiate a transcriptional program (MacDonald et al., 2009; Saito-Diaz et al., 2013). On the other hand, core WNT-PCP pathway components Van Gogh-Like 1 (VANGL1), FZD, Prickle (Pk), DVL, and others function to activate RHOA, c-Jun N-terminal kinase (JNK), and nemo-like kinase (NLK) signaling cascades in order to coordinate tissue polarity and cell motility through regulation of actin dynamics (Glinka et al., 2011).

Ubiquitylation is known to be involved in key regulatory steps of both the canonical WNT and noncanonical WNT-PCP pathways. For example, ubiquitin-mediated regulation of cytoplasmic β-catenin stability is well characterized (Marikawa and Elinson, 1998). In addition, other steps of the WNT pathway upstream of β-catenin

stabilization undergo regulation by the ubiquitin system. Notably, several members of the NEDD4 family of E3 ubiquitin ligases (SMURF1, ITCH, and NEDD4L) have been found to negatively regulate stability of WNT pathway components. SMURF1 interacts with and ubiquitylates AXIN, inhibiting its interaction with the WNT co-receptor LRP5/6 (Ding et al., 2013; Fei et al., 2014; Fei et al., 2013; Tanksley et al., 2013; Wei et al., 2012). Both ITCH and NEDD4L promote degradation of DVL2 (Cadavid et al., 2000; Ding et al., 2013; Fei et al., 2014; Fei et al., 2013; Wei et al., 2012). Additionally, the deubiquitylase (DUB) USP34 was found to antagonize ubiquitylation of AXIN, promoting its stabilization and function in the canonical WNT pathway (Lui et al., 2011). SMURF1 and SMURF2 negatively regulate the WNT-PCP pathway by targeting WNT-PCP receptor component Prickle1 for degradation (Narimatsu et al., 2009). Furthermore, DVL2 is also known to undergo positive regulation by the ubiquitin system. For example, K63-linked ubiquitylation of the N-terminal DAX domain, which is known to mediate dynamic polymerization of DVL2, has been implicated as a positive regulator of DVL2 signal transduction (Schwarz-Romond et al., 2007; Tauriello et al., 2010). These examples highlight the complex regulation of canonical and non-canonical WNT pathways by ubiquitin conjugation and deconjugation machinery.

The NEDD4 family of E3 ubiquitin ligases is conserved from yeast to humans and has been implicated in the ubiquitin-mediated endocytosis of many plasma membrane proteins including surface receptors, ion channels, and nutrient transporters (David et al., 2013; He et al., 2008; Hryciw et al., 2004; Kuratomi et al., 2005; Lee et al., 2011; Lin et al., 2011; MacGurn et al., 2012). There are 9 NEDD4 family E3 ubiquitin ligases encoded in the human genome, each with distinct physiological functions (Rotin

and Kumar, 2009). While not all NEDD4 family E3 ubiquitin ligases have been characterized extensively, several have a strong preference for catalyzing K63-linked polyubiquitin chains *in vitro* (Ingham et al., 2004; Kim and Huibregtse, 2009). Given the broad role of NEDD4 family E3 ubiquitin ligases in the regulation of membrane trafficking and cell signaling, it is not surprising that they are often found to be dysregulated in human diseases including cancer (Bernassola et al., 2008). NEDD4 family members have a conserved domain structure including an N-terminal C2 domain that binds lipids, a C-terminal HECT ubiquitin ligase domain, and 2-4 internal WW domains. The WW domains have a high affinity for PY (Pro-Pro-x-Tyr) motifs and mediate interactions with substrates, adaptors, and regulatory factors (Ingham et al., 2004). Here, we report that the NEDD4 family member WWP1 interacts with USP9X and DVL2, and we find that these associations are governed by interactions between the WW domains of WWP1 and PY motifs present in both USP9X and DVL2. Importantly, we find that these interactions control a ubiquitylation rheostat on DVL2 that regulates both canonical WNT and non-canonical WNT-PCP activation in human breast cancer cells. Thus, we find that this USP9X-DVL2-WWP1 axis is a key regulatory node in the WNT pathway with the potential to influence both canonical and noncanonical WNT signaling in the context of human cancer.

3.3 Results

3.3.1 The WW domains of WWP1 coordinate interactions with USP9X and DVL2

In an attempt to identify factors that regulate WWP1 function we used SILAC-

based quantitative proteomics to generate a WWP1 interaction profile in MDA-MB-231 cells (a triple negative breast cancer cell line). This experiment identified interactions with various plasma membrane (PM) and PM-associated proteins, factors associated with membrane trafficking, signaling factors, and elements of the ubiquitin-proteasome system (**Table 3.1** and **FIG 3.2A**). To validate results obtained by quantitative proteomics, we tested for co-purification of a subset of putative WWP1 interacting proteins with FLAG-WWP1 stably expressed in MDA-MB-231 cells (**FIG 3.1A**). This approach confirmed FLAG-WWP1 interactions with several putative interactors - including USP9X, DVL2 and SPG20 – although some putative interactors such as ARRDC1 and USP24 could not be confirmed by this approach. Considering the possibility that some putative interacting proteins may artificially result from stable overexpression of FLAG-WWP1, we performed native co-immunoprecipitation of WWP1 and identified interactions with USP9X and DVL2 at endogenous expression levels (**FIG 3.2B**). Importantly, other studies have reported interactions between USP9X and NEDD4 family E3 ubiquitin ligases – including SMURF1 (Xie et al., 2013) and ITCH (Mouchantaf et al., 2006). Similarly, DVL2 was previously reported to interact with other NEDD4 family E3 ubiquitin ligases – including WWP2 (Mund et al., 2015) and NEDD4L (Ding et al., 2013; Wei et al., 2012). Notably, both USP9X and DVL2 contain multiple PY motifs capable of binding the WW domains of NEDD4 family E3 ubiquitin ligases (**FIG 3.1B**). Based on our findings and previous reports we decided to further investigate the basis of physical interactions between WWP1, USP9X, and DVL2. Since USP9X and DVL2 both contain multiple PY motifs we hypothesized that the WW domains of WWP1 might function to scaffold these proteins into a complex. To test this,

Category	protein	known function / description	pept. count	H:L ratio	stoich. (norm.)
Bait	WWP1	NEDD4 family E3 ubiquitin ligase (bait)	289	36.01	1.00
membrane traffic	SCAMP3	endosomal recycling	18	37.43	0.16
	ARF4	polarized exocytosis	8	7.13	0.14
	RAB14	regulation of Golgi-to-endosome transport	5	9.22	0.07
	ARF5	endocytosis of integrins	3	12.40	0.05
	SEC23IP	regulates ER exit	9	5.47	0.03
plasma membrane / membrane associated	CCDC85C	function unknown	21	17.47	0.16
	SPG20	function unknown	33	47.71	0.16
	AMOTL2	regulation of cell junctions; Hippo signaling	22	38.39	0.09
	AMOTL1	regulation of cell junctions; Hippo signaling	21	33.19	0.07
	RAPGEF6	function unknown	31	28.00	0.06
	MC1R	melanocortin receptor	3	26.71	0.03
	AXL	receptor tyrosine kinase	8	5.18	0.03
	ERBB2IP	binds and stabilizes ERBB2 receptor	12	9.36	0.03
	FNDC3B	function unknown	10	5.19	0.03
	SLC2A1	facilitative glucose transporter	3	6.67	0.02
	LRP10	putative receptor; function unknown	4	12.62	0.02
	EGFR	epidermal growth factor receptor	6	8.66	0.02
	ADAM9	cell surface metalloproteinase	4	6.04	0.02
	NPC1	intracellular cholesterol transporter	4	8.53	0.01
signaling	WBP2	Hippo pathway and hormone signaling	26	17.07	0.32
	PDLIM7	bone formation and BMP signaling pathways	30	22.18	0.21
	PTPN14	protein tyrosine phosphatase	75	22.11	0.20
	TMEM55B	phosphatidylinositol 4,5-bisphosphate 4-phosphatase	4	6.14	0.05
	DVL2	signal transducer, WNT pathway	9	25.67	0.04
	PTPN21	protein tyrosine phosphatase	4	10.24	0.01
ubiquitin proteasome system	USP9X	deubiquitylase	94	25.37	0.12
	FAM175B	member of the BRISC complex; deubiquitylase	9	13.22	0.07
	TXNIP	thioredoxin interacting protein; may function as E3 adaptor	8	8.86	0.06
	BRCC3	member of the BRISC complex; deubiquitylase	5	21.72	0.05
	ARRDC1	thioredoxin interacting protein; may function as E3 adaptor	6	20.14	0.04
	C19ORF62	member of the BRISC complex; deubiquitylase	3	9.28	0.03
	USP24	deubiquitylase	20	23.66	0.02

TABLE 3.1 WWP1 Interaction Profile using SILAC-MS, Related to Figure 1
Light: MDA-MB-231 cells stably expressing pQCXIP (empty vector); Heavy: MDA-MB-231 cells stably expressing FLAG-WWP1 Selection Criteria: (1) number of peptides quantified ≥ 3; (2) H:L ratio > 5

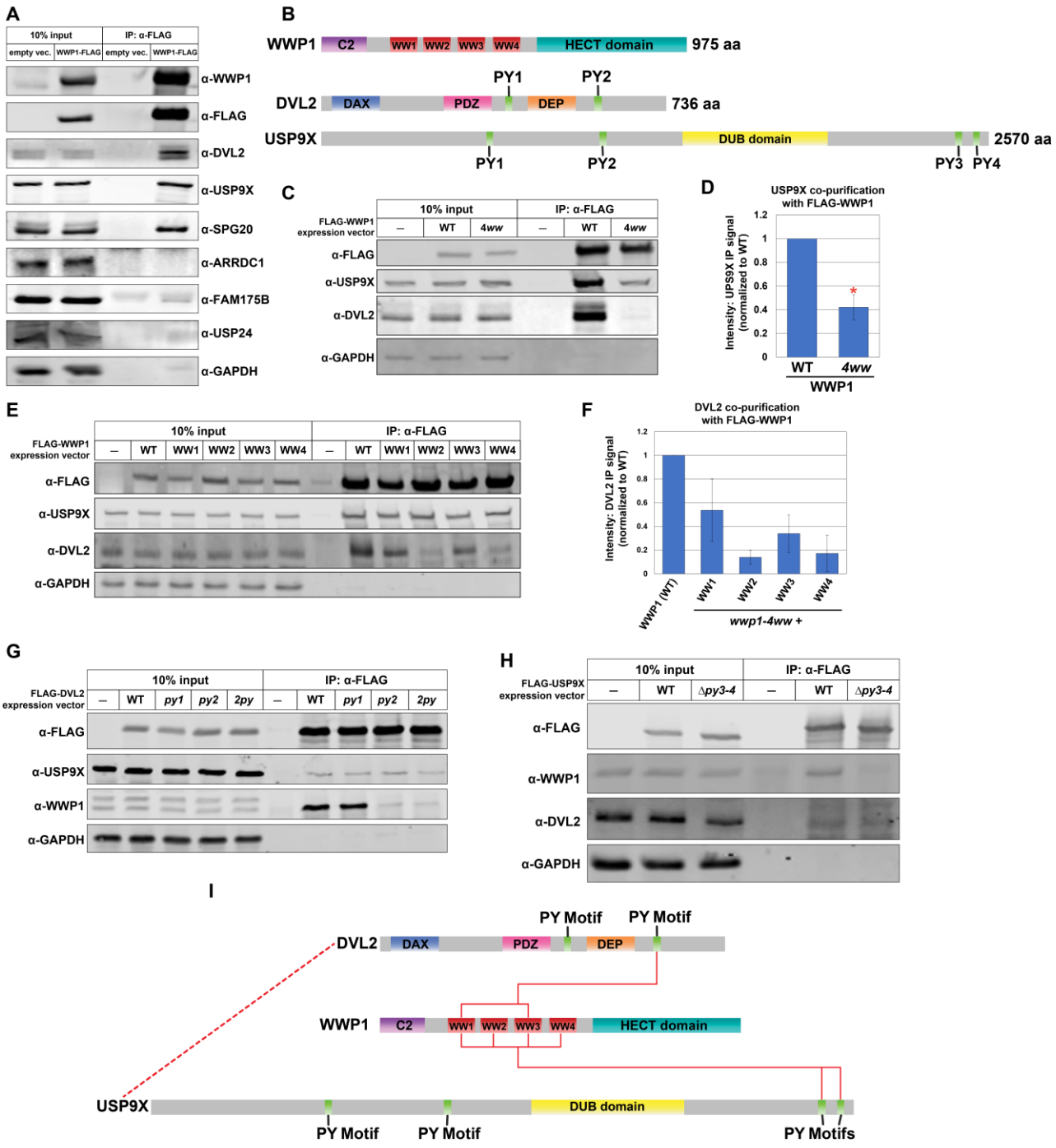

FIGURE 3.1 WWP1 interacts with USP9X and DVL2 in MDA-MB-231 human breast

cancer cells. (**A**) Co-immunoprecipitation analysis testing hits from SILAC-MS analysis in (FIG 3.2A). FLAG-WWP1 was affinity purified from MDA-MB-231 cell lysates. Input and immunoprecipitated (IP) fractions were blotted for the indicated species. **(B)** Schematic of known domains in WWP1, DVL2, and USP9X. **(C)** Analysis of co-purification of DVL2 and USP9X with WWP1 variants. The indicated WWP1 variants were FLAG affinity purified, and quantitative immunoblots were performed to assess co-purification of interacting factors. The *wwp1-4ww* mutant indicates that all four WW domains have been mutated to disrupt the ability to bind PY motifs. **(D)** Quantification of USP9X co-purification with FLAG-WWP1 variants (normalized to WT) over multiple experiments (n=3). Red asterisk indicates a significant difference based on Student's t-test analysis. **(E)** Analysis of co-purification of DVL2 and USP9X with WWP1 variants. The indicated WWP1 variants were FLAG affinity purified, and quantitative immunoblots were performed to assess co-purification of interacting factors. Each mutant variant of WWP1 contains a single intact WW domain (indicated), while the remaining three are mutated to disrupt PY motif binding. **(F)** Quantification of DVL2 co-purification with FLAG-WWP1 variants (normalized to WT) over multiple experiments (n=3). **(G)** Analysis of co-purification of WWP1 and USP9X with DVL2 variants. The indicated mutant DVL2 variants were FLAG affinity purified, and quantitative immunoblots were performed to assess co-purification of interacting factors. Mutant variants of DVL2 included point mutations disrupting the ability of its PY motifs to interact with WW domains. **(H)** Analysis of co-purification of WWP1 and DVL2 with USP9X variants. The indicated USP9X variants were FLAG affinity purified, and quantitative immunoblots were performed to assess co-purification of interacting factors. Mutant variants of USP9X included a small C-terminal truncation which results in deletion of both C-terminal PY motifs. **(I)** A schematic model for how USP9x and DVL2 both interact with WWP1 via PY motif interactions. The data also suggest an interaction between USP9X and DVL2 that is independent of WWP1 (dotted red line).

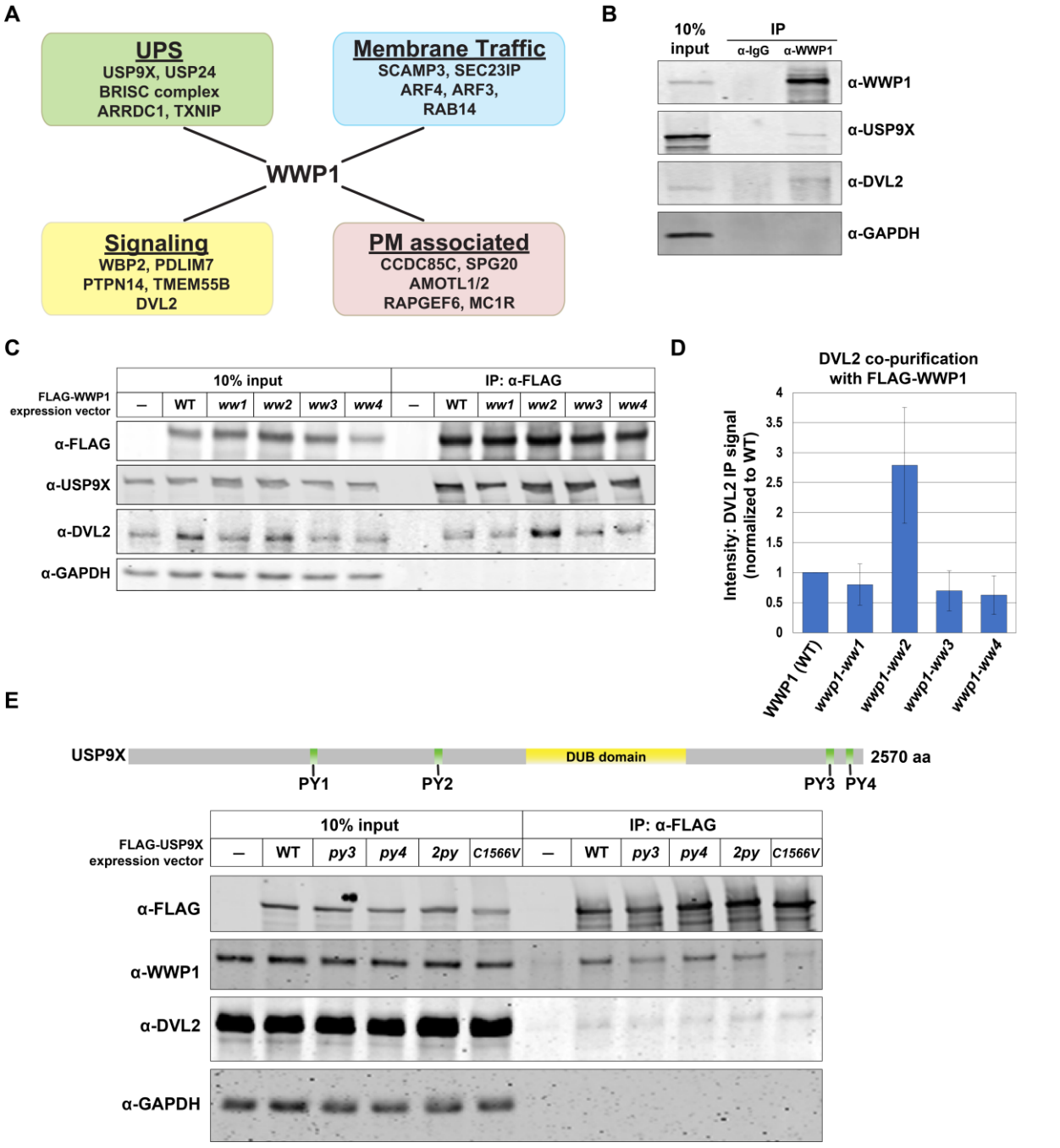

FIGURE 3.2 USP9X, WWP1, and DVL2 interactions are scaffolded by WW-PY interactions **(A)** Schematic summarizing putative WWP1 interacting proteins identified from SILAC-MS. Complete data set for this experiment is reported in Table 3.1. **(B)** Endogenous WWP1 was immunoprecipitated from MDA-MB-231 cells. Input (10%) and immunoprecipitates were resolved by SDS-PAGE and immunoblotted for the indicated species. **(C)** Analysis of co-purification of DVL2 and USP9X with WWP1 variants. The indicated WWP1 variants were FLAG affinity purified, and quantitative immunoblots were performed to assess co-purification of interacting factors. Mutant variants of WWP1 included point mutations disrupting the ability of individual WW domains to bind

PY motifs. **(D)** Quantification of DVL2 co-purification with FLAG-WWP1 variants (normalized to WT) over multiple experiments (n=3). **(E)** Analysis of co-purification of WWP1 and DVL2 with USP9X mutant variants. The indicated mutant USP9X variants were FLAG affinity purified, and quantitative immunoblots were performed to assess co-purification of interacting factors. *py3* and *py4* mutations indicate point mutations in PY3 and PY4, respectively, while *2py* indicates both C-terminal PY motifs were mutated. *C1566V* is mutated at the catalytic cysteine residue of USP9X.

we generated WWP1 WW domain point mutant variants designed to disrupt PY motif interactions (WxxP → FxxA) (Chen et al., 1997; Ermekova et al., 1997; Gajewska et al., 2001) and analyzed DVL2 and USP9X interaction by co-immunoprecipitation. We found that disruption of individual WW domains within WWP1 did not diminish interaction with USP9X or DVL2 (**FIG 3.2C** and **3.2D**). Indeed, we unexpectedly observed that the *wwp1-ww2* mutant exhibited significantly greater interaction with DVL2 (**FIG 3.2C** and **3.2D**). Although individual WW domains were dispensable for interaction with DVL2 and USP9X, we found that a WWP1 variant with point mutations disrupting each WW domain (*wwp1-4ww*) exhibited significantly decreased interaction with USP9X and complete loss of interaction with DVL2 (**FIG 3.1C** and **3.1D**). Together, these findings indicate that ***(i)*** WW domain scaffolding partially contributes to the interaction between WWP1 and USP9X, ***(ii)*** WW domain interactions are required for WWP1 engagement with DVL2, and ***(iii)*** the WW domains of WWP1 function redundantly for interaction with both DVL2 and USP9X.

To further probe the WW domain specificity underpinning WWP1 interactions with DVL2 and USP9X, we generated a panel of WWP1 variants containing only a single intact WW domain (designated as *wwp1*-WW1, *wwp1*-WW2, *wwp1*-WW3, and *wwp1*-WW4). Importantly, we found that any individual WW domain is sufficient to restore interaction with USP9X, suggesting complete redundancy for this interaction (**FIG 3.1E**). In contrast, we found that only WW1 and WW3 were sufficient to restore interaction with DVL2 (**FIG 3.1E** and **3.1F**), indicating that WW2 and WW4 do not contribute to the interaction between WWP1 and DVL2. Furthermore, the observation that *wwp1*-WW2 and *wwp1*-WW4 interact with USP9X but not DVL2 indicates that the

USP9X-WWP1 interaction occurs independent of DVL2 engagement. Overall, these findings suggest that the WW domains of WWP1 scaffold interactions with both USP9X and DVL2 in a manner that is redundant for USP9X and partially redundant for DVL2.

3.3.2 PY motifs in USP9X and DVL2 promote interaction with WWP1

Based on the observation that WW domains of WWP1 are important for interacting with USP9X and DVL2, we hypothesized that PY motifs in USP9X and DVL2 are required to engage WWP1. DVL2 contains two PY motifs ($FPAY_{393}$ and $PPPY_{568}$) that flank the DEP domain (**FIG 3.1B**). To test if either of these PY motifs are required for DVL2 to bind WWP1, we generated DVL2 variants with point mutations at individual PY motifs ($FPAY_{393} \rightarrow FAAA_{393}$ and $PPPY_{568} \rightarrow PAPA_{568}$) and performed co-immunoprecipitation analysis using FLAG-DVL2 as bait. This analysis revealed that PY1 ($FPAY_{393}$) is dispensable for interaction with WWP1 while PY2 ($PPPY_{568}$) is required to interact with WWP1 (**FIG 3.1G**). Furthermore, these results indicate that disruption of the DVL2-WWP1 interaction does not affect DVL2 engagement with USP9X (**FIG 3.1G**). Taken together, our results indicate that the DVL2-WWP1 interaction is governed by binding of the PY2 motif of DVL2 to the WW1 or WW3 domains of WWP1.

We hypothesized that PY motifs in USP9X also contribute to its interaction with WWP1. USP9X contains four PY motifs ($QPQY_{409}$, $HPRY_{1017}$, $NPQY_{2437}$, and $APLY_{2515}$), with the last two occurring at the C-terminus of the protein (**FIG 3.1B**). To test if these C-terminal PY motifs are required for interaction with WWP1, we generated a USP9X variant deleted for the C-terminal portion of the protein ($USP9X_{1\text{-}2433}$, or *usp9x-Δpy3-4*).

Importantly, deletion of the two C-terminal PY motifs resulted in complete loss of interaction with WWP1 (**FIG 3.1H**). However, point mutations in these C-terminal PY motifs ($NPQY_{2437} \rightarrow NAQA_{2437}$ (*py3*) and $APLY_{2515} \rightarrow AALA_{2515}$ (*py4*)) resulted in only partial loss of WWP1 interaction (**FIG 3.2E**). Notably, in each experiment loss of USP9X interaction with WWP1 did not affect its interaction with DVL2, indicating that the USP9X-DVL2 interaction occurs independently of WWP1. Thus, WWP1 engages both USP9X (partially) and DVL2 (primarily) via non-exclusive WW-PY interactions while DVL2 and USP9X exhibit the ability to interact independently of WWP1 (**FIG 3.1I**).

3.3.3 WWP1 and USP9X establish a ubiquitin rheostat on DVL2

DVL2 was previously reported to be a substrate of several NEDD4 family E3 ubiquitin ligases including ITCH, NEDD4L, and NEDL1 (Ding et al., 2013; Miyazaki et al., 2004; Narimatsu et al., 2009; Nethe et al., 2012; Wei et al., 2012) although both positive and negative regulation of DVL2 by NEDD4 family members has been reported. However, WWP1 has not previously been reported to regulate DVL2. Given the physical associations between WWP1 and DVL2 we hypothesized that DVL2 might be subject to ubiquitin conjugation by the E3 activity of WWP1. We found that recombinant WWP1 exhibited ubiquitin conjugation activity toward HA-tagged DVL2 (purified from human STF-293 cell lysates) (**FIG 3.3A** and **FIG 3.4A-B**) and this activity is lost in a lysine-deficient variant of DVL2 (*dvl2-K0*, **FIG 3.4C**). Importantly, we also found that USP9X can reverse the ubiquitylation of DVL2 by WWP1 (**FIG 3.3B**), indicating that DVL2 is a substrate for both WWP1 and USP9X. Strikingly, the K48-specific deubiquitylase OTUB1 and the K63-specific deubiquitylase AMSH did not exhibit activity towards

WWP1-ubiquitylated DVL2 (**FIG 3.3B**), suggesting that WWP1-conjugated ubiquitin on DVL2 is unlikely to contain K63- or K48- linked polymers.

Since WWP1 and USP9X both interact with and operate on DVL2, we hypothesized that the coordination of WWP1 E3 ubiquitin ligase activity and USP9X deubiquitylase activity might serve to establish a ubiquitin rheostat on DVL2. To test this, we incubated DVL2 with different molar ratios of WWP1 and USP9X and analyzed the outcome. Importantly, we found that different molar ratios of WWP1 and USP9X affected the extent of ubiquitylation on DVL2 (**FIG 3.3C-D**, **3.4D** and **3.4E**). These findings indicate that coordinated WWP1 and USP9X activities can establish a ubiquitin rheostat on DVL2.

3.3.4 USP9X promotes canonical WNT activation

Given the established function of DVL2 as a key signal transducing protein in the WNT pathway and given that NEDD4 family members have been reported to negatively regulate WNT signaling (Tanksley et al., 2013) potentially via ubiquitylation of DVL2 (Ding et al., 2013), we decided to test if USP9X regulates WNT signaling. We found that knockdown or knockout of *usp9x* attenuated WNT activation as measured by a TopFLASH reporter assay (**FIG 3.5A** and **3.6A**) and by β–catenin stabilization (**FIG 3.5A**). The WNT signaling defect observed in *usp9x* knockout cells was complemented by transient expression of wildtype FLAG-USP9X but not a catalytic dead (C1556V, or

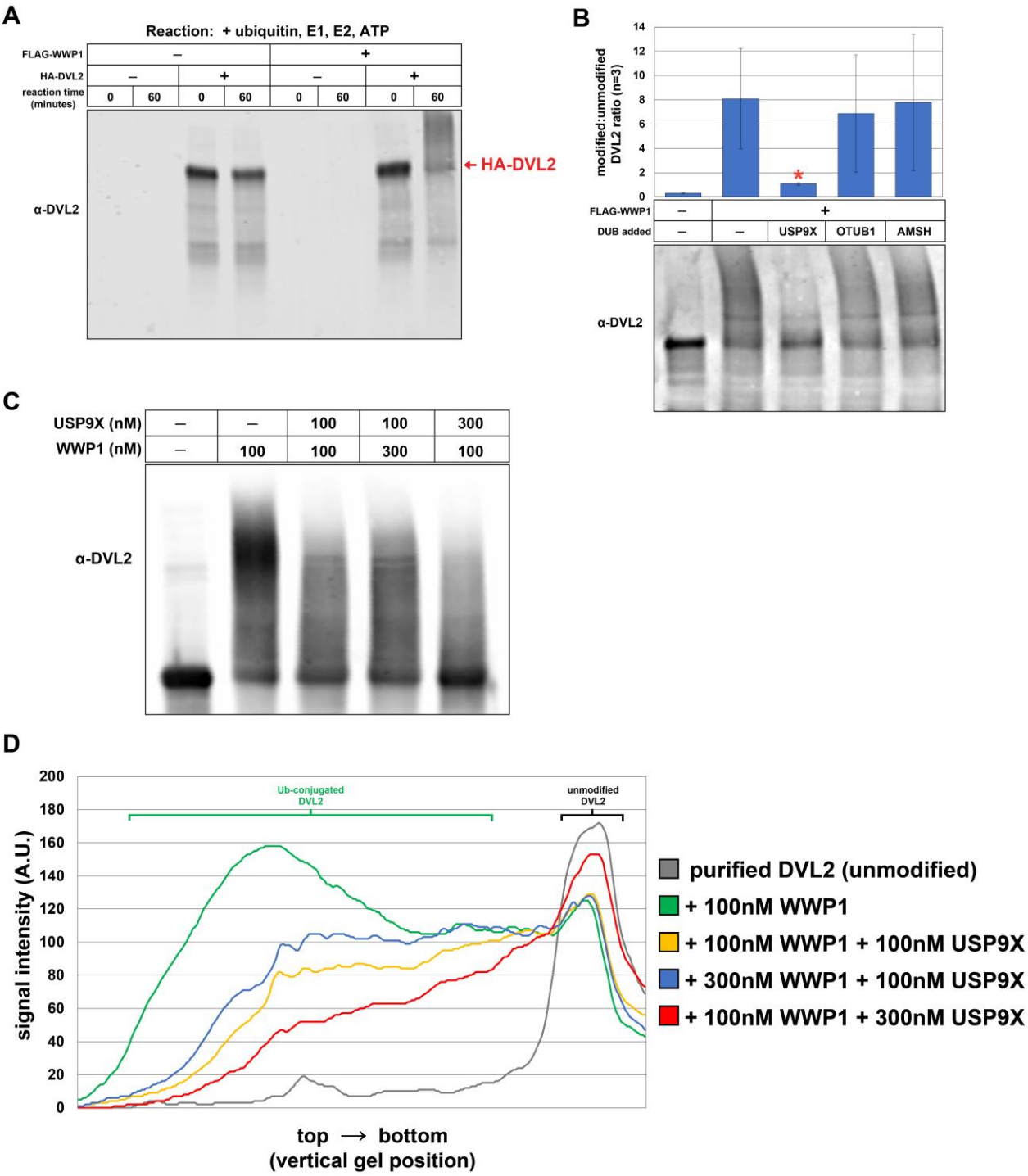

FIGURE 3.3 WWP1 and USP9X operate on DVL2 to establish a ubiquitylation rheostat. **(A)** *In vitro* ubiquitylation reactions were performed using recombinant purified FLAG-WWP1 (60nM) and HA-DVL2 purified from cultured cells. E3 conjugation reactions were allowed to proceed for 60 minutes before the conjugation reaction was terminated. **(B)** Deconjugation assays were performed using HA-DVL2 ubiquitylated *in vitro* by WWP1 (as generated in **(A)**). Equivalent molar ratios of USP9X, OTUB1 and AMSH (100nM)

were added and each reaction was allowed to proceed for 60 minutes before the deconjugation reaction was terminated and HA-DVL2 was resolved by SDS-PAGE and immunoblot (bottom panel). For each sample, a ratio of modified:unmodified HA-DVL2 was measured using ImageJ. The modified:unmodified HA-DVL2 ratio was averaged over multiple replicate experiments (n=3). The red asterisk indicates a statistically significant difference ($p<0.05$) compared to DVL2 that has been modified by WWP1 and subsequently treated with OTUB1 or AMSH. **(C)** Representative immunoblot of *in vitro* ubiquitylation/deubiquitylation reactions (replicate experiments shown in **FIG 3.4D-E**). Experiments were performed using indicated combinations of purified FLAG-WWP1 and 6xHIS-USP9X with HA-DVL2 purified from cultured cells (see **FIG 3.4A-B**). Reactions were allowed to proceed for 60 minutes before being terminated and HA-DVL2 was resolved by SDS-PAGE and immunoblot. **(D)** Line density plots from the HA-DVL2 immunoblot data in **(C)** illustrate differences in extent of ubiquitylation in each sample. Replicate experiments are shown in **FIG 3.4D-E**.

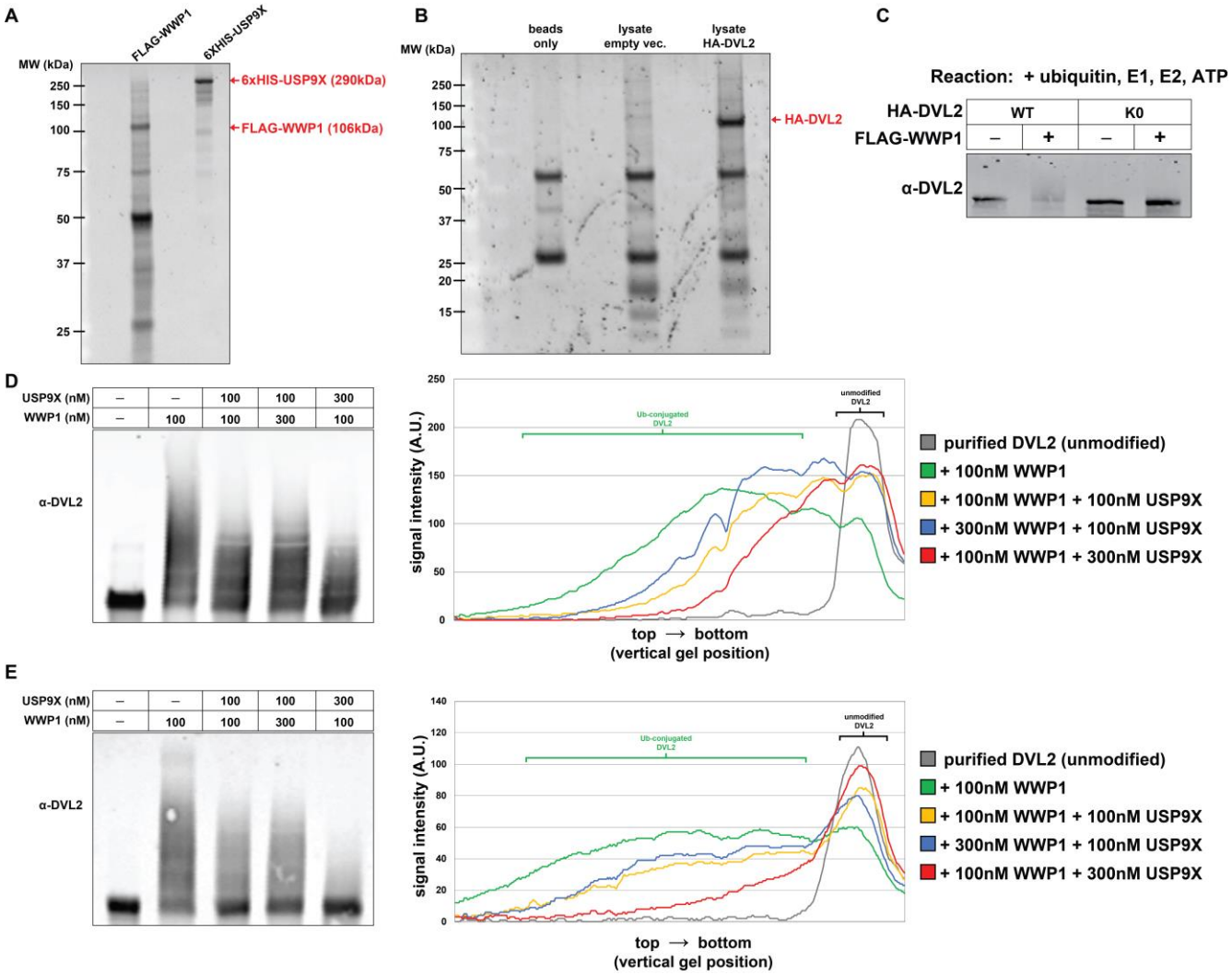

FIGURE 3.4 Analysis of WWP1 and USP9x activity toward DVL2 *in vitro*. **(A)** Purity of recombinant FLAG-WWP1 and 6XHIS-USP9X used in *in vitro* conjugation/deconjugation reactions (FIG 3.3) shown by SYPRO Ruby gel staining. **(B)** Purity of HA-DVL2 (purified from cultured cells) used in *in vitro* conjugation/deconjugation reactions (FIG 3.3) shown by SYPRO Ruby gel staining. **(C)** *In vitro* ubiquitylation reactions were performed using recombinant purified FLAG-WWP1 (60nM) and HA-DVL2 (wildtype and K0, a variant where all lysine residues are mutated to arginine) purified from cultured cells. E3 conjugation reactions were allowed to proceed for 60 minutes before the conjugation reaction was terminated. **(D-E, left panels)** Biological replicates of *in vitro* ubiquitylation rheostat reaction shown in FIG 3.3C-D, experiments were performed using indicated combinations of purified FLAG-WWP1 and 6XHIS-USP9X with HA-DVL2 purified from cultured cells. Reactions were allowed to proceed for 60 minutes before reaction was terminated and HA-DVL2 was resolved by SDS-PAGE and immunoblot. (**D-E, right panels**) Quantification of HA-DVL2 ubiquitylation under indicated conditions using ImageJ line profile analysis of immunoblot.

CD) variant (**FIG 3.5B**), indicating that catalytic activity of USP9X is required for canonical WNT activation. Furthermore, we found that treating cells with WP1130, a small molecule known to inhibit the deubiquitylase activity of USP9X (Kapuria et al., 2010), inhibited canonical WNT activation by WNT3a with an IC_{50} of 2.9μM (**FIG 3.5C**). This result is consistent with our findings that USP9X is required for canonical WNT activation, however WP1130 is known to target other deubiquitylases (USP24, USP5, USP14, and UCH37) (de Las Pozas et al., 2018; Kapuria et al., 2010; Kushwaha et al., 2015; Peterson et al., 2015). Thus, we cannot exclude the possibility that inhibition of multiple DUB activities drives loss of WNT activation in the presence of WP1130. To further explore the possibility that USP9X activity promotes WNT activation we transiently transfected expression vectors for FLAG-USP9X (wildtype or catalytic dead) and measured WNT activation in the context of WNT3a stimulation. Importantly, we found that transient expression of wildtype FLAG-USP9X, but not a catalytic-dead variant, resulted in increased activation of the canonical WNT pathway (**FIG 3.5D**).

We hypothesized that loss of canonical WNT activation in the absence of USP9X may be due to unchecked activity of WWP1 or other NEDD4 family E3 ubiquitin ligases. Importantly, we found that the loss of canonical WNT activation in *usp9x* knockout cells was suppressed by coordinate knockdown of WWP1 or NEDD4L but not WWP2 (**FIG 3.5E**) suggesting that hyper-activation of multiple NEDD4 family members, including NEDD4L and WWP1, may attenuate WNT signaling in the absence of USP9X. Furthermore, we found that transient overexpression of wildtype WWP1, but not a catalytic dead variant (C890S), inhibited TopFLASH activation by WNT3a (**FIG 3.6B** and **3.6C**). Unexpectedly, we also found that expression of the *wwp1-ww2* variant

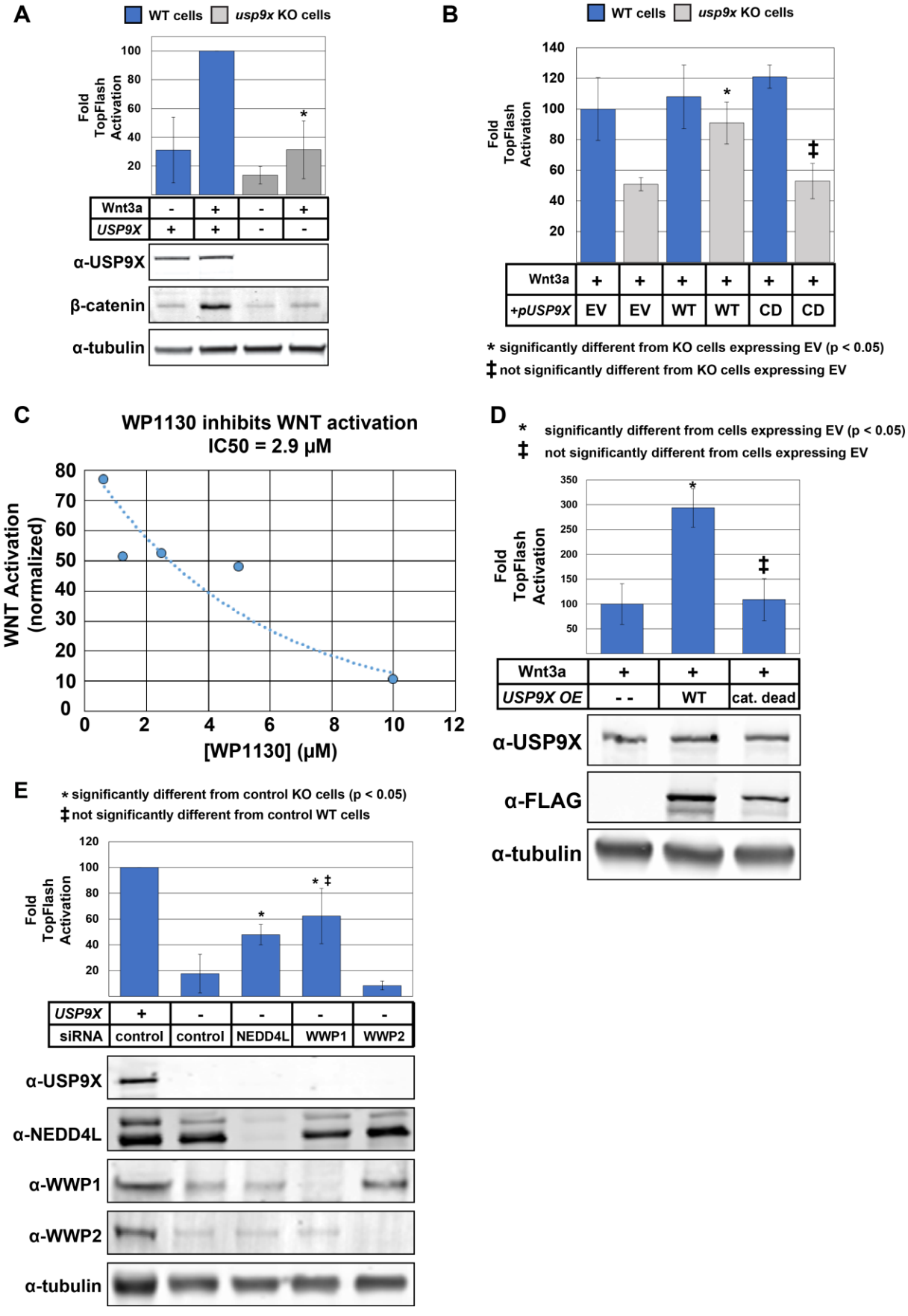
A
WT cells
usp9x KO cells
Fold TopFlash Activation
Wnt3a
USP9X
α-USP9X
β-catenin
α-tubulin
B
WT cells
usp9x KO cells
Fold TopFlash Activation
Wnt3a
+pUSP9X
EV
WT
CD
* significantly different from KO cells expressing EV (p < 0.05)
‡ not significantly different from KO cells expressing EV
C
WP1130 inhibits WNT activation
IC50 = 2.9 μM
WNT Activation (normalized)
[WP1130] (μM)
D
* significantly different from cells expressing EV (p < 0.05)
‡ not significantly different from cells expressing EV
Fold TopFlash Activation
Wnt3a
USP9X OE
WT
cat. dead
α-USP9X
α-FLAG
α-tubulin
E
* significantly different from control KO cells (p < 0.05)
‡ not significantly different from control WT cells
Fold TopFlash Activation
USP9X
siRNA
control
NEDD4L
WWP1
WWP2
α-USP9X
α-NEDD4L
α-WWP1
α-WWP2
α-tubulin

FIGURE 3.5 USP9X promotes canonical WNT activation. **(A)** Analysis of ligand-stimulated WNT activation in MDA-MB-231 cells (blue bars) and *usp9x* knockout equivalents (gray bars). TopFLASH luciferase assays were used to measure WNT activation (top panel) and immunoblotting was performed to assess stabilization of nuclear β-catenin. * indicates WNT activation in *usp9x* knockout cells is significantly decreased ($p<0.05$) compared to sibling MDA-MB-231 cells. **(B)** MDA-MB-231 cells (wildtype and *usp9x* knockout) were stimulated with WNT3a ligand and R-spondin and WNT activation was measured by TopFLASH luciferase assays. Prior to activation, cells were transiently transfected with empty vector (EV) or vector expression USP9X (wildtype (WT) or catalytic dead (CD; C1566V)). One-way ANOVA; *$p<0.05$ **(C)** Ligand-stimulated WNT activation was measured in the presence of indicated concentrations of WP1130. Based on the data an IC50 was estimated. **(D)** MDA-MB-231 cells were transfected with empty vector or plasmids for CMV-driven expression of wildtype (WT) or catalytic dead USP9X. One-way ANOVA; *$p<0.05$ **(E)** Ligand-stimulated WNT activation was measured using TopFLASH luciferase assays for MDA-MB-231 cells and *usp9x* knockout equivalents. Cells were transfected with control siRNA or siRNA targeting knockdown of NEDD4L, WWP1 or WWP2. One-way ANOVA; *$p<0.05$

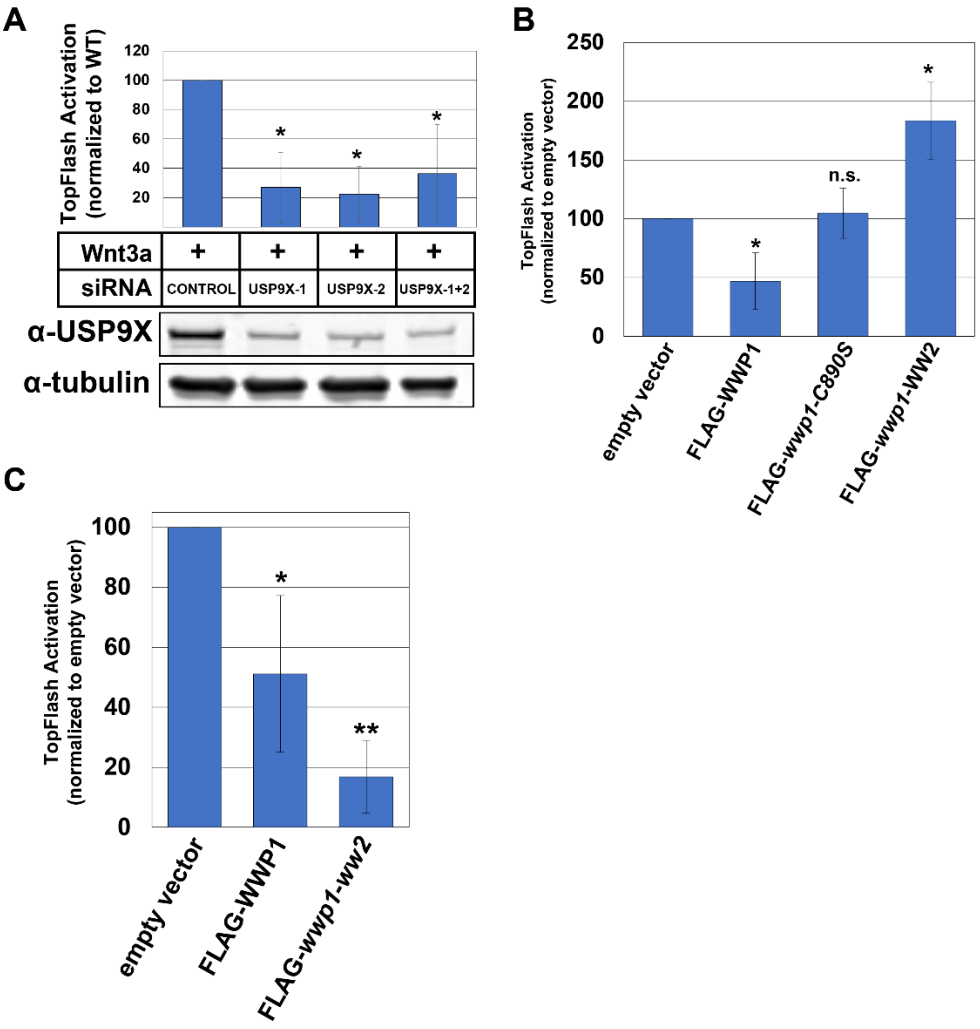

FIGURE 3.6 USP9X and WWP1 regulate canonical WNT activation. **(A)** Analysis of ligand-stimulated WNT activation in the presence of control siRNA or siRNAs targeting USP9X knockdown. TopFLASH luciferase assays were used to measure WNT activation (top panel) and immunoblotting was performed to assess knockdown efficiency (bottom panel). The asterisk indicates significant difference compared to control siRNA treatment ($p<0.05$). **(B)** TopFLASH activation of STF-293 cells transfected with empty vector or plasmids for CMV-driven expression of wildtype (WT) FLAG-WWP1, *wwp1-C890S* (a catalytic dead variant) or *wwp1*-WW2 (a variant with only WW2 intact) (see **FIG 3.1E** and **3.1F**). The asterisk indicates a statistically significant difference compared to the empty vector control ($p<0.05$) while n.s. indicates no significant difference compared to the empty vector control. **(C)** TopFLASH activation of STF-293 cells transfected with empty vector or plasmids for CMV-driven expression of wildtype (WT) FLAG-WWP1 or a *ww2* mutant variant (see **FIG 3.2C** and **3.2D**). One-way ANOVA; Single asterisk indicates statistically significant difference compared to empty vector control ($p<0.05$), while double asterisk indicates statistically significant difference compared to both empty vector control and wildtype WWP1 overexpression ($p<0.005$).

(harboring point mutations in WW2) inhibited canonical WNT activation to a greater extent that wildtype WWP1 (**FIG 3.6C**) while expression of the *wwp1*-WW2 variant (where all WW domains are disrupted except for WW2) exhibited hyperactivation of canonical WNT in the presence of WNT3a (**FIG 3.6B**). Thus, ability of WWP1 to antagonize canonical WNT activation correlates with its ability to bind DVL2 (**FIG 3.1E-F** and **3.2C-D**). Taken together, these findings indicate that USP9X promotes canonical WNT activation while WWP1 antagonizes canonical WNT activation.

3.3.5 USP9X regulation of WNT requires DVL2 deubiquitylation

Given our finding that WWP1 and USP9X interact with and operate on DVL2, we hypothesized that USP9X regulates canonical WNT activation by affecting the ubiquitylation status of DVL2. To address the mechanism of canonical WNT regulation by USP9X, we first tested if USP9X is required for β-catenin stabilization by LiCl – an inhibitor of GSK3. Importantly, LiCl-mediated stabilization did not require USP9X (**FIG 3.8A**), indicating USP9X functions upstream of the β-catenin destruction complex. Importantly, we found that knockdown or knockout of USP9X resulted in decreased steady state abundance of DVL2 protein and mobility shifts by SDS-PAGE consistent with hyper-ubiquitylation (**FIG 3.7A** and **3.8B**). To identify post-translational modifications on DVL2 regulated by USP9X we performed a SILAC-MS on FLAG-DVL2

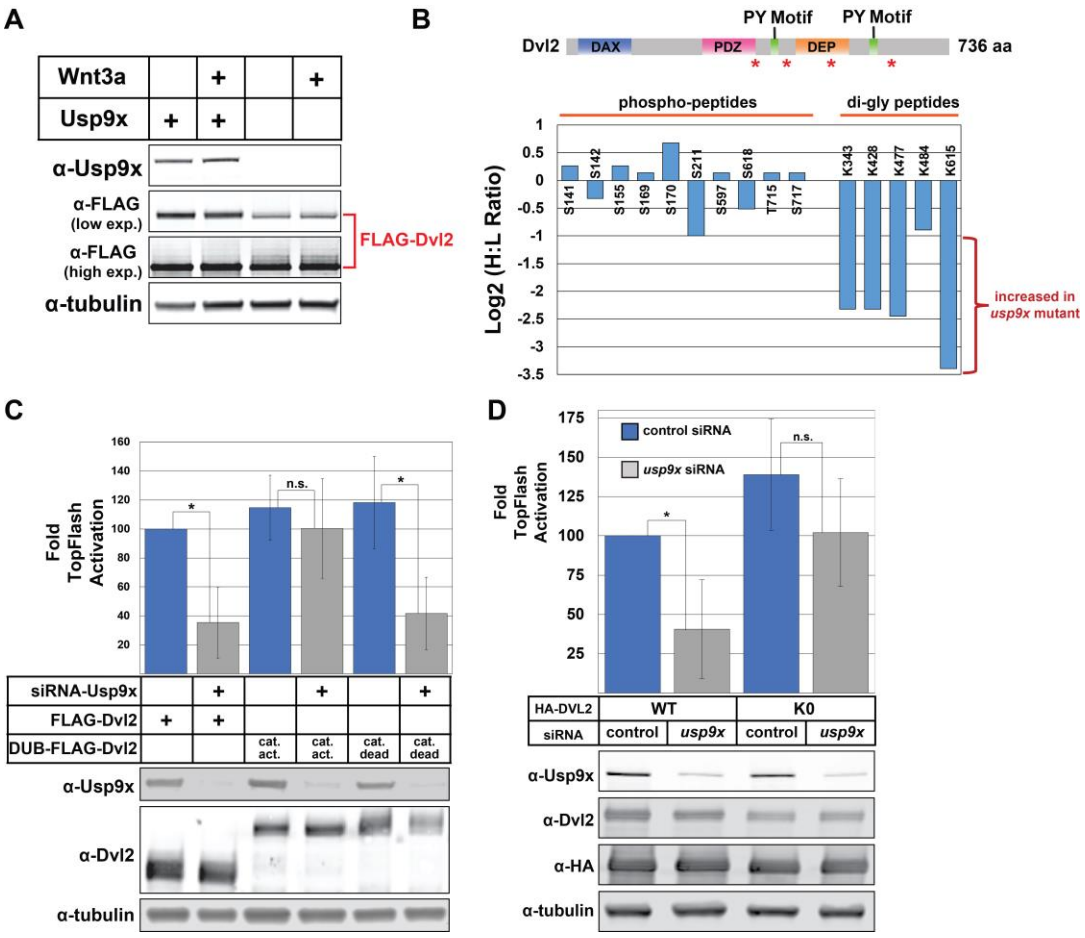

FIGURE 3.7 USP9X promotes canonical WNT activation via deubiquitylation of DVL2. **(A)** Immunoblotting analysis of FLAG-DVL2 mobility by SDS-PAGE from lysates of MDA-MB-231 cells or *usp9x* knockout equivalents. A low exposure α-FLAG blot is shown to illustrate differences in DVL2 abundance, while the higher exposure α-FLAG is shown to illustrate the higher MW species evident in *usp9X* knockout cells. **(B)** SILAC-MS profiling of post-translational modification sites (phosphorylation and ubiquitylation) on DVL2. In this experiment, FLAG-DVL2 purified from MDA-MB-231 cells (heavy) was compared to *usp9x* knockout equivalents (light). A schematic illustrating the domain structure of DVL2 is shown at the top with asterisks to indicate the position of detected ubiquitylation events. **(C)** Analysis of ligand-stimulated WNT activation was measured using TopFLASH reporter assays in STF-293 cells transfected with the indicated expression vectors. UL36 is the DUB domain fused to DVL2 in these experiments. **(D)** Following siRNA knockdown of USP9X, ligand-stimulated WNT activation was measured using TopFLASH reporter assays in STF-293 cells transfected with the indicated HA-DVL2 expression vectors. DVL2-K0 is a variant where all encoded Lys residues are substituted with Arg residues. * represents a statistically significant difference when compared to indicated sample ($p<0.05$). n.s. represents no significant difference relative to indicated comparison.

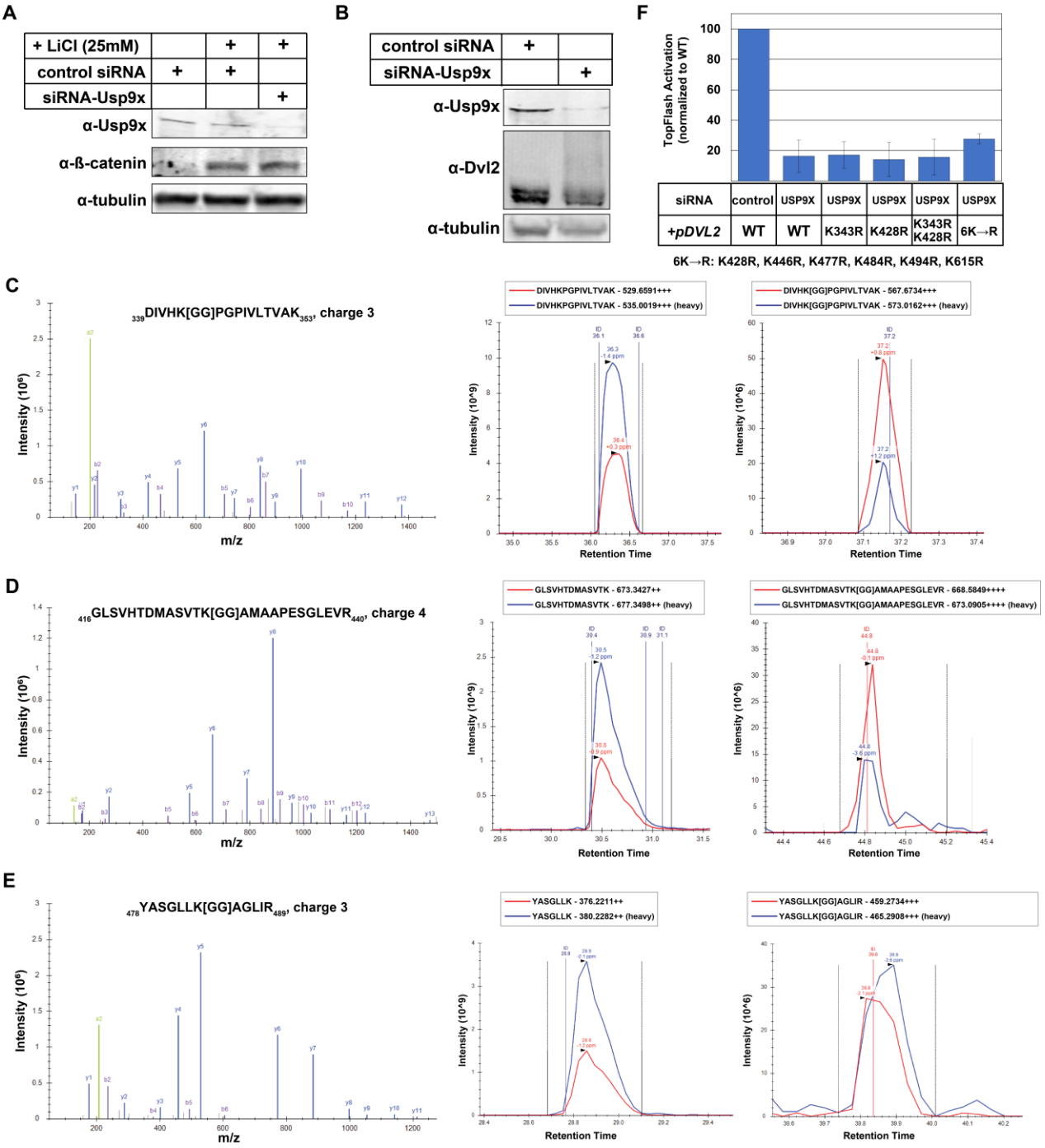

FIGURE 3.8 USP9X regulates DVL2 ubiquitylation state. **(A)** Analysis of LiCl stimulation of WNT activation following transfection with control siRNA or siRNAs targeting USP9X knockdown. Immunoblotting was performed to assess knockdown efficiency and stabilization of nuclear β–catenin. **(B)** Immunoblotting analysis of DVL2 mobility by SDS-PAGE following transfection with control siRNA or siRNAs targeting USP9X knockdown. **(C-E)** Raw data for SILAC quantification (corresponding to **FIG 3.7B**) of individual ubiquitylation events on DVL2 including diGly modification of K343 **(C)**, K428

(D) and K484 **(E)**. MS2 spectra for each diGly peptide is shown in the left panel. To the right of each MS2 spectra, chromatograms are shown for heavy and light unmodified (middle) and diGly-modified (right) peptides, illustrating the quantification of each peptide. In each case, the diGly-modified form of the peptide is significantly elevated in the light sample, which is derived from the *usp9x* mutant sample (see **FIG 3.7B**). **(F)** Functional analysis of DLV2 lysine mutants. STF-293 reporter cells were transiently transfected with the indicated FLAG-DVL2 plasmids and siRNAs and analyzed for WNT activation using the TopFLASH luciferase assay.

affinity purified from MDA-MB-231 cells and *usp9x* knockout equivalents. This analysis resolved many phospho-peptides and ubiquitin remnant (diGly) peptides derived from DVL2 with four internal lysines exhibiting elevated ubiquitylation in the absence of USP9X (**FIG 3.7B** and **FIG 3.8C-E**). Although ubiquitylation at N-terminal lysines of DVL2 has been reported (Madrzak et al., 2015; Tauriello et al., 2010) the ubiquitin modification events described in this study (K343, K428, K477 and K615) have not previously been reported.

To test if USP9X-mediated regulation of WNT signaling requires DVL2 ubiquitylation we expressed DVL2 fused to the UL36 DUB domain (from human herpes virus) and found that this (but not a catalytic dead UL36 fusion) suppressed the WNT activation defect in the absence of USP9X (**FIG 3.7C**). These results indicate that USP9X regulates WNT signaling at (or in very close proximity to) the level of DVL2. To explore the possibility that USP9X-mediated deubiquitylation of DVL2 at specific sites is required for WNT activation we tested a panel of DVL2 lysine mutants (K343R, K429R, K477R and K615R) but found expression of these mutants was insufficient to suppress the WNT signaling defect observed in the absence of USP9X (**FIG 3.8F**). We next considered the possibility that USP9X may regulate multiple ubiquitylation events on DVL2, as suggested by SILAC-MS analysis (**FIG 3.7B**). Importantly, we found that expression of a “lysine-less” DVL2 variant with all encoded lysine residues switched to arginine (DVL2-K0) is sufficient to restore WNT activation in the absence of USP9X (**FIG 3.7D**). Taken together, these results indicate that increased ubiquitylation of DVL2 is required for the attenuation of WNT signaling observed in the absence of USP9X. Thus, the USP9X-mediated deubiquitylation of DVL2 is critical for activation of canonical

WNT signaling.

3.3.6 DVL2 ubiquitylation status regulates interactions with canonical and WNT-PCP factors

We hypothesized that the altered ubiquitylation status of DVL2 in the absence of USP9X regulates its function as a signal transduction protein. To test this hypothesis, we first characterized the DVL2 interaction network in MDA-MB-231 cells using SILAC-MS (**Table 3.2, Table 3.3,** and **FIG 3.9A**). These experiments revealed two near-stoichiometric interactions with the AP-2 clathrin adaptor complex and with the non-canonical WNT factors VANGL1 and cofilin which are known to participate in the planar cell polarity (PCP) pathway (Luga et al., 2012). Additionally, we identified several sub-stoichiometric interactions with NEDD4 family E3 Ub ligases and proteasome subunits (**Table 3.2, Table 3.3,** and **FIG 3.9A**). Many of these interactions had been previously reported (Angers et al., 2006; Yu et al., 2007). Several interactions were confirmed by co-IP (**FIG 3.9B**) and co-localization by immunofluorescence microscopy (**FIG 3.10A**). Consistent with previous reports (Yu et al., 2007; Yu et al., 2010) we also found that knockdown of AP-2 complex subunits inhibited canonical WNT activation in a TopFLASH assay (data not shown).

To quantify how DVL2 interactions are affected by ubiquitylation, we performed SILAC-MS proteomic analysis comparing the interaction profile of catalytic active (light) or catalytic dead (heavy) UL36-DVL2 fusions (also used in **FIG 3.7C**). This revealed that catalytic dead UL36-DVL2 fusion (which can be stably ubiquitylated) interacts more with

Category	protein	known function / description	pept. count	H:L ratio	stoich. (norm.)
Bait	DVL2	WNT pathway signaling protein	29	28.70	1.00
AAA ATPase	ATAD3A	mitochondria-localized AAA ATPase of unknown function	18	8.58	0.72
	ATAD3B		14	**	0.55
endocytosis	AP2M1	AP2 clathrin adpator complex	10	19.79	0.58
	AP2B1		19	8.83	0.51
	AP2A1		18	37.89	0.47
	AP2S1		2	10.99	0.36
	AP2A2		8	**	0.22
	EPS15L1	endocytic adaptor proteins; sort ubiquitylated cargo for endocytosis	3	**	0.09
	EPS15		2	**	0.06
signaling	VANGL1	WNT-PCP signaling protein	5	**	0.24
	DVL3	WNT pathway signaling protein	5	**	0.18
	DVL1		4	**	0.15
	CK1delta	kinase; regulates canonical WNT activation	2	**	0.12
	WDR26	signal transduction protein	2	13.00	0.08
	RANBP9	signal transduction protein	2	**	0.07
ubiquitin proteasome system	NEDD4L	NEDD4 family E3 ubiquitin ligase	4	22.38	0.10
	PSD11	proteasome subunits	2	5.58	0.12
	PSA7		2	36.59	0.20
cytoskeleton	Cofilin-1	regulator of actin dynamics	3	5.70	0.46

TABLE 3.2 DVL2 Interaction Profile using SILAC-MS
Light: MDA-MB-231 cells stably expressing pQCXIP (empty vector)
Heavy: MDA-MB-231 cells stably expressing FLAG-DVL2
Selection Criteria: (1) number of peptides quantified ≥ 2; (2) H:L ratio > 5
** indicates signal in heavy channel but no signal in light channel

category	Protein	known function / description	pept. count	H:L ratio	stoich. (norm.)
bait	DVL2	WNT pathway signaling protein	43	107.20	1.00
AAA ATPase	ATAD3B	mitochondria-localized AAA ATPase of unknown function	15	**	0.40
	ATAD3A		25	62.37	0.67
endocytosis and trafficking	AP2B1	AP2 clathrin adaptor complex	49	52.27	0.90
	AP2M1		17	43.41	0.67
	AP2A1		38	60.82	0.67
	AP2S1		5	71.38	0.60
	AP2A2		30	27.94	0.55
	CAVIN1	caveolae formation and organization	10	18.36	0.44
	CAVIN2		8	**	0.32
	SQSTM1	autophagy receptor	10	10.15	0.39
	EPS15L1	endocytic adaptor proteins; sort ubiquitylated cargo for endocytosis	7	6.31	0.14
	EPS15		2	**	0.04
signaling	VANGL1	WNT-PCP signaling protein	13	**	0.42
	CK1 delta	casein kinase isoforms; regulate canonical WNT activation	17	**	0.70
	CKII beta		7	**	0.56
	CK1 epsilon		12	**	0.49
	CKII alpha		9	**	0.39
	PLK1	polo-like kinase-1	16	**	0.45
	DVL3	WNT pathway signaling protein	15	**	0.36
	RANBP9	signal transduction protein	15	**	0.35
	WDR26	signal transduction protein	13	74.44	0.34
ubiquitin proteasome system	NEDD4L	NEDD4 family E3 ubiquitin ligase	29	35.38	0.51
	WWP2		12	**	0.24
	WWP1		3	**	0.06
	PSA7	proteasome subunits	2	**	0.14
	PRS10		3	**	0.13
	PSA1		2	**	0.13
	PSD11		2	**	0.08
transcription	FOXK2	transcriptional regulators	18	**	0.47
	FOXK1		13	**	0.30
protein folding	BAG3	co-factor for HSP70	14	**	0.42

TABLE 3.3 DVL2 Interaction Profile in WNT-activated cells using SILAC-MS
Light: MDA-MB-231 cells stably expressing pQCXIP (empty vector) stimulated with 200ng/mL mouse-Wnt3a and 100ng/mL mouse-Rspondin
Heavy: MDA-MB-231 cells stably expressing FLAG-DVL2 stimulated with 200ng/mL mouse-Wnt3a and 100ng/mL mouse-Rspondin
Selection Criteria: (1) number of peptides quantified ≥ 2; (2) H:L ratio > 5
** indicates signal in heavy channel but no signal in light channel

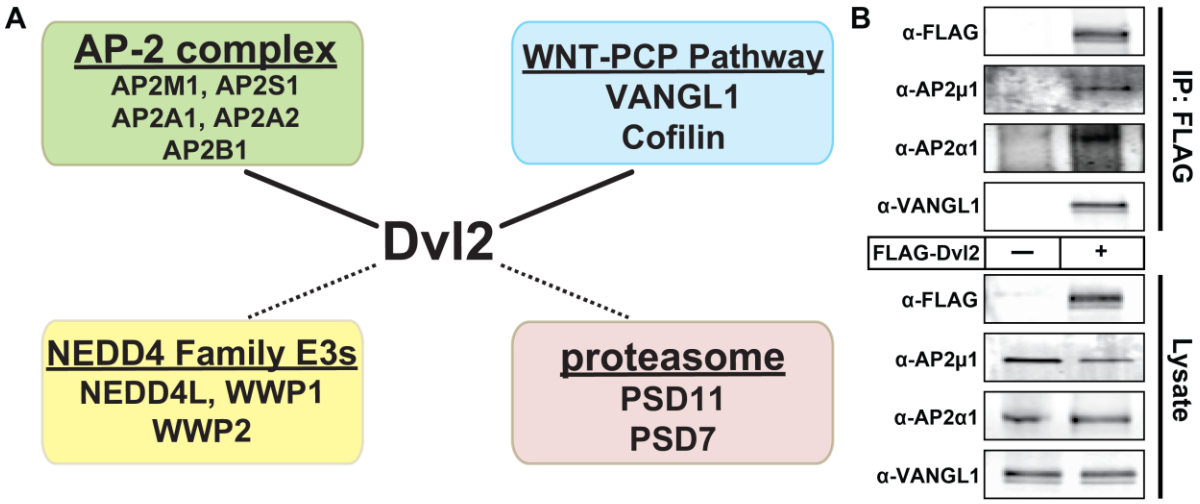
A
AP-2 complex
AP2M1, AP2S1
AP2A1, AP2A2
AP2B1
WNT-PCP Pathway
VANGL1
Cofilin
Dvl2
NEDD4 Family E3s
NEDD4L, WWP1
WWP2
proteasome
PSD11
PSD7
B
α-FLAG
α-AP2μ1
α-AP2α1
α-VANGL1
IP: FLAG
FLAG-Dvl2
—
+
α-FLAG
α-AP2μ1
α-AP2α1
α-VANGL1
Lysate

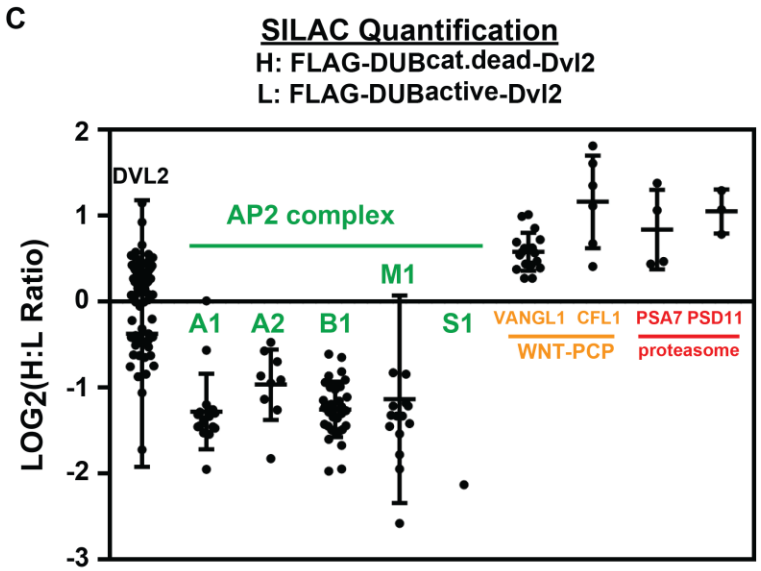
C
SILAC Quantification
H: FLAG-DUBcat.dead-Dvl2
L: FLAG-DUBactive-Dvl2
LOG2(H:L Ratio)
2
1
0
-1
-2
-3
DVL2
AP2 complex
A1
A2
B1
M1
S1
VANGL1
CFL1
WNT-PCP
PSA7
PSD11
proteasome

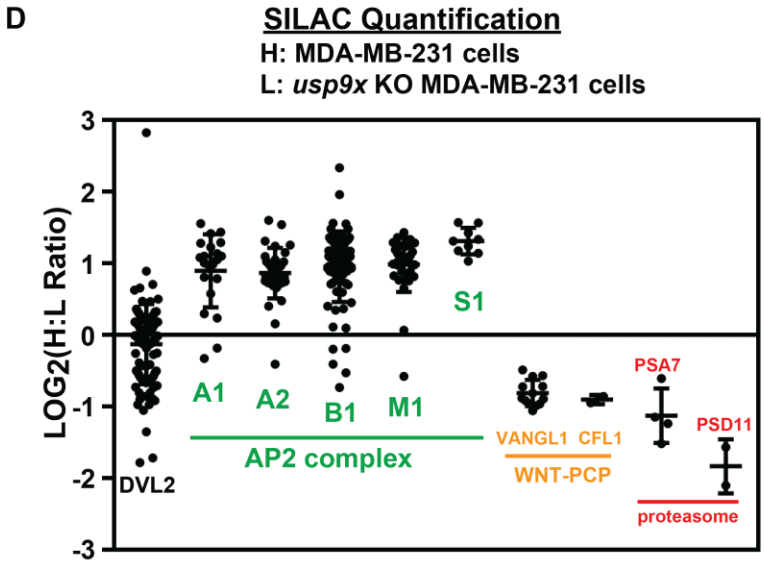
D
SILAC Quantification
H: MDA-MB-231 cells
L: usp9x KO MDA-MB-231 cells
LOG2(H:L Ratio)
3
2
1
0
-1
-2
-3
DVL2
A1
A2
B1
M1
S1
AP2 complex
VANGL1
CFL1
WNT-PCP
PSA7
PSD11
proteasome

FIGURE 3.9 DVL2 ubiquitylation state specifies association with canonical WNT or WNT-PCP pathway factors. **(A)** SILAC-MS was used to resolve the DVL2 interaction network in MDA-MB-231 human breast cancer cells. Near-stoichiometric interactions (solid lines) were detected with the AP-2 clathrin adaptor complex and VANGL1-cofilin, which comprise a subcomplex of the WNT-PCP pathway. Sub-stoichiometric interactions (dotted lines) were identified for NEDD4 family E3 ubiquitin ligases and proteasome subunits. **(B)** Interactions detected by SILAC-MS were confirmed by coimmunoprecipitation. **(C and D)** SILAC-MS analysis was performed to measure how DVL2 interactions are impacted by catalytic active vs. catalytic dead DUB fusion **(C)** or by loss of *USP9X* **(D)**. Scatter plots depict individual H:L measurements (LOG_2 transformed) for each peptide resolved for the indicated proteins. The mean value and standard deviation for each protein is indicated. For the experiment shown in **(C)**, several peptides with extremely low H:L ratios are not depicted here but are shown in **FIG 3.10B**. These outlier peptides correspond to sites of ubiquitin modification (**FIG 3.10C**) shown in **FIG 3.7B**. Differences between DVL2 (bait) and all interacting proteins (AP2 complex, VANGL1, CFL1, and proteasome subunits) are statistically significant ($p<0.005$).

A

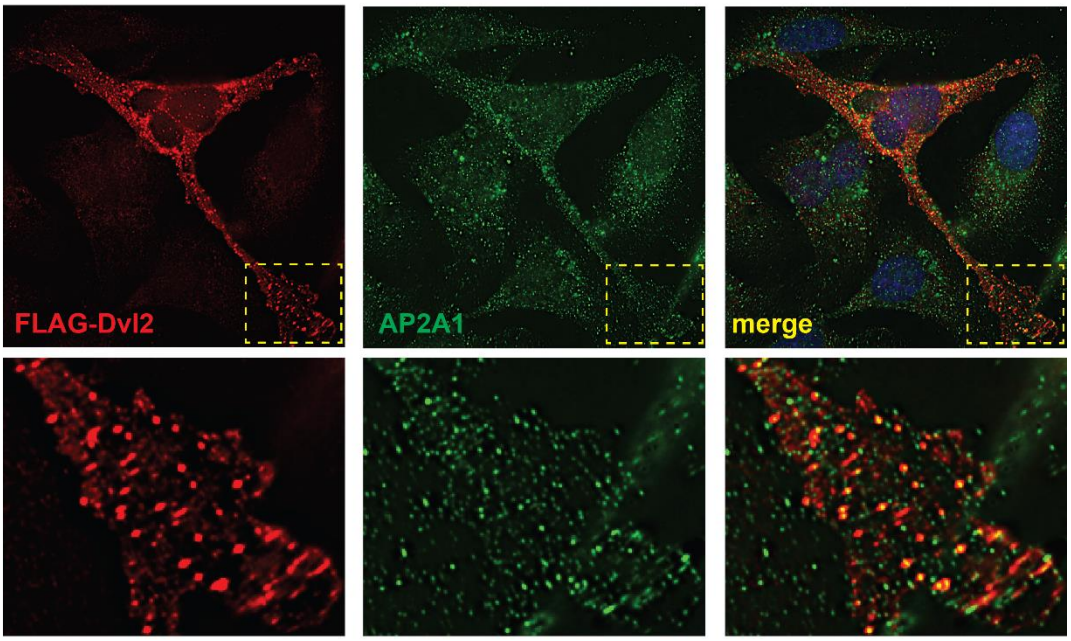

B

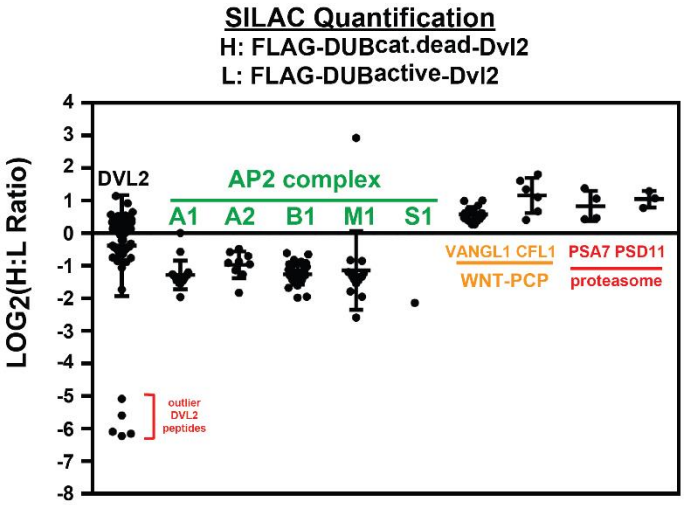

C

Outlier Peptides

Peptide	H:L ratio (normalized)
$_{416}$GLSVHTDMASVTK$_{428}$	0.014791
$_{416}$GLSVHTDMASVTK$_{428}$	0.017268
$_{429}$AMAAPESGLEVR$_{440}$	0.015015
$_{477}$KYASGLLK$_{484}$	0.023585
$_{616}$SGSGSESEPSSR$_{627}$	0.04083

FIGURE 3.10 DVL2 ubiquitylation regulates interactions. **(A)** Immunofluorescence microscopy analysis was performed on MDA-MB-231 breast cancer cells expressing FLAG-DVL2. **(B)** Expanded graph of SILAC-MS analysis in **FIG 3.9C** showing outlier DVL2 peptides**. (C)** Description of outlier DVL2 peptides shown in **(B)** with corresponding normalized H:L ratio.

proteasome subunits and VANGL1/cofilin while the catalytic active UL36-DVL2 fusion (which is not stably ubiquitylated) interacts more with the AP-2 complex (**FIG 3.9C**). Importantly, we noticed in this experiment a small set of peptides derived from the DVL2-UL36 catalytic active fusion protein and absent from the DVL2-UL36 catalytic dead fusion protein (**FIG 3.10B**). Interestingly, these outlier peptides all correspond to tryptic events that can only occur in the absence of ubiquitylation (at positions K428, K477 and K615) (**FIG 3.10C**) indicating that these sites are largely ubiquitin-modified in the DVL2-UL36 catalytic dead fusion protein. We also used SILAC-MS to quantify how DVL2 interactions are altered in *usp9x* knockout cells and found similar results: DVL2 interacted more with VANGL1 and cofilin in *usp9x* knockout cells (where DVL2 ubiquitylation is elevated) but interacted more with AP-2 in the presence of USP9X (where DVL2 is less ubiquitylated) (**FIG 3.9D**). These results indicate ubiquitylated DVL2 interacts more with VANGL1/cofilin – components of the WNT-PCP pathway – while deubiquitylated DVL2 interacts more with the AP-2 complex, which is critical for canonical WNT activation.

3.3.7 USP9X regulates cellular distribution of DVL2 and antagonizes WNT-PCP

Previous studies have reported that VANGL1 and cofilin localize to F-actin rich projections in migrating MDA-MB-231 cells (Hatakeyama et al., 2014) and that DVL2 is required for WNT5a-induced cell migration in these cells (Zhu et al., 2012). Based on our findings that loss of USP9X results in increased ubiquitylation of DVL2 and increased interactions between DVL2 and VANGL1/cofilin we hypothesized that loss of USP9X may result in re-localization of DVL2 to actin-rich projections in MDA-MB-231

cells. To test this, we used immunofluorescence microscopy to characterize FLAG-DVL2 distribution in MDA-MB-231 cells in the presence or absence of USP9X. In MDA-MB-231 cells treated with control siRNAs, DVL2 exhibited a punctate distribution throughout the cell body, reflective of previous descriptions of DVL2 localization (**FIG 3.11A, top panels**) (Schwarz-Romond et al., 2005) whereas MDA-MB-231 siUSP9X knockdown cells displayed a redistribution of DVL2 to actin-rich projections (**FIG 3.11A, middle panels**). Quantification of the cellular distribution of DVL2 in the presence and absence of USP9X reveals a significant increase in DVL2 in actin-rich projections upon loss of USP9X (**FIG 3.11B**). Importantly, coordinate knockdown of WWP1 prevented this re-distribution of DVL2, indicating that WWP1 activity is required for re-distribution of DVL2 to actin-rich projections in the absence of USP9X (**FIG 3.11A, bottom panel** and **FIG 3.11B**). Thus, our data indicates that USP9X promotes DVL2 localization to puncta that also contain AP-2 (**FIG 3.10A**), while loss of USP9X activity results in WWP1-dependent re-distribution of DVL2 to actin-rich projections in MDA-MB-231 breast cancer cells.

One feature of WNT5a-mediated PCP activation is Rho activation, which is DVL2-dependent and required for induction of cell migration by the WNT-PCP pathway (Zhu et al., 2012). Given our findings, we hypothesized that DVL2 re-distribution to actin-rich projections in MDA-MB-231 cells lacking USP9X might result in Rho activation. Indeed, we found that MDA-MB-231 cells normally exhibit about 35% of maximal Rho activation, while cells lacking USP9X exhibit 50% maximal Rho activation (**FIG 3.11C-D**). Taken together, these findings indicate that loss of USP9X in MDA-MB-231 cells results in re-distribution of DVL2 to actin-rich projections and Rho activation,

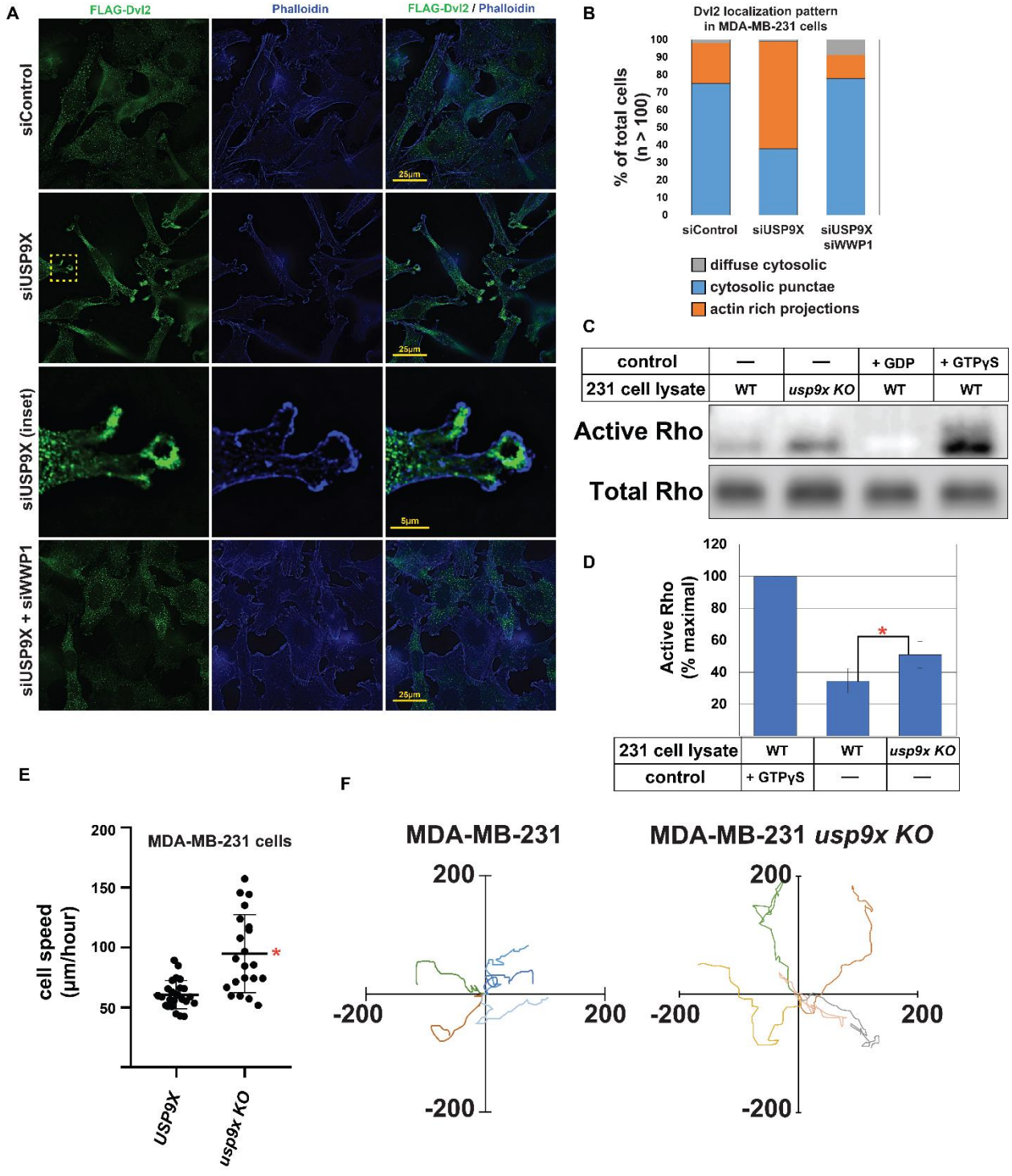

FIGURE 3.11 USP9X regulates DVL2 localization and antagonizes WNT-PCP activation. **(A)** Immunofluorescence imaging of FLAG-DVL2 (green) and actin (phalloidin, blue) in MDA-MB-231 human breast cancer cells transfected with control siRNA (top panels), siRNA targeting USP9X (middle panels), or a combination of siRNA targeting USP9X and siRNA targeting WWP1 (bottom panels). **(B)** Quantification of DVL2 cellular distribution over a population of MDA-MB-231 cells (n > 100). **(C)** WT

MDA-MB-231 and *usp9x* KO variant cell lysates were assayed for active Rho by pulldown assay. Addition of GDP or non-hydrolyzable GTP (GTPɣS) to cell lysates served as negative and positive controls, respectively. **(D)** Quantification of Rho activation shown in **FIG 3.11C** (n=3) was performed by measuring the amount of active Rho detected in parent and *usp9x* knockout cells and normalizing to the GTPγS (maximal activation) control. The red asterisk indicates a significant difference when compared to WT cells ($p<0.05$) **(E)** MDA-MB-231 cells were plated at low density and cell migration (µm/hour) speed was measured. Red asterisk indicates a significant difference between the tested populations (n>30). **(F)** Rose plots showing trajectories of individual MDA-MB-231 cells (left) and *usp9x* knockout equivalents (right).

which is similar to what occurs during WNT5a-mediated activation of the WNT-PCP pathway in these cells (Luga et al., 2012; Zhu et al., 2012).

3.3.8 USP9X regulates cell motility in a manner dependent on DVL2 ubiquitylation

VANGL1, cofilin, and DVL2 are known to coordinate WNT-PCP activation to regulate actin dynamics and promote cell motility, migration and metastasis of MDA-MB-231 cells (Katoh, 2005; Luga et al., 2012; Yang and Mlodzik, 2015; Zhu et al., 2012). Based on these previous studies, we hypothesized that USP9X-mediated regulation of DVL2 may antagonize WNT-PCP-mediated cellular motility. Strikingly, we found that MDA-MB-231 breast cancer cells lacking USP9X exhibited a significant increase in motility compared to wildtype equivalents (**FIG 3.11E-F**). This increase in cell motility was complemented in cells transiently transfected with GFP-USP9X (**FIG 3.12A**). Consistent with this observation, we also found that treatment of MDA-MB-231 cells with WP1130 – a small molecule inhibitor of USP9X – also resulted in a significant increase in the speed of cell motility (**FIG 3.12B**). Importantly, the increased cell speed observed in *usp9x* knockout cells was dependent on VANGL1 (**FIG 3.12C**) indicating the increased motility phenotype requires an intact WNT-PCP pathway. To test if the increase cell motility observed in *usp9x* mutant cells was due to increased autocrine signaling, we treated cells with LGK974, a porcupine inhibitor that blocks the secretion of many WNT ligands, and found this had no effect on the speed of usp9x knockout MDA-MB-231 cells (**FIG 3.12D**). Taken together, these results indicate that loss of USP9X leads to aberrant activation of PCP-mediated motility independent of autocrine signaling.

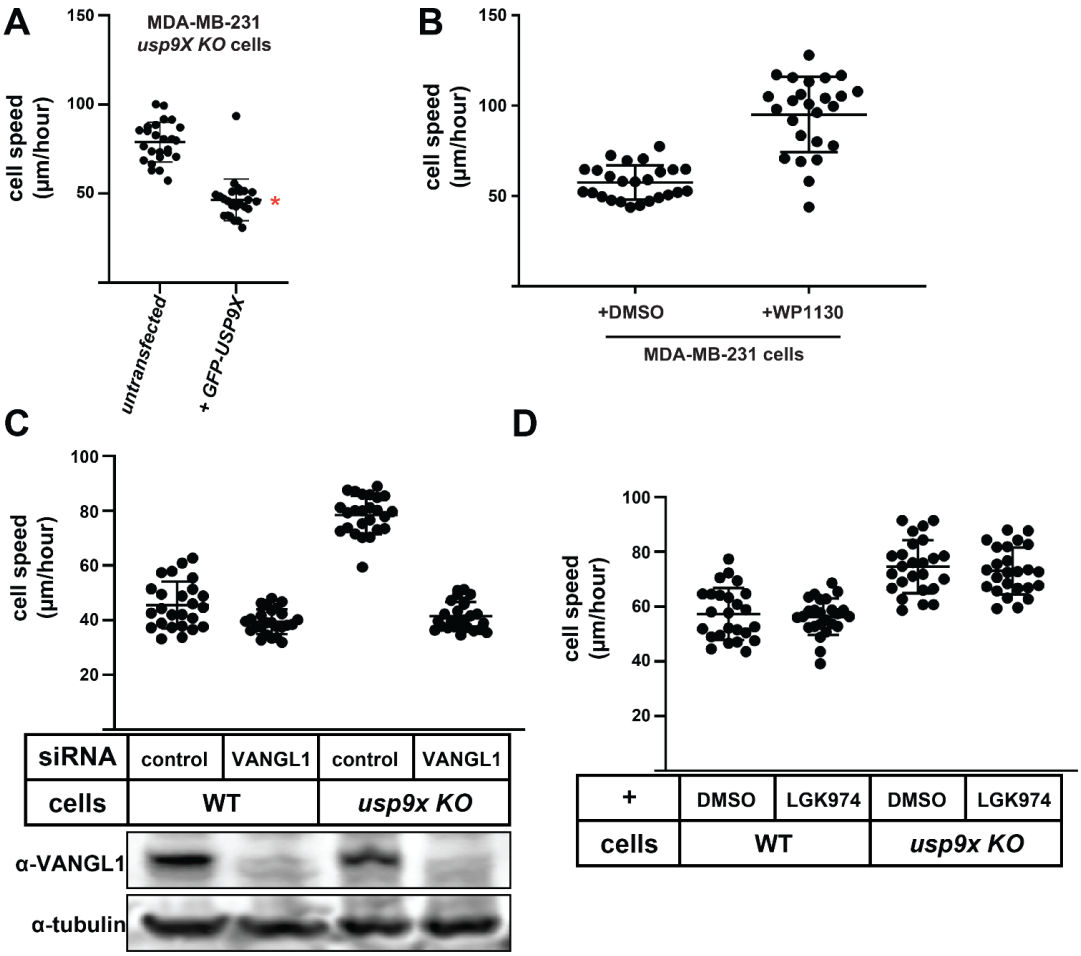

FIGURE 3.12 USP9X antagonizes cell motility. **(A)** The indicated MDA-MB-231 cell lines were transiently transfected with a GFP-USP9X expression vector and cell migration speed was measured for untransfected and transfected (GFP-positive) cells (n=25). The red asterisk represents a statistically significant difference compared to untransfected *usp9x* KO cells. **(B)** Migration speed of MDA-MB-231 cells was measured after treatment with DMSO control or WP1130 (300nM). There is a statistically significant difference when comparing cell speed after WP1130 treatment to DMSO-treated control ($p<0.005$). **(C)** Migration speed of MDA-MB-231 cells was measured after treating with control siRNA or siRNA targeting VANGL1. There was a statistically significant difference ($p<0.05$) in cell speed with VANGL1 knockdown when compared to control siRNA treatment in the indicated cell lines. Bottom panel: Corresponding immunoblots confirming VANGL1 knockdown with siRNA treatment. **(D)** Migration speed of indicated MDA-MB-231 cells after treatment with DMSO control or LGK974 (1nM). There was no significant difference with LGK974 treatment when compared to DMSO control in indicated cell types.

We hypothesized that the elevated ubiquitylation of DVL2 might contribute to the increased motility phenotype observed in usp9x knockout MDA-MB-231 cells. Consistent with this hypothesis, we observed that knockdown of WWP1 suppressed the increased motility phenotype of *usp9x* knockout cells (**FIG 3.13A**), although transient overexpression of WWP1 did not alter speed of MDA-MB-231 cells (**FIG 3.14A**). Notably, MDA-MB-231 cells transiently expressing GFP-DVL2 did not exhibit any change in cell motility compared to untransfected control cells (**FIG 3.14B**), however expression of either wildtype or lysine-deficient (K0) GFP-DVL2 fully suppressed the increased motility phenotype of *usp9x* knockout MDA-MB-231 cells (**FIG 3.14C-D**). This result implicates DVL2 as a mediator of the cell motility phenotype observed for *usp9x* knockout cells, but it does not inform as to the role of ubiquitylation since both wildtype and lysine-deficient DVL2 fully suppress the *usp9x* knockout phenotype. To test the role of ubiquitylation, we analyzed cell motility of MDA-MB-231 cells stably expressing DVL2-UL36 (catalytic active and catalytic dead) DUB fusion proteins. Strikingly, we found that knockdown of *USP9X* resulted in increased motility of control cells and cells expressing catalytic dead DVL2-UL36 fusions, but not of cells expressing catalytic active DVL2-UL36 fusions (**FIG 3.13B).** This result reveals that the increased motility phenotype observed in the absence of *USP9X* requires increased ubiquitylation of DVL2. Finally, we tested if DVL2 ubiquitylation is required for WNT5a-induced cell motility in MDA-MB-231 cells. Interestingly, we found that expression of catalytic active DVL2-UL36 resulted in a significant dampening of WNT5a-induced cell motility

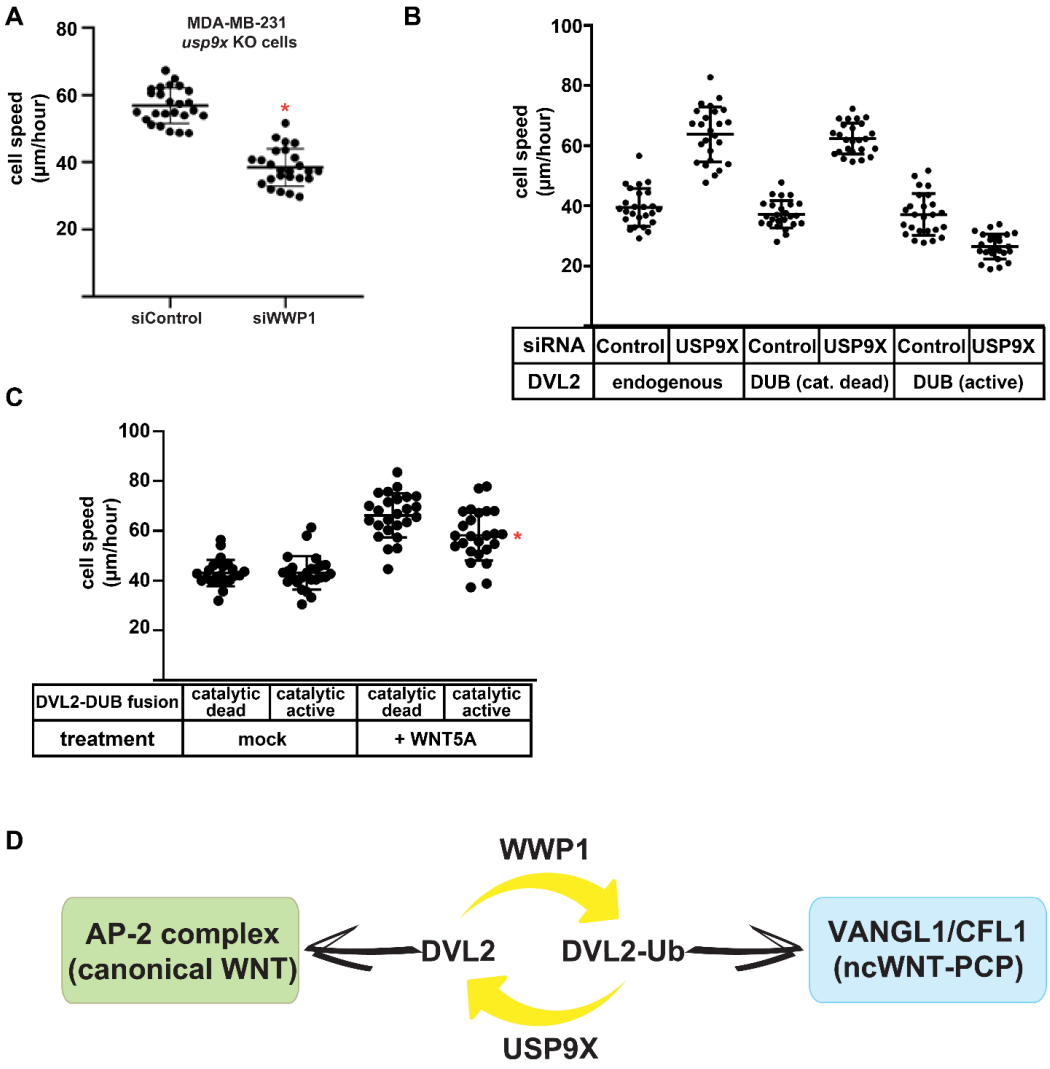

FIGURE 3.13 USP9X-mediated regulation of cell motility requires DVL2 ubiquitylation. **(A)** Migration speed of MDA-MB-231 *usp9x* KO cells treated with either control siRNA or siRNA targeting WWP1 was measured after plating at low density for the indicated conditions. Red asterisk indicates a significant difference compared to control siRNA treated cells ($p<0.005$). **(B)** MDA-MB-231 cell lines stably expressing DVL2-DUB fusions (catalytic active and catalytic dead) were treated with control siRNA or siRNA targeting USP9X and cell speed was measured for 25 cells. **(C)** MDA-MB-231 cell lines stably expressing DVL2-DUB fusions (catalytic active and catalytic dead) underwent mock or WNT5a treatment and cell speed was measured for 25 cells. The red asterisk indicates a statistically significant difference ($p<0.005$) compared to MDA-MB-231 cells stably expressing the catalytic dead DUB-DVL2 fusion treated with WNT5a. **(D)** Model for DVL2 regulation by the USP9X-WWP1 axis to establish a ubiquitin rheostat on DVL2 that influences interaction preference with either the clathrin adaptor AP-2 complex, which is important for canonical WNT signaling, or the VANGL1-cofilin complex, which is important for the WNT-PCP pathway. Thus, the USP9X-WWP1 axis regulates DVL2 ubiquitylation to determine WNT pathway specification.

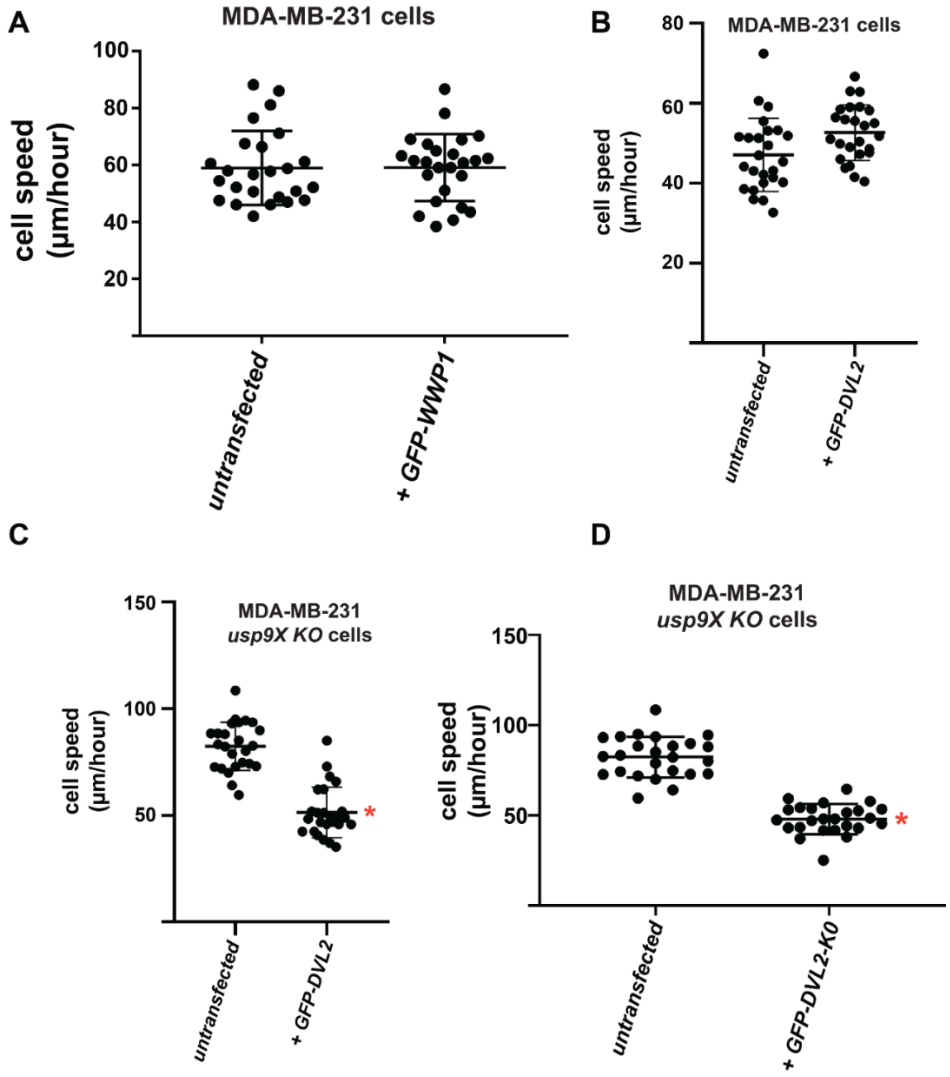

FIGURE 3.14 DVL2 expression suppresses the motility phenotype of *usp9x* knockout cells. **(A)** The indicated MDA-MB-231 cell lines were transiently transfected with a GFP-WWP1 expression vector and cell migration speed was measured for untransfected and transfected (GFP-positive) cells (n=25). There was no significant difference relative to untransfected cells. **(B-C)** The indicated MDA-MB-231 cell lines were transiently transfected with a GFP-DVL2 expression vector and cell migration speed was measured for untransfected and transfected (GFP-positive) cells (n=25). Red asterisk indicates a statistically significant difference ($p<0.005$) when compared to untransfected control in the indicated cell line (n=25). **(D)** The indicated MDA-MB-231 cell lines were transiently transfected with a GFP-DVL2-K0 (a construct in which all lysines have been mutated to arginines) expression vector and cell migration speed was measured for untransfected and transfected (GFP-positive) cells (n=25). Red asterisk indicates a significant difference ($p<0.005$) when compared to untransfected control in the indicated cell line (n=25).

compared to control cells expressing catalytic dead DVL2-UL36, although the observed inhibition was partial (**FIG 3.13C**). These results indicate that USP9X is a critical antagonist of PCP activation and cell motility in MDA-MB-231 cells and that this function is dependent on the ubiquitylation of DVL2. Based on our findings, we propose that the balance of USP9X and WWP1 activities toward DVL2 regulates WNT pathway specification, with USP9X-mediated DVL2 deubiquitylation promoting canonical WNT signaling and WWP1-mediated DVL2 ubiquitylation driving WNT-PCP activation and cell migration (**FIG 3.13D**).

3.4 Discussion

Dishevelled has long been known to play a key role in the transduction of WNT receptor signaling, yet how it is regulated to specify participation in either canonical or non-canonical signaling relays is not well understood. Here, we report that the NEDD4 family E3 ubiquitin ligase WWP1 interacts with DVL2 and the deubiquitylase USP9X, and that these interactions govern a ubiquitylation rheostat on DVL2 critical for both canonical WNT and WNT-PCP activation. Specifically, we have shown that **(I)** USP9X-mediated deubiquitylation of DVL2 promotes canonical WNT activation by enhancing DVL2 interaction with the clathrin adaptor complex AP-2, **(II)** Hyper-ubiquitylation of DVL2 that occurs in the absence of USP9X drives increased DVL2 interaction with WNT-PCP factors VANGL1 and Cofilin and relocalization of DVL2 to actin-rich projections, **(III)** USP9X limits cellular Rho activation and antagonizes noncanonical WNT-PCP activation, **(IV)** USP9X antagonizes cell motility in a WWP1-dependent manner, and **(V)** USPX-mediated regulation of cell motility requires DVL2 ubiquitylation. Based on the

data, we propose that the USP9X-WWP1 axis biases DVL2 engagement with either the canonical WNT pathway or the noncanonical WNT-PCP pathway.

3.4.1 A regulatory axis for WNT pathway specification

The functional diversity of WNT signaling is a result of the complex network design that inter-weaves canonical and non-canonical elements to coordinate multiple specific signaling outputs. Thus, it is important to understand the network design features that couple canonical and non-canonical pathways and contribute to pathway specificity. The role of USP9X in WNT pathway specification draws parallels to diversin, an ankyrin repeat protein also implicated in WNT pathway specification. Knockout of diversin in mice resulted in defective WNT-PCP signaling but hyper-activated signaling through the canonical WNT pathway (Allache et al., 2015; Jones et al., 2014) – phenotypes that are opposite to *usp9x* knockout but suggest a similar mode of pathway coupling. Importantly, diversin has also been reported to be overexpressed in breast cancer cells and contributes to both proliferation and invasion (Yu et al., 2014). Shared use of certain signaling factors - like dishevelled and diversin - between canonical and non-canonical WNT pathways may facilitate mechanisms of pathway specification based on inverse coupling – effectively operating as a “zero sum game”. For example, if a shared component like dishevelled or diversin is limiting for pathway activation then engagement by one pathway may consequently prevent activation of the coupled pathway. Thus, regulatory mechanisms that impact stability of shared factors or their interaction networks have strong potential to contribute to pathway specification.

DVL2 has been reported to undergo both positive and negative regulation by the

ubiquitin system through the action of multiple different E3 ubiquitin ligases and deubiquitylating enzymes. For example, both ITCH and NEDD4L have been shown to negatively regulate DVL2 stability by conjugating K48-linked polyubiquitin chains on DVL2, targeting it to the proteasome for degradation (Ding et al., 2013; Liu et al., 2014a; Marikawa and Elinson, 1998; Mukai et al., 2010; Tauriello et al., 2010; Wei et al., 2012). On the other hand, K63-linked polyubiquitin modifications of the DVL2 DIX domain were reported to enhance canonical WNT activation (Tauriello et al., 2010) while other reports have suggested these modifications may antagonize canonical WNT activation (Madrzak et al., 2015). The apparent regulation of DVL2 by multiple members of the NEDD4 family could result from functional redundancy, but could also reflect differential regulation based on expression in different contexts or different cell types. Our finding that siRNA targeting of NEDD4L or WWP1 partially rescued WNT activation in the absence of USP9X (**FIG 3.5E**) is consistent with a redundancy model, but it does not exclude the possibility that USP9X antagonizes multiple exclusive ubiquitylation events on DVL2 mediated by different E3 ubiquitin ligases. Indeed, our data indicates that functional regulation of DVL2 by USP9X involves reversal of multiple distinct ubiquitylation events (**FIG 3.7B**) – possibly mediated by multiple E3 ubiquitin ligases - since no single K→R mutation was capable of suppressing the loss of WNT activation phenotype observed in the absence of USP9X (**FIG 3.8F**). Furthermore, the *in vitro* analysis of USP9X activity presented here suggests that USP9X may be unique in its ability to operate on WWP1-ubiquitylated DVL2, and that it may have activity toward atypical ubiquitin polymers (**FIG 3.3B-D**). These results are consistent with a recent study of USP9X structure and activity that reported a strong preference for K11-linked

polyubiquitin chain substrates (Paudel et al., 2019). Although our studies indicate that these ubiquitylation events on DVL2 are important for WNT pathway specification, data presented here do not address the specific polyubiquitin linkage types involved or the contribution of other NEDD4 family ligases. Therefore, additional biochemical and genetic studies will be required to fully elucidate how USP9X operates on distinct ubiquitin modifications on DVL2 that may be mediated by multiple E3 ubiquitin ligases, and how the sum of these activities contribute to the ubiquitin rheostat on DVL2 and WNT pathway specification.

Previous studies have reported conflicting roles for USP9X with respect to canonical WNT activation. Specifically, USP9X has previously been reported to positively regulate the stability of β-catenin in glioma cells (Yang et al., 2016). However, USP9X was also reported to negatively regulate the stability of β-catenin in mouse neural progenitor cells (Premarathne et al., 2017). Our studies are consistent with a positive role for USP9X in canonical WNT pathway activation and our data indicate that USP9X functions upstream of the destruction complex (**FIG 3.8A**). Although our findings are consistent with a role for USP9X in the regulation of WNT at the level of DVL2 we cannot exclude the possibility of a context-dependent role for USP9X at other tiers of the WNT pathway. Furthermore, it is possible that expression of different NEDD4 family members, other USP9X-interactors, or substrate adaptors and targeting factors could modify USP9X function in a context-specific manner.

Previous studies reported that Wnt5a-mediated activation of the WNT-PCP pathway in human breast cancer cells causes increased cell migration as a result of DVL2/Daam1-dependent activation of RhoA (Zhu et al., 2012). While a role for DVL2 in

regulation of WNT-PCP and migration was evident, a role for USP9X in WNT-PCP and migration had not been clearly defined. Data presented here suggest that USP9X and WWP1 interact to provide fine-tuned regulation of DVL2 ubiquitylation state in order to regulate DVL2 localization to actin-rich projections, Rho activation, and motility in breast cancer cells. These studies address how ubiquitylation of DVL2 influences activation of the canonical and non-canonical WNT pathways, but they do not address how activation of WNT and WNT-PCP by WNT3a and WNT5a (respectively) may impact DVL2 ubiquitylation status. Future studies will be required to determine if WNT pathway activation contributes to the ubiquitin rheostat on DVL2, perhaps functioning to tune DVL2 ubiquitylation and provide regulatory feedback.

3.4.2 USP9X: a complex factor in cancer

Given that USP9X has been implicated in the regulation of multiple receptor signaling and trafficking pathways, it is not surprising that in recent years USP9X dysregulation has been linked to many different types of cancers. USP9X has been suggested to exhibit oncogenic behavior in some cancer contexts including multiple myeloma, melanoma, lung cancer, and breast cancer (Kushwaha et al., 2015; Li et al., 2017; Potu et al., 2017; Schwickart et al., 2010). In contrast, USP9X has also been proposed to have tumor suppressor activity in other cancers including pancreatic ductal adenocarcinoma (Pérez-Mancera et al., 2012) and colorectal adenocarcinoma (Khan et al., 2018). Recently, USP9X has been shown to be required for the attenuation of EGFR signaling (Savio et al., 2016) which is suggestive of a tumor suppressor function. Taken together, these reports suggest a complex role for USP9X in cancer progression that

may be highly context-dependent. Our findings suggest that USP9X functions together with WWP1 to regulate a ubiquitin rheostat on DVL2. The ubiquitylation status of DVL2 determines its engagement with either canonical or non-canonical WNT factors. Based on these findings we hypothesize that in some cellular contexts increased USP9X activity may sensitize cells to activation of the canonical WNT pathway (**FIG 3.5D**), which promotes proliferation and tumor growth, while simultaneously antagonizing the non-canonical WNT-PCP pathway which is involved in cell motility and metastasis (**FIG 3.11C-F**). These results indicate that dysregulation of USP9X can function to promote canonical WNT-driven proliferation while simultaneously guarding against migration and metastasis mediated by the WNT-PCP pathway. Based on these findings, we propose that small molecule inhibitors of USP9X may be effective as antagonists of WNT-based proliferation (**FIG 3.5C**) but they may also ultimately promote migration and metastasis (**FIG 3.12B**).

3.4.3 Regulation of cell signaling pathways by DUB-E3 interactions

The ubiquitin proteasome system contributes to the tight spatial and temporal regulation of protein trafficking, localization, and stability. Recently, several examples of interactions between E3 ubiquitin ligases and DUBs have been reported, raising questions about the regulatory significance and design logic of such interactions. In principle, DUB-E3 interactions could facilitate a number of useful design features, including E3 antagonization, E3 deubiquitylation, or polyubiquitin chain editing on substrates. E3 antagonization has the potential to result in a futile cycle, but coordinated regulation of ligase and DUB activities could also establish a ubiquitin rheostat on a

shared substrate. Such a rheostat has been reported to occur in the context of ER quality control machinery, where DUB activities can sharpen the distinction between folded and misfolded membrane proteins (Zhang et al., 2013). Another striking example involves the DUB USP7, which was shown to interact with the MAGE-L2-TRIM27 E3 ubiquitin ligase to regulate the ubiquitylation status of WASH, a shared substrate, on the endosome (Wu et al., 2014). Interestingly, USP7 has been reported to interact with multiple E3 ubiquitin ligases (Kim and Sixma, 2017) but the functional significance of many of these interactions remain unclear. E3-DUB interactions have also been reported to protect E3 ubiquitin ligases from degradation, thus promoting E3 activity. For example, the DUB USP19 promotes cellular proliferation by stabilizing KPC1 (also known as RNF123), a ubiquitin ligase for the cyclin-dependent kinase inhibitor p27Kip1 (also known as CDKN1B) (Lu et al., 2009). A striking example of polyubiquitin chain editing occurs with the protein A20, a potent inhibitor of the NFkB signaling pathway that contains both a DUB domain and an E3 ubiquitin ligase domain (Wertz et al., 2004). The DUB domain of A20 removes a K63-linked polyubiquitin chain from the Receptor Interacting Protein (RIP), a protein essential for NFkB signaling. Subsequently, the E3 ubiquitin ligase domain of A20 conjugates a K48-linked polyubiquitin chain to RIP targeting it for degradation by the proteasome - thus inhibiting the NFkB pathway. Thus, there are numerous examples of E3-DUB interactions that establish ubiquitin rheostats on substrates, protect and stabilize E3 ubiquitin ligases, and coordinate activities to achieve polyubiquitin chain editing in signaling complexes.

We have identified an E3-DUB interaction that functions to provide layered regulation of the WNT pathway. Our results indicate that the activities of WWP1 and

USP9X are antagonistic and function to establish a ubiquitin rheostat on DVL2 that is a critical regulator of WNT pathway specification. Functionally, USP9X antagonizes WWP1 activity towards DVL2 (**FIG 3.3C-D**), although our data cannot exclude the possibility that WWP1-USP9x interactions function in a chain-editing capacity on polyubiquitinated DVL2. Ultimately, rigorous biochemical analysis dissecting mechanisms that regulate the balance of different ubiquitylation and deubiquitylation activities toward DVL2 will be critical to understand how its specification for either canonical or noncanonical WNT signaling pathways is determined.

CHAPTER 4

Biochemical Characterization of a Ubiquitin Rheostat on DVL2

4.1 Summary

In **Chapter 3** of this thesis I reported that USP9X and WWP1 regulate a ubiquitin rheostat on DVL2. My findings reveal that USP9X-mediated deubiquitylation of DVL2 is required for canonical WNT activation, while increased DVL2 ubiquitylation is associated with localization to actin-rich projections and activation of the planar cell polarity (PCP) pathway. However, several biochemical details remain to be elucidated; (i) The lysine residues of DVL2 modified and regulated by the USP9X-WWP1 axis, (ii) the linkage specificity of both USP9X and WWP1 toward DVL2, and (ii) how NEDD4L, and possibly other NEDD4 family members, contribute to the ubiquitin rheostat on DVL2.

Here, I further investigate the activities associated with this ubiquitin rheostat on DVL2 and I also characterize the activity of NEDD4L toward DVL2. While previous results indicated that both WWP1- and NEDD4L-mediated ubiquitylation contribute to USP9X-mediated regulation of the WNT pathway (**Chapter 3**, **FIG 3.5E**), here I show that these E3s exhibit differential polyubiquitin linkage specificity toward DVL2. I also examine in further detail the activities of USP9X both *in vitro* and in cells. Altogether, these findings have important implications for our understanding of how ubiquitin can function as a rheostat in cells

4.2 Introduction

The word *rheostat* comes from the merging of the Greek word *rheos* (“a flowing stream”) and the English word *stat* (“a regulating device”). It is not surprising that a word whose origin evokes such vivid imagery has been used to describe the complex mechanism of tuning a single input signal to elicit multiple different outputs. The term *rheostat* was originally used in 1843 by the English inventor Charles Wheatstone to describe the tuning of electrical currents through a circuit. But since its original use, it has been used to describe many different regulatory/tuning mechanisms ranging from controlling the speed of a motor in a car to the regulation of macromolecules in a human cell.

Molecular rheostats are important for biology because some signals benefit from a tunable output rather than just a binary “on/off” response. There are many cellular contexts where a binary signal output is required such as the biochemical switches that control transitions between phases of the cell cycle (Santos and Ferrell, 2008). However, some physiological processes are better managed with a tunable response. For example, cells often respond to environmental stress with a response that is commensurate with the stress observed (Matus et al., 2008). This allows cells to respond appropriately depending on the extent of the stress rather than initiating apoptosis at the detection of any degree of stress. One example of a molecular rheostat can be found in *Neisseria meningitidis*, the bacteria that causes bacterial meningitis and septicemia. This bacteria has RNA thermometers within mRNAs that control expression of bacterial immune evasion factors in response to temperature changes (Barnwal et al., 2016). Interestingly, small increases in temperature cause the RNA structure to

gradually open up to allow progressively increased access to the ribosome binding site. These examples highlight that many factors can impart rheostatic control on a molecular mechanism. They also underscore the importance of a tunable signal in certain cellular conditions.

There are also reports of molecular rheostats that are regulated by post-translation modifications including ubiquitin. In these mechanisms, the coordinated regulation of ligase and DUB activities function to establish a ubiquitin rheostat on a shared substrate. Such a rheostat has been reported to occur in the context of ER quality control machinery, where DUB activities can sharpen the distinction between folded and misfolded membrane proteins (Zhang et al., 2013). In this mechanism, small differences in interactions between the E3 ubiquitin ligase and substrate can be amplified into greater differences in net substrate degradation.

There are additional examples of balanced activities of DUBs and E3s regulating a ubiquitin rheostat on a shared substrate. Of note, the DUB USP7 has been reported to function as a molecular rheostat which fine-tunes endosomal F-actin levels by antagonizing auto-ubiquitylation and degradation of the E3 ubiquitin ligase TRIM27 (Hao et al., 2015). This subsequently inhibits overactivation of the actin-nucleating protein WASH through directly deubiquitinating it. These studies showed that K63-linked ubiquitylation regulates WASH function as an actin-nucleating protein during endosomal protein recycling and the USP7-TRIM27 rheostat functions to tune WASH ubiquitylation and consequently, endosomal protein recycling (Hao et al., 2013; Hao et al., 2015). These studies also identified mutations of USP7 in individuals with a human neurodevelopmental disorder. In this case, mechanistic insight into the biochemical

activities of a ubiquitin rheostat revealed a promising drug target for the treatment of neurodevelopmental diseases.

In **Chapter 3** of this thesis I identified and characterized a novel ubiquitin rheostat on DVL2 that functions to regulate WNT pathway specification in breast cancer cells. Here, I characterize the biochemical features of this mechanism and address the contributions of other NEDD4 family members. This information will be important for understanding the dynamics of ubiquitin rheostats and how they can contribute to the regulation of WNT pathways.

4.3 Results

4.3.1 In-frame ubiquitin fusion to DVL2 doesn't alter canonical WNT activation

While it deubiquitylation of DVL2 drives canonical WNT activation and ubiquitylation drives noncanonical WNT-PCP activation, the types of ubiquitin modifications dictating these functions was not clear (Nielsen et al., 2019). Based on our model (**FIG 3.13D**), I hypothesized that fusion of one ubiquitin to DVL2 would inhibit canonical WNT activation. To test this, I generated a DVL2 variant with one ubiquitin fused in-frame to the C-terminus and found that transient expression of this DVL2-Ub fusion did not significantly affect WNT activation (**FIG 4.1**). Additionally, this ubiquitin fusion had no effect on DVL2 stability (**FIG 4.1**). This suggests that placement of a single ubiquitin on DVL2 is not sufficient to mimic the loss of usp9x phenotype. One caveat to interpreting this data is that in-frame fusion of ubiquitin to DVL2 is not the same as the typical isopeptide bond formed between ubiquitin and DVL2 in cells.

Furthermore, this placement of ubiquitin on the tertiary structure may differ from the placement by an E3 ubiquitin ligase. Our ability to interpret these results is also impacted by the fact that these results are preliminary and there is great variability between the three biological replicates. However, this experiment suggests that addition of a single ubiquitin to the C-terminus of DVL2 does not replicate the phenotype observed in the absence of USP9X. One interpretation is that this regulation may involve more complex polyubiquitin modifications or site-specific regulation of DVL2.

4.3.2 WWP1 ubiquitylates DVL2 at multiple lysine residues

In **Chapter 3** I identified several lysine residues of DVL2 (K343, K428, K477 and K615) that undergo increased ubiquitylation in the absence of USP9X (**FIG 3.7B**). Based on these findings, I hypothesized that WWP1-mediated ubiquitylation of DVL2 may be site-specific. To test this, I generated DVL2 variants in which ubiquitylation can only occur at one site (DVL2 variants containing only one lysine, all other lysines are mutated to arginine). Using these reagents I performed a pilot *in vitro* ubiquitin conjugation assay and found that WWP1 exhibits limited conjugation activity toward each of the single-lysine DVL2 variants (**FIG 4.2A-B**). These results suggest that restoring a single lysine in DVL2 is not sufficient to reconstitute WWP1 activity toward DVL2. While these studies are preliminary and need to be repeated, these results indicate that WWP1 likely ubiquitylates more than one lysine residue of DVL2.

Since no single lysine was sufficient to fully account for WWP1 activity, I next tested if localized groups of lysines could account for WWP1 activity. To test this I

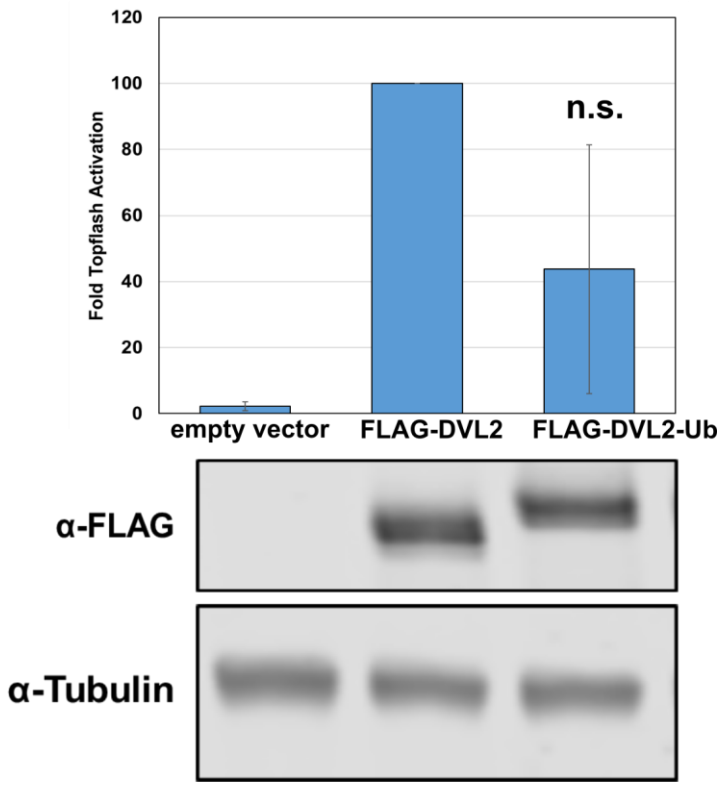

FIGURE 4.1 Effect of fusing ubiquitin to DVL2 on canonical WNT activation. Analysis of ligand-stimulated WNT activation was measured using TopFLASH reporter assays in STF-293 cells transfected with the indicated FLAG-DVL2 expression vectors. FLAG-DVL2-Ub: Expression construcut in which ubiquitin is fused to the C-terminus of DVL2. n.s. represents no significant difference relative to FLAG-DVL2 sample ($p<0.05$).

generated DVL2 variants with either only the N-terminal lysines (K15, K30, K44, K54, K58, K68, K234, K241, K274, K301, K343, K353) or only the C-terminal lysines (K428, K446, K477, K484, K494, K615) intact. Here I found that restoration of either the N-terminal or the C-terminal lysines was sufficient to fully reconstitute WWP1 activity toward DVL2 (**FIG 4.2 C-D**). These results indicate that WWP1 is hitting multiple lysines across DVL2. Further studies will be required to identify the combination of residues of DVL2 that are regulated by WWP1.

4.3.3 WWP1 activity toward DVL2 is linkage-specific

I next wanted to characterized the types of ubiquitin modifications being added to DVL2 by WWP1. I performed *in vitro* ubiquitin conjugation reactions using HA-DVL2 purified from HEK293 cells, purified recombinant WWP1, and purified recombinant ubiquitin variants that are linkage restricted (i.e. lacking every lysine except one) (**FIG 4.3**). From these experiments, I was able to draw several conclusions; **(1)** WWP1 can conjugate multiple mono-ubiquitins to DVL2 (**FIG 4.3 A,B**). This is evident from the K0 lane of **FIG 4.3A**. Using a K0 ubiquitin (a ubiquitin variant in which every lysine is mutated to arginine) ensures that only mono-ubiquitylation modification events can occur. However, I cannot exclude the possibility that linear polyubiquitin chains are being formed, although this is unlikely. In this experiment I observed a mass shift of approximately 50 kDa when using K0 ubiquitin. Since the molecular weight of one ubiquitin moiety is only 8 kDa, this indicates that multiple lysine residues (as many as 6) of DVL2 are being modified with mono-ubiquitin in this reaction. To directly test whether these modifications represent multiple monoubiquitylation events or linear polyubiquitin

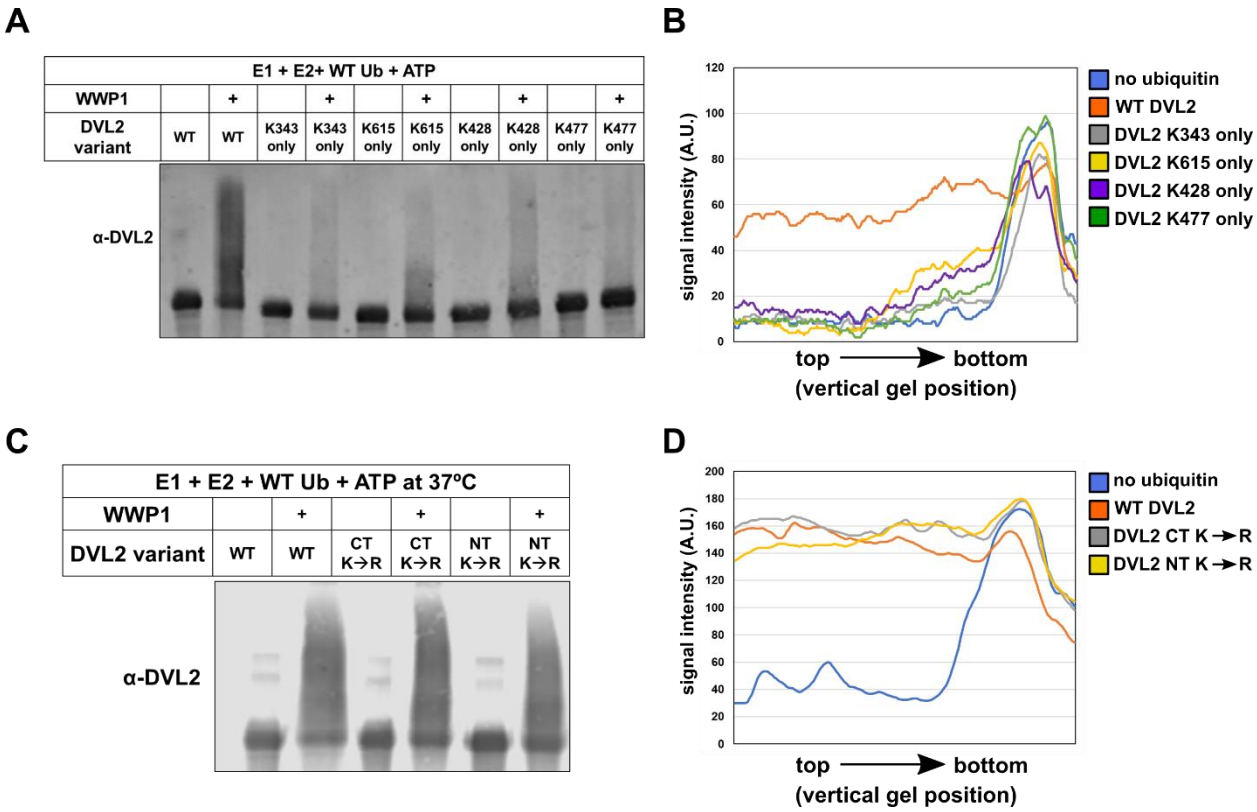

FIGURE 4.2 Analysis of polyubiquitin chain formation by WWP1 on DVL2 variants. (A) Immunoblot showing WWP1-mediated ubiquitin conjugation to DVL2 variants lacking every lysine except one. The conjugation was allowed to proceed for 30 minutes at 37°C. (B) Quantification of (A) using line density analysis in ImageJ. (C) Immunoblot showing WWP1-mediated ubiquitin conjugation to DVL2 variants with all N-terminal lysine residues intact (CT K→R) or all C-terminal lysine residues intact (NT K→R). (D) Quantification of (C) using line density analysis in ImageJ.

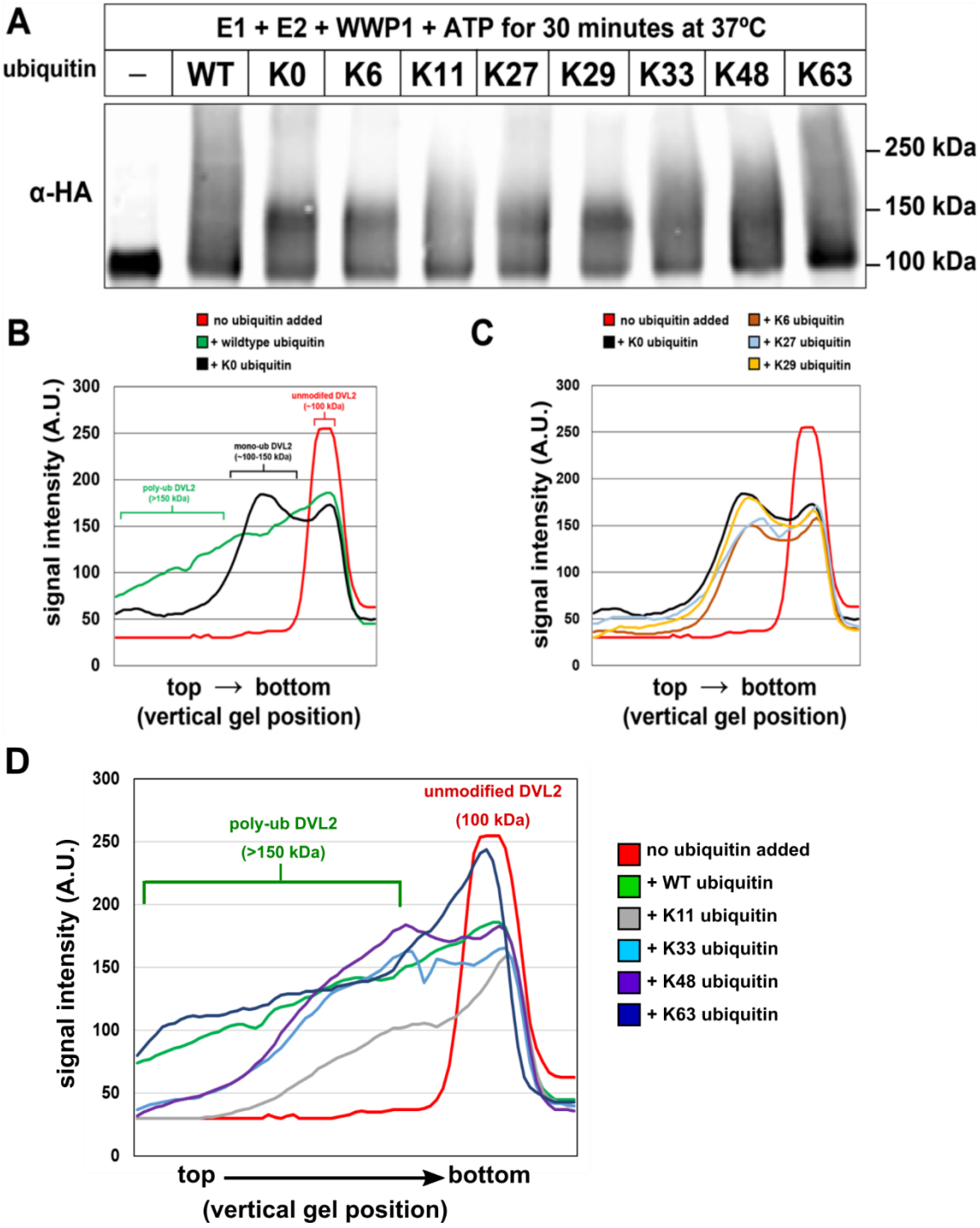

FIGURE 4.3 Analysis of polyubiquitin chain formation by WWP1 on DVL2. (A) Immunoblot showing WWP1-mediated ubiquitin conjugation to DVL2 using the indicated linkage-restricted ubiquitin variants. The conjugation was allowed to proceed for 30 minutes at 37°C. (B-D) Quantification of (A) using line density analysis in Image

this conjugation reaction would have to be performed on DVL2 variants expressing only one lysine residue. **(2)** WWP1 does not form K6-, K27-, or K29-linked polymers on DVL2 (**FIG 4.3 A,C**), and **(3)** WWP1 can form K63-, K48-, K33-, and K11- linked polymers on DVL2 (**FIG 4.3 A,D**). These results indicate that the activity of WWP1 toward DVL2 has some linkage restrictions.

4.3.4 USP9X activity in vitro and in cells is linkage specific

My previous analysis revealed that USP9X operates on ubiquitylated DVL2 while OTUB1 and AMSH could not (**FIG 3.3B**). These results suggest that WWP1-mediated ubiquitylation of DVL2 does not involve K48- or K63-linked polyubiquitin. From these experiments I can conclude that USP9X is able to remove the ubiquitin modifications that WWP1 adds to DVL2. I next aimed to characterize the specificity of USP9X activity toward ubiquitylated DVL2. To further characterize this, I first wanted to characterize USP9X activity *in vitro* toward unanchored polyubiquitin chains of distinct linkage types (**FIG 4.4**). Here I found that USP9X exhibits the most efficient deubiquitylase activity K6-, K11-, K29-, and K33-linked polyubiquitin chains. USP9X showed far lower efficiency in processing K48- and K63-linked polyubiquitin chains and no activity toward linear polyubiquitin chains. Previous reports, using only the USP9X catalytic domain, suggest that the USP9X has a strong preference for K11-linked polyubiquitin and less efficient activity toward K63-, K48-, and K6-linked polyubiquitin (Paudel et al., 2019). My studies employed the full-length USP9X and indicate that full-length USP9X exhibits linkage preferences toward unanchored polyubiquitin chains *in vitro*.

I next sought to determine if loss of USP9X affects global abundance of specific

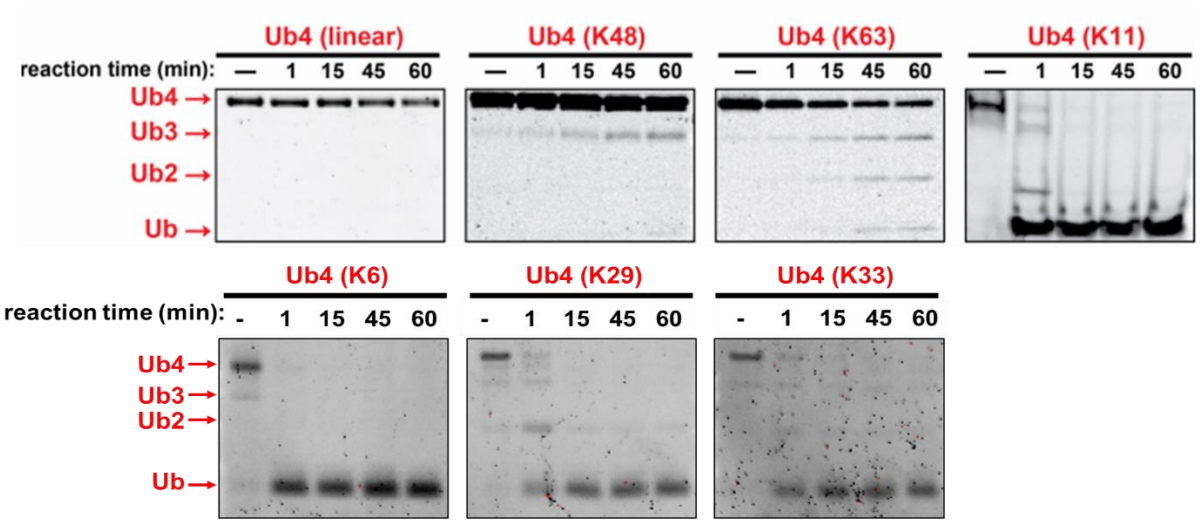

FIGURE 4.4 Analysis of USP9X activity *in vitro.* SYPRO-stained gels showing USP9X deconjugation activity toward unanchored tetra-ubiquitin chains of indicated linkage type. Deconjugation reactions were allowed to proceed at at 37°C and time points were collected as indicated. Reactions were stopped by addition of sample buffer.

polyubiquitin linkage types. To accomplish this, I used a SILAC-MS proteomics approach combined with a diGlycine motif enrichment step which allows for enrichment of ubiquitin-modified peptides to define the ubiquitin-modified proteome (Fulzele and Bennett, 2018; Kim et al., 2011). In this experiment I compared the ubiquitin modified proteomes of MDA-MB-231 cells in the presence and absence of USP9X (**TABLE 4.1**). These results represent pooled data from 2 biological replicates of a pilot experiment and every linkage type was not identified in each replicate. However, over 2 biological replicates I was able to detect almost all of the polyubiquitin chain linkage types except for linear polyubiquitin. I found that K27-linked polyubiquitin chains increased in abundance in the absence of USP9X (**TABLE 4.1**). K27-linkages are not commonly detected in cells and very little is known about their biochemical properties. It is important to note that I was unable to test USP9X activity toward unanchored K27-linked polyubiquitin *in vitro* because this reagent is not currently commercially available.

Surprisingly, these results also suggest that K6- and K63-linked polyubiquitin chains decrease in the absence of USP9X (**TABLE 4.1**). It is possible that USP9X may function to stabilize E3 ubiquitin ligases that typically forms K6- and K63-linked polyubiquitin in the cell. This is consistent with a role for USP9X in stabilizing NEDD4 family E3 ubiquitin ligases. However, the low magnitude of these changes suggests that USP9X does not grossly alter the abundance of most linkage-types in cells.

To further explore the activity of USP9X toward DVL2 I used WWP1 to generate linkage-restricted polyubiquitin modifications on DVL2 and treated these samples with USP9X. Here I found that USP9X was able to remove K11-, K33-, and K63-linked polyubiquitin modifications from DVL2 (**FIG 4.5**). Consistent with the *in vitro* activity

SILAC Quantification

H: MDA-MB-231 cells
L: *usp9x* KO MDA-MB-231 cells

Linkage	H:L Ratio
K6	1.65, 2.63
K11	1.15
K27	0.23
K29	0.96
K33	1.3
K48	1.19, 1.02
K63	1.4

TABLE 4.1 SILAC quantitation of polyubiquitin chain linkage-types in MDA-MB-231 cells with a WT or *usp9x* KO background (Heavy condition: WT MDA-MB-231 cells; Light condition: *usp9x* KO MDA-MB-231 cells)

experiments using the unanchored polyubiquitin chains (**FIG 4.4**), USP9X showed less efficient activity toward K48-linked polyubiquitin conjugated to DVL2, converting only about 50% of modified DVL2 to an unmodified form (**FIG 4.5**). Taken together, these results suggest that USP9X exhibits linkage preference toward ubiquitylated DVL2.

4.3.5 Characterizing interactions between USP9X, NEDD4L, and DVL2

In **Chapter 3** of this thesis I showed that USP9X-mediated regulation of the canonical WNT pathway is partially dependent on both WWP1 and NEDD4L (**FIG 3.5E**). While it was already known that NEDD4L interacts with DVL2 (Ding et al., 2013), and I have previously determined that DVL2 interacts with USP9X (**FIG 3.1**), it was not clear whether USP9X, NEDD4L, and DVL2 were able to interact in a complex. Using co-immunoprecipitation analysis with FLAG-DVL2 as bait, I found that DVL2 co-purified with both NEDD4L and USP9X (**FIG 4.6A**) and these interactions were disrupted when the second PY motif of DVL2 was mutated (**FIG 4.6B**). In these experiments I used a catalytic dead variant of NEDD4L because transient overexpression of WT NEDD4L resulted in degradation of DVL2 (**data not shown**). These results indicate that DVL2 interaction with both NEDD4L and USP9X are scaffolded by the second PY motif of DVL2. Taken together, this suggests that NEDD4L may be able to interact with both USP9X and DVL2 in a complex, but additional co-immunoprecipitation experiments using NEDD4L and USP9X as bait are required to specifically test this.

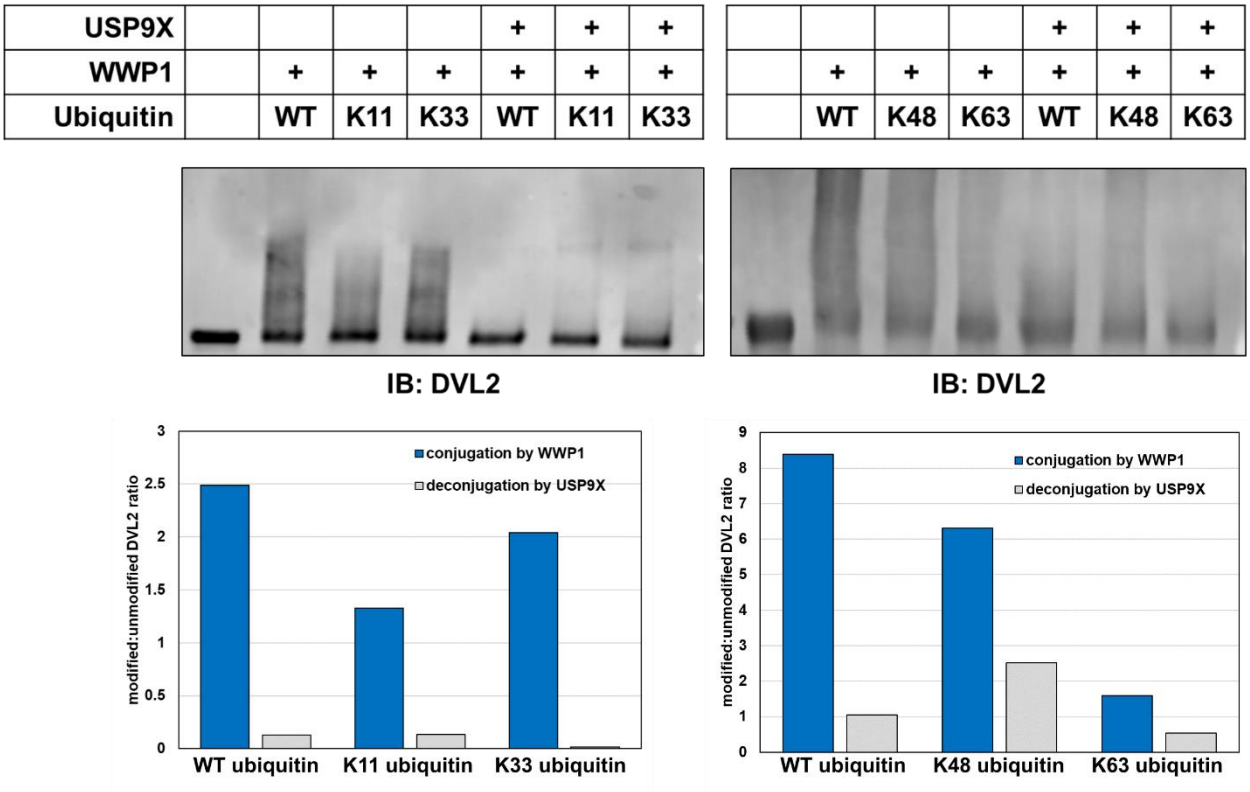

FIGURE 4.5 Activity of USP9X toward linkage-restricted ubiquitin modifications of DVL2 mediated by WWP1. Top: Immunoblot showing WWP1-mediated ubiquitin conjugation to DVL2 using the indicated ubiquitin variants and subsequent deconjugation by USP9X. The conjugation was allowed to proceed for 30 minutes at 37°C and deconjugation reaction consisted of a 60 minute incubation at 37°C. Bottom: For each sample, a ratio of modified:unmodified HA-DVL2 was measured using ImageJ. The modified:unmodified HA-DVL2 ratio for the conjugation reaction is shown in blue and the modified:unmodified HA-DVL2 ratio for the deconjugation reaction is shown in grey.

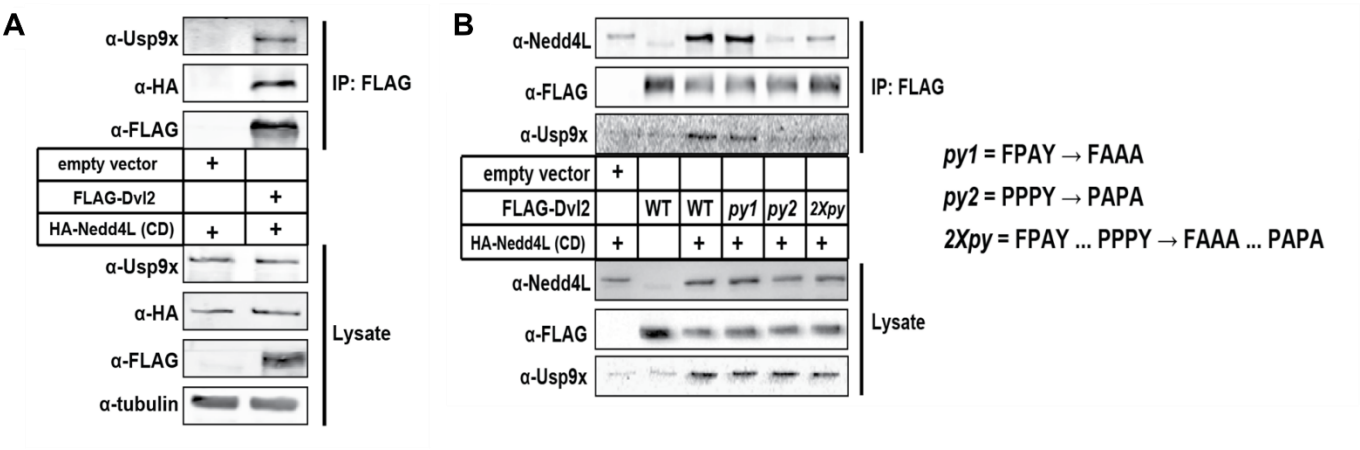

FIGURE 4.6 NEDD4L interactions with USP9X and DVL2 are scaffolded by DVL2 PY motifs. (A) Co-immunoprecipitation analysis in which FLAG-DVL2 was affinity purified from HEK293 cell lysates. Input and immunoprecipitated (IP) fractions were blotted for the indicated species. (B) Co-immunoprecipitation analysis in which indicated FLAG-DVL2 variants were affinity purified from HEK293 cell lysates. Input and immunoprecipitated (IP) fractions were blotted for the indicated species.

Experiments performed by a former post-doctoral fellow in the MacGurn lab, Dr. Kristin Jernigan, revealed that siRNA-mediated knockdown of USP9X resulted in decreased stability of a WT HA-NEDD4L but not a catalytic dead variant (**FIG 4.7A**). This suggests that USP9X regulates NEDD4L stability via removal of autoubiquitylation events. Interestingly, Dr. Jernigan's experiments also revealed that siRNA-mediated knockdown of USP9X had no effect on the stability of NEDD4, another member of the NEDD4 family (**FIG 4.7B**). Further analysis will be required to determine if USP9X interactions with NEDD4s through DVL2 complexes are required to mediate this effect.

4.3.6 NEDD4L activity toward DVL2 differs from WWP1

In **Chapter 3** I characterized WWP1-mediated regulation of DVL2. However, there is mounting evidence that multiple NEDD4 family members may also regulate DVL2. The contribution of multiple NEDD4s may suggest either (i) redundancy among the NEDD4s, or (ii) multiple NEDD4s contributing different activities toward one substrate. I hypothesized that NEDD4L and WWP1 contribute different ubiquitin modifications on DVL2 that are each regulated by USP9X. To test this I first performed linkage-restricted conjugation assays with NEDD4L (**FIG 4.8**). Interestingly, the activity of NEDD4L differed from that of WWP1. Here I found that: **(1)** NEDD4L can conjugate single mono-ubiquitin modifications to DVL2 (evident from K0 lane)(**FIG 4.8 A, B)**, **(2)** NEDD4L does not form K6-, K11-, K27-, K29-, K33-, or K48-linked polymers on DVL2 (**FIG 4.8 A, C**), and **(3)** NEDD4L can form K63-linked ubiquitin polymers on DVL2 but it appears that this occurs to a lesser extent than the conjugation that occurs in the presence of WT ubiquitin (**FIG 4.8 A,D**). This data is not consistent with previous reports

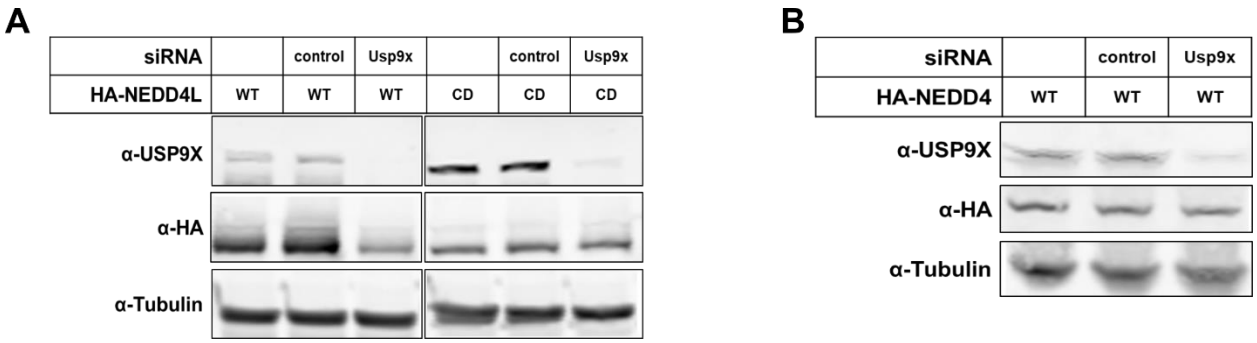

FIGURE 4.7 USP9X regulates the stability of NEDD4L *Data from Dr. Kristin Jernigan*. (A) Immunoblot of whole-cell lysates expressing WT or catalytic dead (CD) HA-NEDD4L treated with indicated siRNA. (B) Immunoblot of whole-cell lysates expressing HA-NEDD4 treated with indicated siRNA

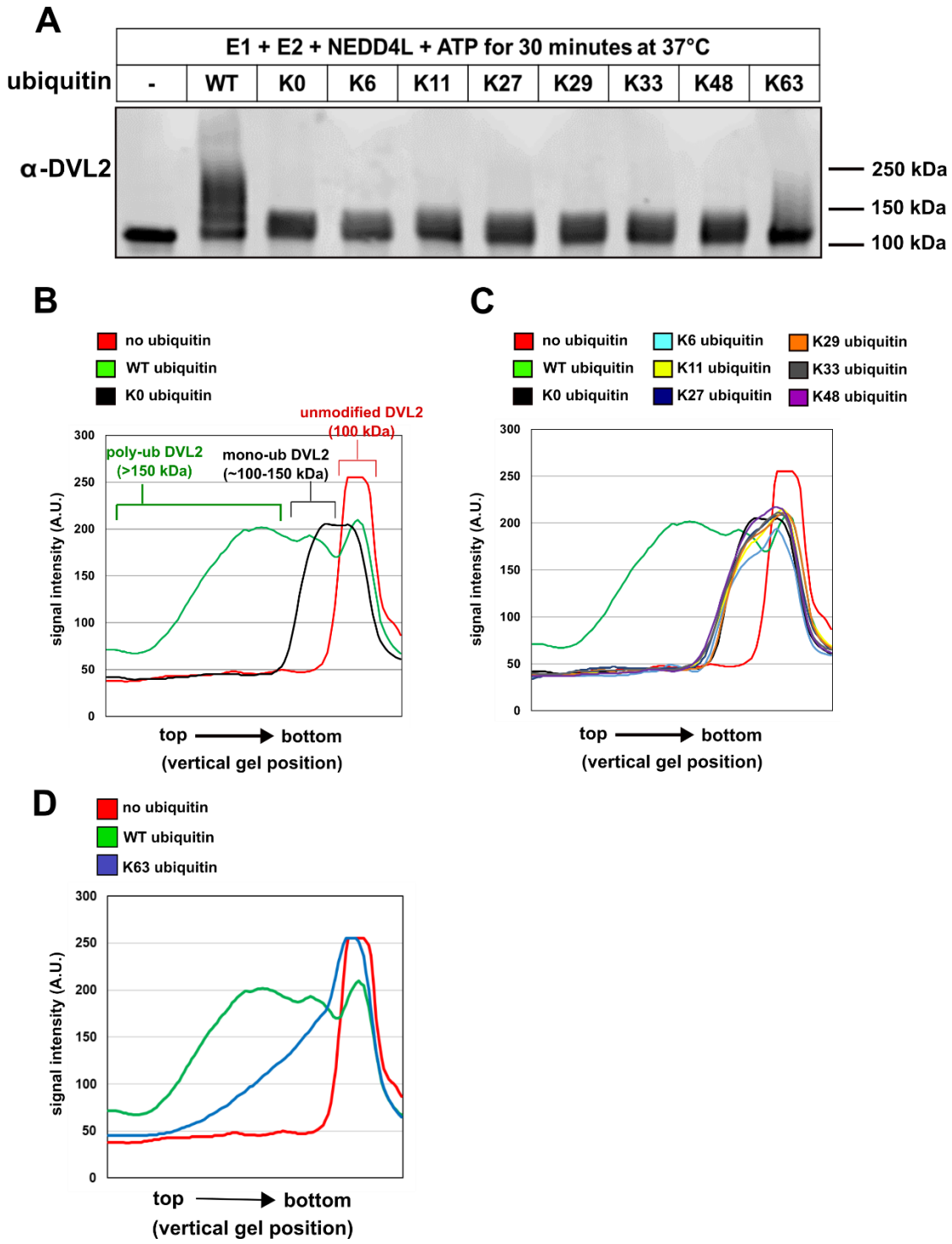

FIGURE 4.8 Analysis of polyubiquitin chain formation by NEDD4L on DVL2. (A) Immunoblot showing NEDD4L-mediated ubiquitin conjugation to DVL2 using the indicated linkage-restricted ubiquitin variants. The conjugation was allowed to proceed for 30 minutes at 37°C. (B-D) Quantification of (A) using line density analysis in ImageJ.

which indicated that NEDD4L conjugates K6-, K27-, and K29-linked polyubiquitin to DVL2 (Ding et al., 2013) although it is important to note that these assays were performed differently. The previous studies of NEDD4L activity toward DVL2 utilized an *in vitro* translation system to generate DVL2, here I use DVL2 purified from HEK293 cells. Furthermore, the finding that no single polyubiquitin linkage type can fully reconstitute NEDD4L activity suggests that NEDD4L may conjugate heterogeneous linkage types and/or branched polyubiquitin chains to DVL2. Further analysis utilizing MS approaches to characterize the ubiquitylation events added to DVL2 by NEDD4L could be informative. Alternatively, recombinant ubiquitin variants containing different combinations of 2-3 lysine residues for use in *in vitro* reconstitution experiments may also shed light on the critical determinants of these modifications.

I next aimed to determine if USP9X has activity toward DVL2 ubiquitylated by NEDD4L. Here I found that USP9X is able to effectively remove both WWP1- and NEDD4L-mediated ubiquitylation events on DVL2 (**FIG 4.9**). I next aimed to determine if this activity is linkage-specific. Here I found that USP9X is less efficient at removing K63-linked polyubiquitin from NEDD4L-ubiquitylated DVL2 (**FIG 4.10**). The interpretation of these results is complicated by the fact that that linkage-restricted conjugation of K63-linked polyubiquitin to DVL2 is far less efficient than formation of polyubiquitin chains with WT chains (**FIG 4.10 B-D**). This could indicate that NEDD4L forms unique polyubiquitin chains on DVL2 that are not homogenous. Such chains may be branched and exhibit multiple linkage-types making them impossible to replicate with linkage-restricted ubiquitylation experiments *in vitro*. As a result, dissecting the exact types of ubiquitin modifications of DVL2 that are regulated by the USP9X/NEDD4L axis

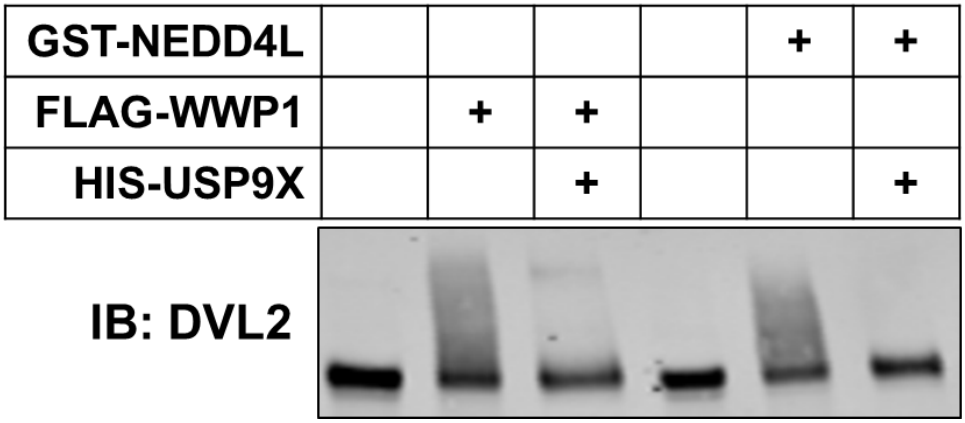

FIGURE 4.9 USP9X activity toward DVL2 ubiquitylated by WWP1 and NEDD4L. Immunoblot showing WWP1-mediated ubiquitin conjugation to DVL2 using WT ubiquitin (lanes 1-2) and subsequent deconjugation by USP9X (lane 3) and NEDD4L-mediated conjugation to DVL2 using WT ubiquitin (lanes 4-5) and subsequent deconjugation by USP9X (lane 6). The conjugation was allowed to proceed for 30 minutes at 37°C and deconjugation reaction consisted of a 60 minute incubation at 37°C.

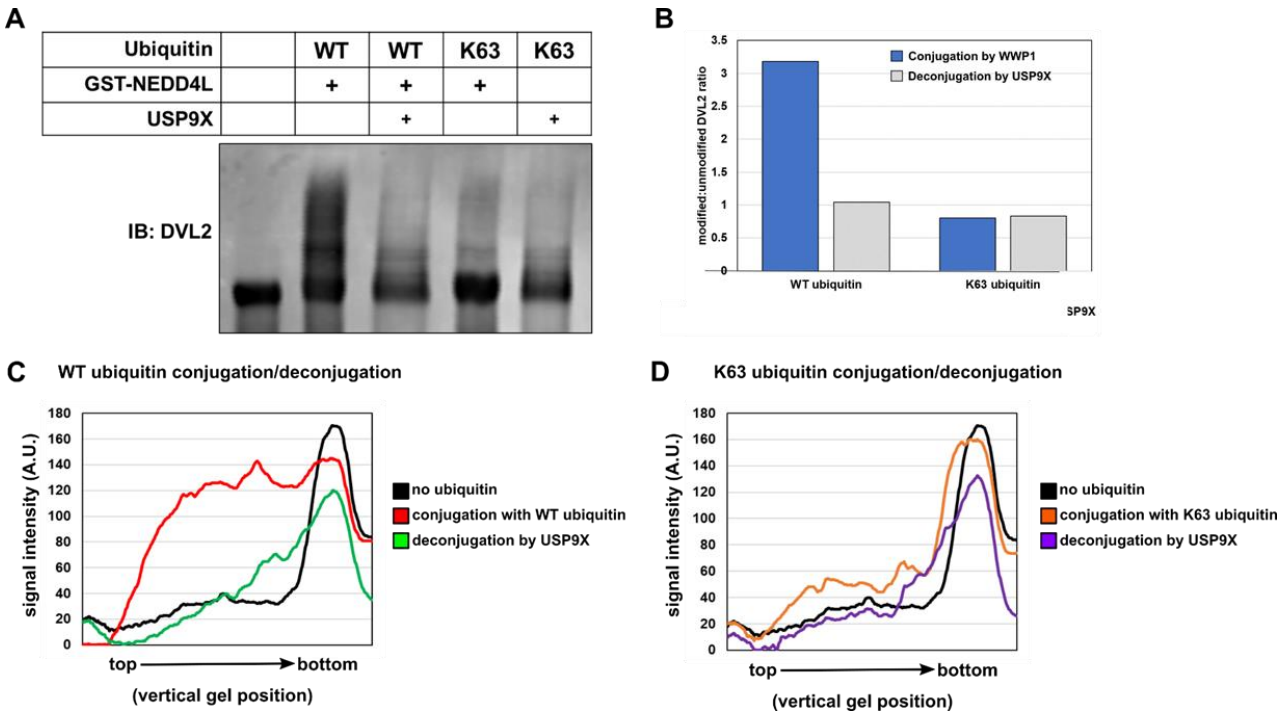

FIGURE 4.10 Activity of USP9X toward linkage-restricted ubiquitin modifications of DVL2 mediated by NEDD4L. (A) Immunoblot showing NEDD4L-mediated ubiquitin conjugation to DVL2 using the indicated ubiquitin variants and subsequent deconjugation by USP9X. The conjugation was allowed to proceed for 30 minutes at 37°C and deconjugation reaction consisted of a 60 minute incubation at 37°C. (B) For each sample, a ratio of modified:unmodified HA-DVL2 was measured using ImageJ. The modified:unmodified HA-DVL2 ratio for the conjugation reaction is shown in blue and the modified:unmodified HA-DVL2 ratio for the deconjugation reaction is shown in grey. (C-D) Quantification of (A) using line density analysis in ImageJ

may be technically challenging and will require additional analysis.

4.4 Discussion

Taken together, these findings suggest that WWP1 and NEDD4L contribute distinct ubiquitin modifications to DVL2 and these modifications are subject to varying degrees of regulation by USP9X. Specifically, I have shown that **(i)** USP9X can interact with both NEDD4L and DVL2; these interactions are scaffolded by DVL2 PY motifs **(ii)** WWP1 can conjugate K11-, K33-, K48-, and K63-linked polyubiquitin to DVL2, **(iii)** NEDD4L can conjugate K63-linked polyubiquitin to DVL2 but only to a far lesser extent than the polyubiquitin modifications formed on DVL2 using WT ubiquitin, **(iv)** USP9X exhibits preferential activity toward unanchored K6-, K11-, K29-, and K33-linked polyubiquitin *in vitro,* **(v)** USP9X can remove polyubiquitin modifications on DVL2 generated by both WWP1 and NEDD4L, **(vi)** USP9X can effectively reverse K11- and K33-linked polyubiquitylation on DVL2 generated by WWP1, and **(vii)** USP9X is less effective at removing K63-linked polyubiquitylation on DVL2 generated by NEDD4L. Altogether, these results give insight into the types of ubiquitin modifications on DVL2 that may be critical to driving this rheostat.

4.4.1 Linkage-specific regulation of DVL2

To further understand the importance of this differential regulation of DVL2 by WWP1 and NEDD4L, it will be important to dissect the type of polyubiquitin modification conjugated to DVL2 by NEDD4L. My findings suggest that NEDD4L forms heterogeneous or branched polyubiquitin chains on DVL2 containing multiple linkage-

types. While the function of mixed or branched ubiquitin chains is not well understood, some examples of branched ubiquitin chains have been characterized and shown to target substrate proteins for degradation by the proteasome (Meyer and Rape, 2014). Formation of branched polyubiquitin chains on DVL2 may have important consequences for WNT signaling.

DVL2 contains 18 lysine residues that span several functional domains and is known to undergo ubiquitin modification within these domains that can elicit positive and negative outcomes. For example, K63-linked polyubiquitin modifications of the DVL2 DIX domain have been reported to enhance canonical WNT activation by enhancing DVL2 polymerization (Tauriello et al., 2010). Interestingly, other reports have suggested modifications of the DVL2 DIX domain may antagonize DVL2 and canonical WNT activation (Madrzak et al., 2015). Site of ubiquitin modification within the DVL2 structure may dictate the functional output of the given ubiquitin signal. My data suggests that USP9X and WWP1 regulate ubiquitin modifications at multiple lysine residues that span multiple regions of DVL2 in order to bias DVL2 participation in either the canonical or noncanonical WNT-PCP pathway. As such, determining the lysine residues of DVL2 that are modified and regulated by NEDD4L, WWP1, and USP9X will be very informative for understanding the functional significance of these DUB-E3 regulatory complexes.

4.4.2 Differential activity of NEDD4s may provide context-specificity to rheostat

DVL2 is known to undergo differential regulation by multiple members of the ubiquitin proteasome system in which the type of ubiquitin modification can elicit very

different fates for DVL2. Of note, ITCH and NEDD4L have been proposed to negatively regulate DVL2 stability by conjugating K48-linked (ITCH) or K6-, K27-, and K29-linked (NEDD4L) polyubiquitin chains on DVL2 targeting it for proteasomal degradation (Ding et al., 2013; Liu et al., 2014a; Marikawa and Elinson, 1998; Mukai et al., 2010; Tauriello et al., 2010; Wei et al., 2012). Additionally, my findings outlined in **Chapter 3** of this thesis indicate that the WWP1-USP9X axis regulates DVL2 ubiquitylation state to elicit a non-degradative outcome and regulate WNT pathway specification. DVL2 regulation mediated by multiple members of the NEDD4 family could result from functional redundancy, but could also reflect differential regulation based on expression in different contexts or different cell types. Based on my findings that NEDD4L and WWP1 contribute distinct ubiquitin modifications on DVL2 that are regulated by USP9X, I speculate that differential expression levels of NEDD4s in distinct cell types or contexts likely dictates the types of ubiquitin modifications on DVL2 that are regulating its stability and function. It could be very informative to test whether other USP9X-interacting NEDD4 family members such as ITCH and SMURF also exhibit linkage-specific activity toward DVL2.

Overall, the findings presented in this chapter provide mechanistic details for USP9X and NEDD4-mediated regulation of DVL2 and shed light on the expanding complexity of ubiquitin-mediated regulation

Chapter 5

Discussion & Future Directions

5.1 Summary

In **Chapter 3** of this thesis I provided evidence supporting that USP9X, a deubiquitylase, and WWP1, an E3 ubiquitin ligase, regulate a ubiquitin rheostat on DVL2, a cytoplasmic transducer of the WNT signaling pathway. In **Chapter 4** of this thesis I provided biochemical characterization of the activities of USP9X, WWP1, and NEDD4L toward DVL2. Here I will discuss the implications of these findings and future directions for this research.

5.2 A complicated role for USP9X in breast cancer

Although there is mounting evidence of a role for USP9X in cancer, the literature regarding the molecular function of USP9X is conflicting. USP9X has been suggested to exhibit oncogenic behavior in some cancer contexts including multiple myeloma, melanoma, and lung cancer but it has also been proposed to have tumor suppressor activity in other cancers such as pancreatic ductal adenocarcinoma (Kushwaha et al., 2015; Potu et al., 2017; Pérez-Mancera et al., 2012; Schwickart et al., 2010). Genetic alterations in *usp9x* have been identified in a variety of human cancers (**TABLE 5.1**). Not surprisingly, USP9X has emerged as a candidate therapeutic target for the treatment of several cancers including hematologic malignancies, melanoma, and ERG-

Cancer type	*usp9x* mutation
Uterine cancer	Mutated in 15.7% of cases
Melanoma	Mutated in 10.9% of cases
Head and neck cancer	Mutated or deleted in 7.5% of cases
Colorectal cancer	Mutated in 5.9% of cases
Stomach cancer	Mutated in 5.0% of cases
Lung adenocarcinoma	Mutated in 4.1% of cases
Breast cancer	Mutated in 3.0% of cases
Sarcoma	Amplified in 2.8% of cases

TABLE 5.1 Prevalence of genetic alterations in usp9x in human cancers. List of top reported genetic alterations in USP9X occurring in different cancer types as reported on the CBioPortal DataBase http://www.cbioportal.org

positive prostate tumors (Potu et al., 2017; Schwickart et al., 2010; Wang et al., 2014b). Given its promise as a potential therapeutic target for the treatment of cancer, it will be important to fully understand the molecular function of USP9X at a biochemical and cellular level.

The data presented in this thesis support a role for the USP9X-WWP1 axis in regulation of the WNT pathway in breast cancer cells (**FIG 5.1**). USP9X is mutated in 3.0% of breast cancer cases (**TABLE 5.1**) and my studies indicate that USP9X has properties that may promote or suppress tumor growth in this context. I have shown that hyperactivation of USP9X potentiates canonical WNT signaling, whereas inhibition of USP9X drives noncanonical WNT-PCP signaling and migration. As such, chemical inhibition of USP9X for the treatment of breast cancer has the potential to result in: (1) decreased canonical WNT signaling and consequently WNT-driven proliferation, as well as (2) increased cell migration and metastatic behavior. On the other hand, our results suggest that chemical hyperactivation of USP9X would likely: (1) antagonize migration of breast cancer cells, and (2) promote WNT-driven proliferation of breast cancer cells. Thus, chemical modulation of USP9X in the context of breast cancer may be problematic. However, it is currently unclear to what extent dysregulation of USP9X or WWP1 may contribute to the progression of breast cancer.

5.2.1 Sub-cellular localization of USP9X

While the findings presented in this thesis provide insight into the role of USP9X

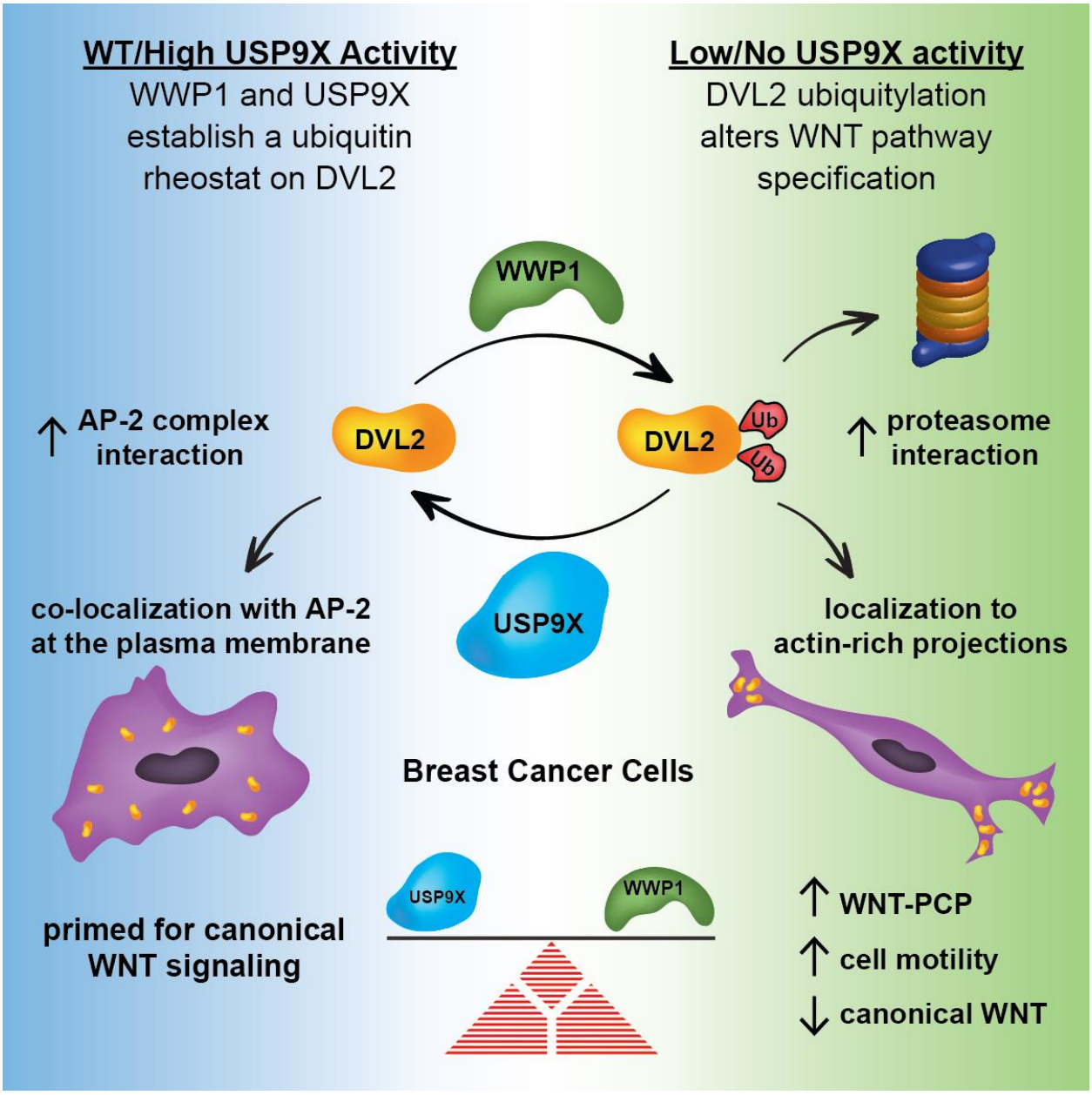

FIGURE 5.1 USP9X and WWP1 regulate a ubiquitin rheostat on DVL2 that determines WNT pathway specification

dichotomous role of USP9X in cancer. To further characterize USP9X, I think it will be critical to define the interaction profile of USP9X in several relevant cancer contexts.

In order to define the interaction network and localization of USP9X in MDA-MB-231 breast cancer cells I have used a CRISPR/Cas-9 genome editing approach to endogenously tag Usp9x with a FLAG-mNeon tag at both the N- and C-termini in MDA-MB-231 cells. I screened for clones that underwent successful endogenous tagging of USP9X using western blot analysis and found that some clones displayed a complete shift of USP9X signal to higher molecular weight species indicating that 100% of endogenous USP9X has been tagged with FLAG-mNeon whereas other clones exhibited only a partial shift suggesting tagging was successful at only one locus (**FIG 5.2A**). To confirm that this epitope tag does not disrupt USP9X function I tested canonical WNT activation in these cell lines using a Topflash assay and found that these cells are able to effectively activate the canonical WNT pathway (**FIG 5.2B**). Using live-cell imaging techniques with these cells I was able to determine that the localization of USP9X in MDA-MB-231 cells is cytoplasmic and displays a distinct pattern with several large USP9X puncta per cell that appear to be perinuclear (**FIG 5.2C**). The localization pattern of USP9X that I observe in these cells is different from what is suggested in the literature, suggesting a context-dependent localization and perhaps context-dependent function of USP9X (Han et al., 2012; Murtaza et al., 2015). This reagent will be useful for further studies of USP9X activity in breast cancer cells. Similar reagents in other relevant cancer cell lines (**TABLE 5.1**) should be generated in order to define the role of USP9X in each of these cancers. Such studies have the

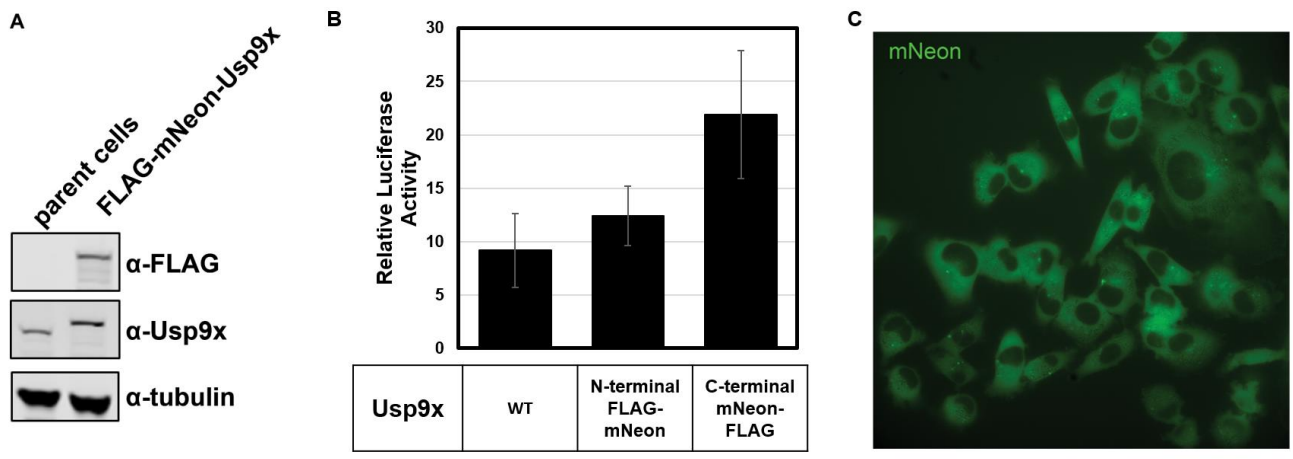

FIGURE 5.2: Endogenous tagging of Usp9x. (A) Immunoblot analysis of endogenous Usp9x in WT MDA-MB-231 cells and representative MDA-MB-231 clone expressing endogenously tagged FLAG-mNeon-Usp9x**.** (B) Topflash reporter assays of indicated cells treated with Wnt3a ligand and R-spondin. Luciferase activity is normalized to activation in untreated WT cells**.** (C) Representative epifluorescence imaging of MDA-MB-231 cells expressing endogenously FLAG-mNeon tagged Usp9x

potential to define USP9X mechanism-of-action in these disease contexts and uncover novel drug targets for treatment of these diseases.

5.2.2 USP9X substrate profiling in breast cancer cells

My data indicate that DVL2 is a substrate of USP9X in MDA-MB-231 cells and this mechanism contributes to WNT pathway specification. However, there may be other substrates of USP9X contributing to this cellular behavior. In an unbiased and quantitative approach, I used a peptide antibody-based affinity reagent to enrich for and identify endogenously ubiquitylated proteins in MDA-MB-231 cells with a WT or *usp9x* KO background. This antibody reagent recognizes the Lys-ϵ-Gly-Gly (diGLY) remnant that is generated after trypsin digestion of ubiquitylated proteins (Fulzele and Bennett, 2018). These peptides can then be identified using mass spectrometry. In this pilot experiment I identified several potential substrate proteins that undergo increased ubiquitylation in the absence of USP9X. One candidate was Spg20, a protein commonly involved in regulation of plasma membrane trafficking events (**TABLE 5.2**). Interestingly, I also identified Spg20 in the WWP1 interaction profile generated in MDA-MB-231 cells (**TABLE 3.1**). Consistent with previously published reports, I also identified Eps15 to be a potential substrate of USP9X which exhibited increased ubiquitylation in the absence of USP9X (**TABLE 5.2**) (Savio et al., 2016). Importantly, other studies have reported that Spg20 interacts with Eps15 to regulate endocytic trafficking, and impairment of Spg20 drives axonopathy and a neurological disorder known as Troyer syndrome (Bakowska et al., 2005). I hypothesize that USP9X may contribute a layer of regulation to this trafficking mechanism through associations with

Potential Usp9x substrates

Protein	Site(s) Modified	H:L Ratios
Profilin-1	K105	0.50, 0.50
Spg20	K370, K377	0.46, 0.25, 0.31
Stam1	K170, K171	0.43, 0.42, 0.43
*Eps15	K793	0.37
**EGFR	K739	1.10

* Identified in 1 out of 3 biological replicates, does exhibit Usp9x-dependent change
** Identified in 1 out of 3 biological replicates, does not exhibit Usp9x-dependent change

TABLE 5.2 USP9X substrates in MDA-MB-231 cells based on SILAC-MS. SILAC quantitation of potential substrates of USP9X identified in proteomic analysis (Heavy condition: WT MDA-MB-231 cells; Light condition: *usp9x* KO MDA-MB-231 cells). Criteria includes hits that were identified in at least 2 of the 3 biological replicates of this experiment and exhibited a relative change of at least 2-fold between WT and *usp9x* knockout conditions.

Spg20 and Eps15. Further studies of the functional significance of USP9X interaction with Spg20 and Eps15 will be very informative.

Another candidate substrate identified in this analysis was STAM1, a component of the ESCRT0 complex (**TABLE 5.2**). This result was not surprising because, the NEDD4 family member ITCH, a known substrate of USP9X, is reported to ubiquitylate and regulate STAM1 (Malik et al., 2012; Mouchantaf et al., 2006). I hypothesize that USP9X may function to deubiquitylate ITCH, STAM1, or other components of the ESCRT machinery to impact dynamic endocytic trafficking.

Additionally, I was able to detect ubiquitylation events on EGFR but no USP9X-dependent change was observed (**TABLE 5.2**). These results are consistent with previously published reports suggesting that USP9X regulates EGFR trafficking via regulation of Eps15 ubiquitylation state (Savio et al., 2016). Taken together, these findings suggest a broader role for USP9X in the regulation of important endocytic trafficking pathways.

Profilin-1, an important regulator of actin dynamics, was also identified as a candidate substrate in this analysis (**TABLE 5.2**) (Cao et al., 1992). My previous findings indicate that USP9X alters actin dynamics by regulating activation of the GTPase Rho (**FIG 3.11**). Overall, this suggests USP9X may be involved in several mechanisms for regulating actin dynamics. Further studies of the effect of USP9X on actin dynamics and how this impacts cell migration will be important.

While this analysis did reveal several candidate substrates these results are preliminary and I expect deeper analysis will allow us to uncover high confidence hits and identify more substrates of USP9X. Comprehensive quantification of these

substrates would require protocol optimization and substantial effort.

5.2.3 USP9X functions in both WNT and Hippo signaling

In addition to the research presented here, there are several other studies that have sought to characterize the function of USP9X in breast cancer. These reports indicated that increased USP9X expression correlates with increased protein levels of the oncogene YAP1 in human breast cancer cell lines and patient samples (Li et al., 2018). This study reported that USP9X deubiquitylates and stabilizes YAP1 in breast cancer and thus promotes cell survival and chemoresistance through YAP1 stabilization. Interestingly, YAP1 is a major mediator of the Hippo pathway, a key receptor signaling pathway known to have significant cross-talk with the WNT pathway (Kim and Jho, 2014). Hippo signaling has been reported to antagonize WNT signaling (Imajo et al., 2012). In this mechanism, YAP and TAZ, another mediator of Hippo signaling, were reported to negatively regulate canonical WNT activation through interactions with β-catenin that inhibit its nuclear localization (Imajo et al., 2012). YAP and TAZ also inhibit canonical WNT activation by inhibiting DVL2 interaction with Casein-kinase 1 (CK1) (Varelas et al., 2010) (Imajo et al., 2012). This mechanism of USP9X-mediated regulation of Hippo signaling suggests USP9X may promote tumor progression in breast cancer.

While USP9X plays a clear role in both WNT and Hippo signaling pathways, the interplay between these pathways is not well understood. First, it will be important to understand the biochemical determinants of USP9X-mediated regulation of YAP/TAZ. Interestingly, YAP has WW domains and thus may bind USP9X directly through

interactions with its PY motifs (Iglesias-Bexiga et al., 2015). I hypothesize that a subset of USP9X PY motifs function to engage WW domains within WNT pathway components, while other PY motifs of USP9X associate with WW domains of Hippo pathway components. Rigorous characterization of the role of USP9X in both the Hippo and WNT pathways will be extremely informative in understanding USP9X function in breast cancer.

Interestingly, USP9X has also been proposed to suppress pancreatic tumor growth through deubiquitylation and stabilization of the Hippo kinase LATS in pancreatic cancer cells (Toloczko et al., 2017). The LATS kinases are core kinases in the Hippo signaling pathway that function to phosphorylate and inhibit the downstream transcriptional activators of the pathway, YAP and TAZ. USP9X functions as a synergizing component of the Hippo pathway that deubiquitylates and stabilizes the LATS kinase to negatively regulate YAP/TAZ and in turn suppress pancreatic tumor growth. These studies suggest a context-dependent function of USP9X. This also underscores the need to further characterize the role of USP9X in the regulation of Hippo signaling in these contexts.

5.3 NEDD4 family E3 ubiquitin ligases in cancer

Many NEDD4 family E3 ubiquitin ligases have been linked to human cancer progression (**TABLE 5.3**) (Chen and Matesic, 2007; Eide et al., 2013). For example, many colorectal carcinomas and colon cancer cell lines exhibit amplified NEDD4 and this amplification correlates with increased cell growth rates (Eide et al., 2013). WWP1 has been reported to be amplified in 7.5% of invasive breast carcinomas (**TABLE 5.3**).

In **Chapter 3** of this thesis I defined the interaction profile of WWP1 in MDA-MB-231 breast cancer cells and this information guided the identification and characterization of a novel mechanism regulating WNT pathway specification in breast cancer cells. Based on my findings, I speculate that amplification of WWP1 drives hyper-activation of the WNT-PCP pathway which results in increased invasion and migration of breast cancer cells and ultimately drives breast cancer metastasis. These studies suggest that WWP1 may be a promising target for the treatment of invasive breast carcinoma. However, targeting WWP1 may be complicated by the potential for redundant functions among NEDD4 family members. Thus, targeting multiple NEDD4 family members may be required to efficiently modulate the activity of interest.

5.3.1 NEDD4L interaction profile in breast cancer cells

To characterize the interaction network of NEDD4L in breast cancer cells I performed SILAC-MS in MDA-MB-231 cells stably expressing FLAG-NEDD4L (**TABLE 5.4**). I chose to define the interaction profile of NEDD4L in the MDA-MB-231 breast cancer cells based on the results outlined in **Chapter 3** suggesting that USP9X-mediated regulation of the WNT pathway in MDA-MB-231 cells is partially dependent on NEDD4L. In these studies, the most stoichiometric interactors identified were the

NEDD4 Family Member	Human Disease
NEDD4	Mutated: Uterine cancer (8.1%) Mutated: Colorectal adenocarcinoma (3.4%)
NEDD4L	Mutated: Uterine cancer (7%) Mutated: Melanoma (6.3%)
WWP1	Amplified: Uterine cancer (8.8%) Amplified: Breast invasive carcinoma (7.5%)
WWP2	Mutated: Uterine cancer (5.3%) Mutated: Stomach adenocarcinoma (3.4%)
ITCH	Amplified: Colorectal adenocarcinoma (8.4%) Mutation: Uterine cancer (6.4%)
SMURF1	Amplified: Esophageal cancer (11%) Amplified: Stomach adenocarcinoma (6.6%)
SMURF2	Mutated: Uterine cancer (6.2%) Amplified: Breast invasive carcinoma (5.7%)
NEDL1	Mutated: Skin cutaneous melanoma (15.9%) Mutated: Uterine cancer (12.1%)
NEDL2	Mutated: Skin cutaneous melanoma (17.7%) Mutated: Uterine cancer (12.7%)

TABLE 5.3 Prevalence of genetic alterations in NEDD4 family members in human cancers. List of top reported genetic alterations occurring in different cancer types as reported on the CBioPortal DataBase http://www.cbioportal.org

Table 5.4. SILAC-based interaction profile of NEDD4L in MDA-MB-231 cells				
Protein	**function / description**	**pept. count**	**H:L ratio**	**% seq coverage**
NEDD4L	NEDD4 family member (bait)	59	168.18	61.2
14-3-3 β	14-3-3 family members; known to antagonize NEDD4L	12	33.67	53.3
14-3-3 γ		13	27.06	52.2
14-3-3 ε		15	31.31	51.4
14-3-3 ξ		11	17.16	48.2
14-3-3 η		10	34.05	41.1
AMOTL1	angiomotin-like 1	20	67.65	28.1

TABLE 5.4 SILAC-based interaction profile of NEDD4L in MDA-MB-231 cells. Heavy condition: MDA-MB-231 cells stably expressing FLAG-NEDD4L; Light condition: MDA-MB-231 cells stably expressing empty vector

members of the 14-3-3 family of proteins, which are known to interact with NEDD4L and contribute to NEDD4L-mediated regulation of ENaC (Ichimura et al., 2005). It has been shown that the ability of NEDD4L to interact with ENaC is regulated by an SGK1-dependent mechanism in which phosphorylation of NEDD4L by SGK1 recruits the 14-3-3 proteins to directly interact with NEDD4L which keeps the E3 ubiquitin ligase in an inactive state (Debonneville et al., 2001; Ichimura et al., 2005). However, it is important to note that there are several caveats that complicate our ability to interpret this data, (1) MDA-MB-231 cells stably expressing FLAG-NEDD4L grow significantly slower than WT MDA-MB-231 cells. Thus, it is possible that stable overexpression of NEDD4L may have off-target effects that could be making the cells sick. (2) 14-3-3 proteins are known to be inhibitory to NEDD4L activity. Since these interactions were super-stoichiometric, it is possible that the cells are coping with NEDD4L overexpression by upregulating this inhibitory mechanism. One major consequence of this would be that the interactors we identified may not be the relevant interactors in this cellular context.

In this NEDD4L interactome profile I also identified a sub-stoichiometric interaction with the angiomotin-like 1 protein (AMOTL1), which is a membrane-associated protein that typically controls cell polarity and migration in endothelial cells (Troyanovsky et al., 2001). The NEDD4L-AMOTL1 interaction was previously reported and these studies showed that NEDD4L regulates AMOTL1 stability by targeting it for proteasomal degradation (Wang et al., 2012). Interestingly, we did not identify USP9X or DVL2 in this pilot experiment which could indicate that USP9X and DVL2 are not major stoichiometric interactors of NEDD4L in this context. However, I cannot exclude

the possibility that the quality of this experiment was low and USP9X and DVL2 peptides were missed. As such, it will be important to repeat these experiments and also perform fractionation of the tryptic peptides before analysis by MS to obtain an increased amount of high-confidence hits and better coverage of sub-stoichiometric interactors. It is also important to note that in order to perform this experiment, I had to stably incorporate FLAG-NEDD4L into the genome of MDA-MB-231 breast cancer cells using a retroviral system and the stable expression of FLAG-NEDD4L is approximately 10-fold higher than that of endogenous NEDD4L. As such, we cannot exclude the possibility that overexpression of NEDD4L may be artificially driving some of the observed interactions, potentially masking other interactions. Therefore, endogenous chromosomal tagging of NEDD4L using a CRISPR-Cas9 system may yield results that are more representative of the steady state NEDD4L interaction profile. While there are caveats to interpreting the results of this preliminary interaction profile, we can speculate that NEDD4L is primarily engaging 14-3-3 proteins in MDA-MB-231 cells and is therefore likely in an inactive state in this context.

Overall, I think that defining the interaction profiles of NEDD4s in relevant cancer contexts could provide important information about NEDD4 substrates as well as how NEDD4s are regulated. These studies have the potential to offer great insight into the role of NEDD4s in disease progression and may also elucidate novel drug targets for the treatment of these diseases.

5.3.2 Chemical modulation of NEDD4L

While there are no known chemical modulators that directly target NEDD4s,

there is a mechanism to indirectly stimulate the activity of NEDD4L. NEDD4L has been well characterized in epithelial kidney cells as a key regulator of ENaC surface stability (Abriel et al., 1999). It is known that the kinase SGK1 regulates NEDD4L activity by phosphorylation which inhibit its E3 ubiquitin ligase activity which in turn regulates surface expression of ENaC (Debonneville et al., 2001). There is an SGK1 inhibitor, GSK650394, available that inhibits SGK1 activity which inhibits phosphorylation of NEDD4L and results in accumulation of dephosphorylated/active NEDD4L (**FIG 5.3A**) (Sherk et al., 2008). Based on the findings presented in **Chapter 3 and 4** of this thesis, I hypothesized that treatment with GSK650394 would inhibit canonical WNT activation. As expected, I found that activation of NEDD4L via inhibition of SGK1 attenuated canonical WNT signaling. Since this inhibitor has the potential to be a very useful tool for specific activation of NEDD4L in future studies, I also generated a dose-response curve and calculated an IC_{50} for this compound (**FIG 5.3B**).

Based on the model established in **Chapter 3**, I hypothesized that hyperactivation of NEDD4L may increase noncanonical WNT-PCP-driven cell migration. Here I found that treatment with GSK650394 resulted in a significant increase in MDA-MB-231 cell migration speed (**FIG 5.3C**).

Interestingly, the 14-3-3 proteins, which were the most stoichiometric interactors of NEDD4L identified in the NEDD4L interaction profiling (**TABLE 5.4**), associate with NEDD4L in an SGK1-dependent manner (Ichimura et al., 2005). I hypothesize that

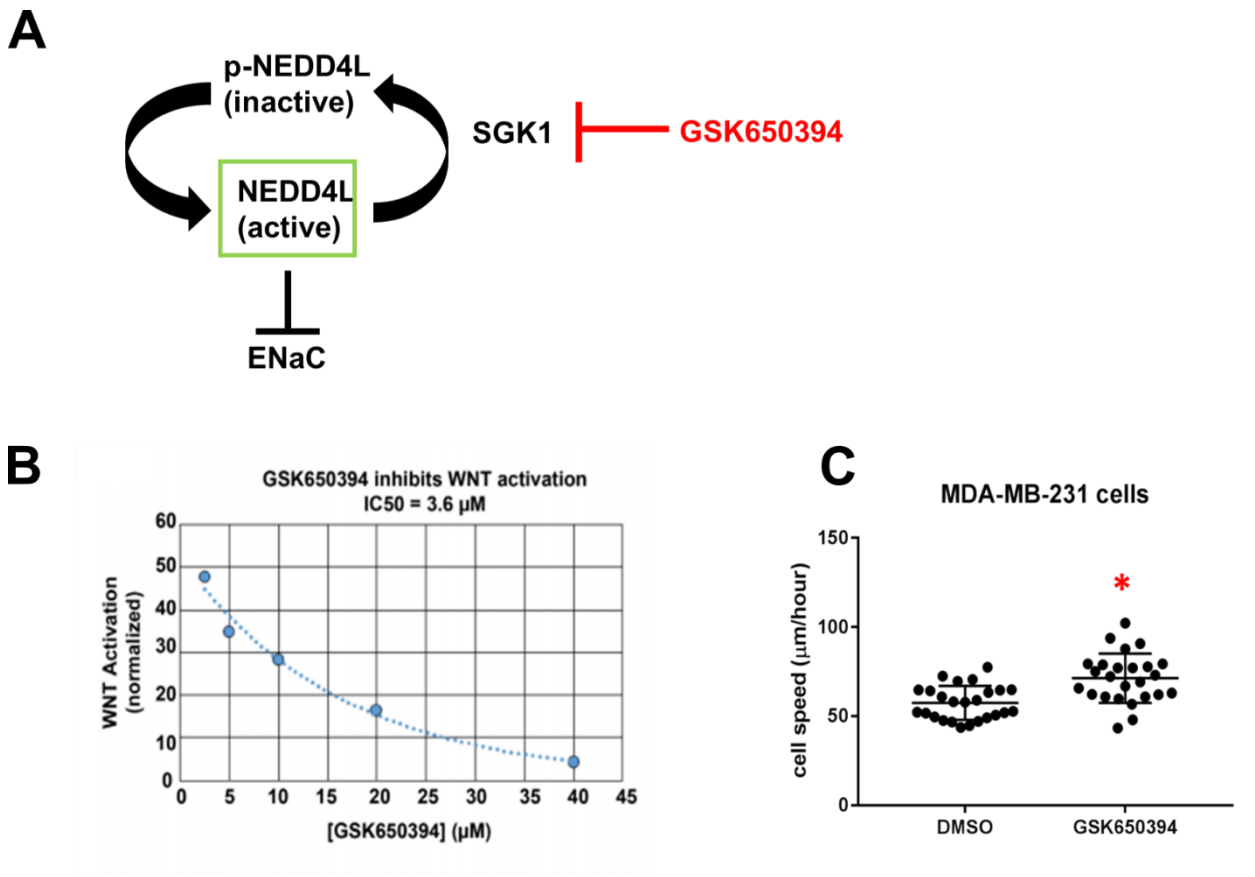

FIGURE 5.3 Effect of SGK1 inhibitor (GSK650394) on canonical and noncanonical WNT activation. (A) Model for GSK650394 activation of NEDD4L. GSK650295 inhibits SGK1 activity, allowing accumulation of dephosphorylated/active NEDD4L. (B)Ligand-stimulated WNT activation was measured in the presence of indicated concentrations of GSK650394. Based on the data an IC50 was estimated. (C) Migration speed of MDA-MB-231 cells was measured after treatment with DMSO control or GSK650394 (300nM). There is a statistically significant difference when comparing cell speed after GSK650394 treatment to DMSO-treated control ($p<0.005$)

treatment with GSK650394, leaving NEDD4L in an active state, would likely free NEDD4L from association with the 14-3-3 proteins and may potentially allow for identification of other interactors. Characterizing the NEDD4L interaction profile after treatment with GSK650394 may be extremely informative for understanding the cellular function of NEDD4L in MDA-MB-231 cells and perhaps other contexts.

APPENDIX A

Reported DUB-E3 interactions

DUB	E3	Pathway	Interaction/ model	Methodology	Citation
UCH-L1	PARK2	neurons/ parkinson's disease	PARK2 targets UCH-L1 for degradation	affinity capture-western, biochemical activity, reconstituted complex	McKeon JE (2014)
UCH-L1	TRAF6	NFKB pathway; innate immune response	UCH-L1 antagonizes TRAF6-mediated ubiquitylation of TRAF3	affinity capture-western	Karim R (2013)
UCH-L1	MDM2	p53 signaling	UCH-L1 antagonizes MDM2-mediated ubiquitylation of p53	affinity capture-western	Li L (2010)
UCH-L1	TRIM63	-	-	Biochemical activity (high throughput)	Loch CM (2012)
BAP1	TRIM63	-	-	Biochemical activity (high throughput)	Loch CM (2012)
BAP1	MAP3K1	JNK signaling		high throughput protein microarray profiling	Charlaftis N (2014)
UCHL5	UBE3A			affinity capture-MS, biochemical activity	Huttlin EL (2015)
UCHL5	PJA1	-	-	Biochemical activity (high throughput)	Loch CM (2012)
UCHL5	TRIM63	-	-	Biochemical activity (high throughput)	Loch CM (2012)
UCHL5	RFFL	-	-	Biochemical activity (high throughput)	Loch CM (2012)
UCHL5	RNF20	-	-	genomics/bioinformatics	Wan C (2015)
UCHL5	HUWE1	-	-	proteomics screen	Thompson JW (2014)
UCHL5	MAP3K1	JNK signaling	-	high throughput biochemical activity	Charlaftis N (2014)
UHCL5	HERC2	-	-	affinity capture-MS high throughput	Huttlin EL (2015)
CYLD	MIB2	Notch signaling	CYLD stabilizes MIB2 to antagonize Notch	affinity capture-MS, affinity capture-western, biochemical activity	Rajan N (2014)

DUB	E3	Pathway	Interaction/ model	Methodology	Citation
CYLD	TRAF6	Streptococcus pneumoniae induced Plasminogen Activator Inhibitor-1 (PAI-1) and acute lung injury; NFKB pathway	CYLD exhibits anti-PAI1 activity through direct regulation of TRAF-6; CYLD attenuates NFKB pathway activation in response to TLR engagement by deubiquitylating TRAF6	affinity capture-western, biochemical activity	Wu J (2015)
CYLD	ITCH	inflammatory signaling	Itch-CYLD complex first cleves K63-linked ubiquitin from Tak1 and then subsequently adds K48-linked ubiquitin to terminate inflammatory signaling via tumor necrosis factor	affinity capture-western, reconstituted complex	Ahmed N (2011)
USP1	DTX3	-	-	Two-hybrid, high throughput	Hayes SD (2012)
USP1	TRAF6	-	-	Two-hybrid, high throughput	Hayes SD (2012)
USP2	TRAF6	T cell receptor signaling	USP2a deSUMOylates TRAF6 and mediates TRAF6-MALT1 interactions to regulate NFKB signaling	Affinity capture-western, biochemical activity, two-hybrid (high throughput)	Li Y (2013)
USP2	MDM2	p53 pathway	USP2a regualtes the p53 pathway by deubiquitylating and stabilizing MDM2	Affinity capture-wester, reconstituted complex, two-hybrid	Stevenson LF (2007)
USP2	TRIM63	-	-	Biochemical activity (high throughput)	Loch CM (2012)
USP2	CBLC	-	-	Two-hybrid, high throughput	Hayes SD (2012)
USP2	DTX3	-	-	Two-hybrid, high throughput	Hayes SD (2012)
USP2	RNF125	-	-	Two-hybrid, high throughput	Hayes SD (2012)

DUB	E3	Pathway	Interaction/model	Methodology	Citation
USP4	TRAF2	NFKB pathway	USP4 deubiquitylates TRAF2 and TRAF6 and inhibits TNFalpha-induced cancer cell migration	affinity capture-western, biochemical activity, reconstituted complex	Xiao N (2011)
USP4	TRAF6	NFKB pathway	USP4 deubiquitylates TRAF2 and TRAF6 and inhibits TNFalpha-induced cancer cell migration	affinity capture-western, biochemical activity, reconstituted complex	Xiao N (2011)
USP4	HUWE1	p53 pathway	USP4 deubiquitylates and stabilizes HUWE1 resulting in decreased p53 levels	affinity capture-western, biochemical activity	Zhang X (2011)
USP4	TRIM63	-	-	Biochemical activity (high throughput)	Loch CM (2012)
USP5	SMURF1	inflammatory signaling	Smurf1 interacts with and ubiquitylates USP5 to target for proteasomal degradation, and thereby inhibits the production of TNF-alpha	Affinity capture-western, biochemical activity (high throughput)	Qian G (2016)
USP5	RAD18	DNA damage repair	Rad18 ubiquitylates sites of DNA damage to recruit repair proteins. USP5 interacts with RAD18 to remove ubiquitin modifications to eliminate ubiquitin signals after repair is complete	Affinity capture-western	Nakajima S (2014)
USP5	ITCH	-	-	Affinity capture-MS	O'Connor HF (2015)
USP5	STUB1	-	-	Co-fractionation (high throughput)	Wan C (2015)
USP5	HERC4	-	-	Co-fractionation (high throughput)	Kristensen AR (2012)

DUB	E3	Pathway	Interaction/model	Methodology	Citation
USP5	RFFL	-	-	Biochemical activity (high throughput)	Loch CM (2012)
USP5	TRIM63	-	-	Biochemical activity (high throughput)	Loch CM (2012)
USP5	PJA1	-	-	Biochemical activity (high throughput)	Loch CM (2012)
USP5	TRAF6	-	-	Biochemical activity	Bremm A (2010)
USP5	UBR1	-	-	Co-fractionation (high throughput)	Havugimana PC (2012)
USP5	XIAP	-	-	Co-fractionation (high throughput)	Havugimana PC (2012)
USP7	MDM2	p53 pathway		Affinity capture-western, co-crystal structure, co-fractionation, protein-peptide, reconstituted complex	Lu X (2007)
USP7	HUWE1	Hypoxia-induced tumor progression	HUWE1 interacts with and ubiquitylates USP7 to enhance its activity in order to deubiquitylate and stabilizew HIF-1alpha and promote tumor progression, metastasis, and tumor resistance	Affinity capture-MS, affinity capture-western, biochemical activity	Sowa ME (2009)
USP7	MARCH7-	immune, neuronal, and embryonic stem cell pathways	MARCH7 undergoes compartment specific-deubiquitylation by USP9X in the cytosol and USP7 in the nucleus	Affinity capture-Western, Two-hybrid (high throughput)	Nathan JA (2008)
USP7	UHRF2	DNA methylation maintenance	USP7 identified as interacting partner of UHRF2 in a proteomics screen	Affinity capture-MS, two hybrid (high throughput)	Liu Y (2016)
USP7	CHFR	mitotic stress checkpoint; cell cycle control	USP7-mediated deubiquitylation of CHFR results in accumulation and activation of CHFR to regulate cell cycle progression	Affinity capture-MS, affinity capture-western	Oh YM (2009)

DUB	E3	Pathway	Interaction/model	Methodology	Citation
USP7	TRAF6	TLR-mediated NFKB and JNK signaling		affinity capture-western, biochemical activity, reconstituted complex	Daubeuf S (2009)
USP7	RAD18	DNA damage repair	USP7 deubiquitylates and stabilizes RAD18 to promote ubiquitin-dependent DNA damage signaling	Affinity capture-wester, biochemical activity, reconstituted complex	Zlatanou A (2016)
USP7	RNF168	DNA damage repair	USP7 deubiquitylates and stabilizes RNF168 to promote ubiquitin-dependent DNA damage signaling	Affinity capture-wesstern, reconstituted complex	Zhu Q (2015)
USP7	WWP2	Ataxias	-	Affinity capture-MS, two hybrid (high throughput)	Chaudhary N (2014)
USP7	PJA1	-	-	affinity capture-MS, biochemical activity	Huttlin EL (2017)
USP7	UBE2E3	-	-	Affinity capture-MS	Huttlin EL (2017)
USP7	TRIM63	-	-	Biochemical activity (high throughput)	Loch CM (2012)
USP7	RFFL	-	-	Biochemical activity (high throughput)	Loch CM (2012)
USP7	HECW1	Ataxias	-	Two-hybrid (high throughput)	Lim J (2006)
Usp7	RNF169	DNA damage repair	USP7 deubiquitylates and stabilizes RNF169 to promote double-strand break repair	Affinity capture-MS, affinity capture-western, biochemical activity, co-crystal structure, reconstituted complex	Hein MY (2015)

DUB	E3	Pathway	Interaction/ model	Methodology	Citation
Usp7	TRIM27	TNF-α-induced apoptosis	TRIM27 functions to regulate TNF-α-induced apoptosis by forming a complex with USP7 to deubiquitylate RIP1	Affinity capture-MS, affinity capture-western, two-hybrid (high throughput)	Hein MY (2015)
Usp7	UHRF1	DNA damage repair	USP7 interacts with UHRF1 in a trimeric complex with DNA methyltransferase -1 (DNMT1) whereby USP7 deubiquitylates and stabilizes UHRF1 and stimulates the methylation activity of DNMT1	Affinity capture-MS, affinity capture-western, biochemical activity, co-crystal structure, reconstituted complex	Ma H (2012)
USP8	NRDP1/ RNF41	Membrane receptor trafficking/cytokine receptor sorting and processing	Balanced reciprocal cross-regulation of RNF41 and USP8 regulates receptor trafficking and stability	Affinity capture-MS, affinity capture-western, co-crystal structure, FRET, reconstituted complex, two-hybrid	Cao Z (2007)
USP8	RNF128/ GRAIL	T cell receptor signaling; T cell anergy	USP8 interacts in a complex with otubain 1 and GRAIL in order to regulate GRAIL ubiquitylation state	Affinity capture-Western	Soares L (2004)
USP8	PJA1	-	-	Biochemical activity (high throughput)	Loch CM (2012)
USP8	TRIM63	-	-	Biochemical activity (high throughput)	Loch CM (2012)
USP9X	ITCH	Receptor signaling pathways (EGFR)	USP9X stabilizes ITCH by removing autoubiquitylation events	Affinity capture-MS, affinity capture-western, reconstituted complex	O'Connor HF (2015)
USP9X	SMURF1	Receptor signaling and trafficking	USP9X stabilizes SMURF by removing autoubiquitylation events	Affinity capture-MS, affinity capture-western, reconstituted complex	Xie Y (2013)

DUB	E3	Pathway	Interaction/ model	Methodology	Citation
USP9X	MARCH7-	immune, neuronal, and embryonic stem cell pathways	MARCH7 undergoes compartment specific-deubiquitylation by USP9X in the cytosol and USP7 in the nucleus	Affinity capture-MS, affinity capture-western	Agrawal P (2012)
USP9X	VHL	Cell proliferation	USP9X destabilizes pVHL to promote cell proliferation	Affinity capture-western, reconstituted complex	Zhang C (2016)
USP9X	HUWE1/MULE	Cell proliferation	USP9X interacts in a coplex with MULE and the pro-survival protein MCL1 to regulate MCL1 stability and promote tumour cell survival	Affinity capture-western	Gomez-Bougie P (2011)
USP9X	WWP1	-	-	Affinity capture-MS	Huttlin EL (2014/pre-pub)
USP9X	WWP2	-	-	Affinity capture-MS	Chaudhary N (2014)
USP9X	MIB1	DNA damage repair	-	Affinity capture-MS	Wang J (2013)
USP9X	PJA1	mTOR signaling	USP9X is a negative regulator of mTOR activity and muscle differentiation	Affinity capture-MS	Agrawal P (2012)
USP9X	UBR4	-	-	Co-fractionation (high throughput)	Havugimana PC (2012)
USP9X	LNX1	-	-	Affinity capture-MS	Lenihan JA (2017)
USP9X	HECW2/NEDL2	-	-	Affinity capture-MS	Lu L (2013)
USP10	RNF168	Topoisomerase II function/DNA replication, recombination, and transcription	USP10 interacts with RNF168 and opposes RNF168-mediated ubiquitylation of TOP2α and restricts TOP2α binding to chromatin	Affinity capture-MS, affinity capture-western	Guturi KK (2016)

DUB	E3	Pathway	Interaction/ model	Methodology	Citation
USP10	TRAF6	NFκB signaling	USP10 interacts in a complex with TANK and MCPIP1 in order to deubiquitylate TRAF6 and attenuate NFκB activation	Affinity capture-western	Wang W (2015)
USP10	MDM2	p53 pathway	After DNA damage USP10 translocates into the nucleus and reverses the activity of MDM2 to stabilize p53	Affinity capture-western	Yuan J (2010)
USP10	HECW2/NEDL2	-	-	Affinity capture-MS	Lu L (2013)
USP11	XIAP	Apoptosis	USP11 exhibits pro-survival activity by stabilizing XIAP and promoting tumor initiation and progression	Affinity capture-MS, Affinity capture-western	Sowa ME (2009)
USP11	MYCB2	-	-	Affinity capture-MS	Sowa ME (2009)
USP12	ITCH	Notch signaling	USP12 acts as a negative regulator of the Notch pathway by reversing ITCH-mediated ubiquitylation of Notch ligand	Affinity capture-western, proximity label-MS	Moretti J (2012)
USP12	CBLB	T-cell receptor signaling	Usp12 deubiquitylates and prevents lysosomal degradation of LAT and Trat1 to maintain the proximal TCR complex for the duration of signaling	Proximity label-MS	Jahan AS (2016)
USP12	MDM2	p53 pathway	USP12 negatively regulates p53 stability by deubiquitylating MDM2	Affinity capture-western	McClurg UL (2018)

DUB	E3	Pathway	Interaction/ model	Methodology	Citation
USP13	gp78/AMFR	ERAD	USP13 reverses gp78-mediated ubiquitylation of UBL4A to promote ERAD	Affinity capture-western, reconstituted complex	Liu Y (2014)
USP13	SIAH2	Hypoxia; MAPK signaling	USP13 Enzyme Regulates Siah2 Ligase Stability and Activity via Noncatalytic Ubiquitin-binding Domains	Affinity capture-western, reconstituted complex	Scortegagna M (2011)
USP13	TRIM63/MURF1	-	-	Two-hybrid	McElhinny AS (2002)
USP13	ITCH	-	-	Affinity capture-MS	Sowa ME (2009)
USP13	SKP2	Cell cycle control	nuclear Ufd1 recruits the deubiquitinating enzyme USP13 to counteract APC/C(Cdh1)-mediated ubiquitination of Skp2	Affinity capture-western	Chen M (2011)
USP13	UBE3C	-	-	Co-fractionation (high throughput)	Havugimana PC (2012)
USP14	UBE3A	-	-	Co-fractionation (high throughput), Affinity capture-MS	Havugimana PC (2012)
USP15	RNF40	-	-	Affinity capture-MS, Affinity capture-western	Sowa ME (2009)
USP15	SMURF2	TGFβ signaling pathway	USP15 deubiquitylates SMURF2 which results in enhanced stability of TGFβ receptor and downstream pathway activation	Affinity capture-western, biochemical activity	Iyengar PV (2015)
USP15	MYCBP2	-	-	Affinity capture-MS	Huttlin EL (2014/pre-pub)

DUB	E3	Pathway	Interaction/ model	Methodology	Citation
USP15	RNF20	Transcription; histone ubiquitylation	In the nucleus USP15 indirectly associates with the RNF20/RNF40 E3 ubiquitin ligase complex and the splicing machinery component SART3. USP15 association with SART3 promotes deubiquitylation of histone 2B (H2B)	Affinity capture-MS, Affinity capture-western	Huttlin EL (2014/pre-pub)
USP15	WWP2	-	-	Affinity capture-MS	Chaudhary N (2014)
USP15	MDM2	p53 pathway; TGFβ signaling	TGFβ signaling upregulates translation of USP15 to promote p53 stability. USP15 competitively recognizes both p53 and MDM2.	Reconstituted complex	Liu WT (2016)
USP15	HERC1	-	-	Affinity capture-MS	Kotani Y (2017)
USP15	β-TrCP	WNT signaling	USP15 antagonizes β-TrCP-mediated ubiquitylation of β-catenin, preventing its proteasomal degradation	Affinity capture-western	Greenblatt MB (2016)
USP15	TRIM63	-	-	Biochemical activity (high throughput)	Loch CM (2012)
USP15	TRAF6	-	USP15 interacts with TRAF6 and removes K63-linked polyubiquitylation of TRAF6	Biochemical activity	Bremm A (2010)
USP15	HUWE1	-	-	Affinity capture-MS	Thompson JW (2014)
USP15	SMURF1	-	-	Affinity capture-MS	Xie Y (2013)

DUB	E3	Pathway	Interaction/ model	Methodology	Citation
USP16	HERC2	DNA damage repair	USP16 interacts with HERC2 to fine-tune the ubiquitylation state of histone H2A during DNA damage repair	Affinity capture-MS, affinity capture-western	Sowa ME (2009)
USP16	NEURL4	-	-	Affinity capture-MS	Huttlin EL (2017)
USP16	RNF8	DNA damage repair	USP16 interacts in a complex with RNF8 and HERC2 to negatively regulate cellular response to DNA damage	Affinity capture-western	Zhang Z (2014)
USP18	SKP2	Type 1 IFN signaling	SKP2 regulates the stability of USP18, an ISG15 isopeptidase	Affinity capture-western, reconstituted complex, two-hybrid	Tokarz S (2004)
USP18	HERC1	-	-	Affinity capture-MS	Huttlin EL (2015)
USP19	SIAH1	Hypoxia	SIAH1 and SIAH2 promote USP19 ubiquitylation and proteasomal degradation	Affinity capture-western, co-crystal structure, protein-peptide, reconstituted complex, two-hybrid	Velasco K (2013)
USP19	SIAH2	Hypoxia	SIAH1 and SIAH2 promote USP19 ubiquitylation and proteasomal degradation	Affinity capture-western, two-hybrid	Altun M (2012)
USP19	SKP2	-	-	Affinity capture-MS	Huttlin EL (2017)
USP19	STUB1/CHIP	ERAD	USP19 interacts with the E3 ubiquitin ligase CHIP and the chaperone HSP90 in order to regulate the ubiquitylation status of misfolded proteins to promote ERAD	Affinity capture-western	He WT (2016)

DUB	E3	Pathway	Interaction/ model	Methodology	Citation
USP19	HERC2	-	-	Affinity capture-MS	Sowa ME (2009)
USP19	XIAP	TNF-α-induced apoptosis	USP19 regulates the stability of XIAP and enhances TNFα-induced caspase activation and apoptosis	Affinity capture-western	Mei Y (2011)
USP19	NEURL4	-	-	Affinity capture-MS	Sowa ME (2009)
USP20	HERC2	DNA damage repair; DNA replication stress response	HERC2-USP20 axis regulates DNA damage checkpoint through Claspin	Affinity capture-MS, affinity capture-western, Biochemical activity	Sowa ME (2009)
USP20	VHL	-	USP20 can be ubiquitylated and degraded in a pVHL-dependent manner	Affinity capture-western, biochemical activity, reconstituted complex, two-hybrid	Li Z (2002)
USP20	TRAF6	NFκB signaling	USP20 interacts with and deubiquitylates TRAF6 in a β-arrestin2-dependent manner. USP20 functions as a negative regulator of TLR4-mediated activation of NFκB signaling by reversing ubiquitylation of β-arrestin2	Affinity capture-western, reconstituted complex	Jean-Charles PY (2016)
USP20	NEURL4	-	-	Affinity capture-MS, affinity capture-western	Sowa ME (2009)
USP20	PJA1	-	-	Biochemical activity (high throughput)	Loch CM (2012)
USP21/USP23	TRIM63	-	-	Biochemical activity (high throughput)	Loch CM (2012)
USP21/USP23	TRAF6	-	-	Biochemical activity	Bremm A (2010)
USP21/USP23	HECW2/NEDL2	-	-	Affinity capture-MS	Lu L (2013)

DUB	E3	Pathway	Interaction/ model	Methodology	Publication
USP21/ USP23	CBL	-	-	Two-hybrid (high throughput)	Hayes SD (2012)
USP21/ USP23	CBLC	-	-	Two-hybrid (high throughput)	Hayes SD (2012)
USP24	WWP2	-	-	Affinity capture-MS	Chaudhary N (2014)
USP25	RNF41	-	-	Affinity capture-MS	Huttlin EL (2014/pre-pub)
USP26	MDM2	p53 pathway	USP26 deubiquitylates and stabilizes MDM2 resulting in decreased stability of the tumor suppressor p53	Affinity capture-western	Lahav-Baratz S (2017)
USP28	RCHY1/PIRH2	DNA damage repair	USP28 interacts in a complex with PIRH2 and the DNA damage checkpoint protein CHK2. USP28 antagonizes PIRH2-mediated polyubiquitylation and proteasomal degradation of CHK2	Affinity capture-western	Bohgaki M (2013)
USP28	MAP3K1	-	-	Biochemical activity	Charlaftis N (2014)
USP28	FBXW7	MYC	USP28 is required for MYC stability. USP28 binds MYC through an interaction with FBXW7, an F-box protein that is part of an SCF-type E3 ubiquitin ligase. USP28 stabilizes MYC in the nucleus. In the nucleolus FBXW7 ubiquitylates MYC and targets it for degradation	Affinity capture-western	Popov N (2007)
USP28	RFFL	-	-	Biochemical activity (high throughput)	Loch CM (2012)
USP28	PJA1	-	-	Biochemical activity (high throughput)	Loch CM (2012)

DUB	E3	Pathway	Interaction/model	Methodology	Citation
USP28	TRIM63	-	-	Biochemical activity (high throughput)	Loch CM (2012)
USP30	PARK2	Mitophagy	Parkin interacts with and ubiquitylates USP30 to target USP30 for degradation. USP30 antagonizes mitophagy by deubiquitylating mitochondrial proteins.	Biochemical activity	Gersch M (2017)
USP33	VHL	-	pVHL ubiquitylates and destabilizes USP33	Affinity capture-western, biochemical activity, reconstituted complex, two-hybrid	Li Z (2002)
USP33	TRAF6	NFκB signaling	USP33 negatively regulates NFκB activation by deubiquitylating TRAF6	Affinity capture-western	Yasunaga J (2011)
USP33	β-TrCP	β-catenin signaling	USP33 is negatively regulated by β-TrCP and ubiquitin-dependent proteolysis	Affinity capture-western	Cheng Q (2017)
USP33	NEURL4	Centorsome biogenesis	USP33 interacts in a complex with NEURL4 centriolar protein CP110 to regulate CP110 ubiquitylation state and stability	Affinity capture-western	Li J (2013)
USP33	TRIM63	-	-	Biochemical activity (high throughput)	Loch CM (2012)
USP35	SMURF2	-	-	Affinity capture-MS (high throughput)	Hein MY (2015)
USP36	NEDD4L	Neurotrophin receptor signaling	USP36 regulates degradation of TrkA neurotrophin receptor by regulating NEDD4L interactions with TrKA	Affinity capture-Western	Anta B (2016)

DUB	E3	Pathway	Interaction/ model	Methodology	Citation
USP36	FBXW7	Myc	USP36 reverses FBXW7-mediated ubiquitylation of MYC to stabilize MYC and promote cancer progression	Affinity capture-western	Sun XX (2015)
USP36	PJA1	-	-	Affinity capture-MS	Huttlin EL (2015)
USP36	SHPRH	-	-	Affinity capture-MS	Sowa ME (2009)
UP37	β-TrCP	Cell cycle control	SCF-BTRCP regulates USP37 stability during G2-phase to promote mitotic entry	Affinity capture-MS, affinity capture-western, biochemical activity, proximity label-MS	Huttlin EL (2017)
USP39	TRAF6	-	-	Two-hybrid (high throughput)	Hayes SD (2012)
USP39	ARIH1	-	-	Affinity capture-MS	Scott DC (2016)
USP42	MDM2	p53 signaling	USP42 forms a direct complex with p53 and controls level of ubiquitination during the early phase of the response to a range of stress signals	Affinity capture-western	Hock AK (2011)
USP42	HERC2	-	-	Affinity capture-MS	Sowa ME (2009)
USP46	PJA2	-	-	Affinity capture-MS	Sowa ME (2009)
USP47	β-TrCP	Cell cycle control	USP47 interacts with BTRCP to regulate cell growth and survival	Affinity capture-MS, Affinity capture-western, proximity label-MS	Sowa ME (2009)
USP48	MDM2	p53 signaling	USP48 binds Mdm2 and promotes Mdm2 stability and enhances Mdm2-mediated p53 ubiquitination and degradation	Affinity capture-western	Cetkovska K (2017)
USP49	UBR5	-	-	Affinity capture-MS	Sowa ME (2009)

DUB	E3	Pathway	Interaction/ model	Methodology	Citation
USP49	SHPRH	-	-	Affinity capture-MS	Sowa ME (2009)
USP49	HUWE1	-	-	Affinity capture-MS	Sowa ME (2009)
USP50	HUWE1	-	-	Affinity capture-MS	Sowa ME (2009)
USP51	PJA1	-	-	Biochemical activity (high throughput)	Loch CM (2012)
USP54	BTRC	Cellular stress response	-	Proximity label-MS (high throughput)	Coyaud E (2015)
A20	TRAF6	NFKB pathway	The NFκB response to TLR activation is attenuated through a mechanism in which TRAF6 is deubiquitylated by A20	Affinity capture-western, biochemical activity, two-hybrid	Heyninck K (1999)
A20	RNF168	DNA damage response	A20/TNFAIP3 binds and inhibits the E3 ubiquitin ligase RNF168, which is responsible for regulating histone H2A turnover critical for proper DNA repair	Affinity capture-western, reconstituted complex	Yang C (2018)
A20	NEDD4L	-	-	Affinity capture-MS	Huttlin EL (2017)
A20	ARIH1	-	-	Affinity capture-MS	Huttlin EL (2017)
A20	RNF5	-	-	Two-hybrid (high throughput)	Hayes SD (2012)
VCIP135	RNF411	-	-	Affinity capture-MS	Huttlin EL (2014/pre-pub)
VCIP135	HUWE1	-	-	Affinity capture-MS	Sowa ME (2009)
VCIP135	BTRC	-	-	Proximity label-MS	Coyaud E (2015)
VCIP135	MDM2	p53 signaling	-	Affinity capture-MS	Zhao K (2018)
POH1	UBE3A	Proteasomal regulation	-	Affinity capture-MS, affinity capture-Western	Wang X (2007)

DUB	E3	Pathway	Interaction/ model	Methodology	Citation
POH1	HUWE1	-	-	Affinity capture-MS, affinity capture-western	Thompson JW (2014)
POH1	UBE3C	Proteasomal regulation	-	Affinity capture-MS, affinity capture-Western	Wang X (2007)
POH1	HERC2	Proteasomal regulation	-	Affinity capture-MS, Affinity capture-western	Jacobson AD (2014)
POH1	UBR4	Proteasomal regulation	-	Affinity capture-MS, affinity capture-western	Jacobson AD (2014)
POH1	STUB1	-	-	Co-fractionation	Havugimana PC (2012)
POH1	PARK2	Mitophagy	-	Affinity capture-MS	Sarraf SA (2013)
POH1	AMFR	ERAD	-	Affinity capture-MS	Christianson JC (2012)
AMSH	SMURF2	-	RNF11 recruits AMSH to Smurf2 for ubiquitination, leading to its degradation by the 26S proteasome	Affinity capture-western	Li H (2004)
AMSH	TRAF6	-	-	Biochemical activity	Bremm A (2010)
AMSH	PJA1	-	-	Biochemical activity (high throughput)	Loch CM (2012)
CSN5	DTL	DNA damage response	-	Affinity capture-MS, affinity capture-western	Bennett EJ (2010)
CSN5	MDM2	p53 signaling	CSN5 stabilizes MDM2 through reducing MDM2 self-ubiquitination and decelerating turnover rate of MDM2 and thereby regulates p53 stability	Affinity capture-western, reconstituted complex	Zhang XC (2008)
CSN5	SKP2	-	-	Affinity capture-MS	Sowa ME (2009)
CSN5	RNF138	-	-	Affinity capture-MS	Bennett EJ (2010)
CSN5	RFWD2	-	-	Affinity capture-MS	Olma MH (2009)

DUB	E3	Pathway	Interaction/ model	Methodology	Citation
CSN5	RBX1	-	-	Affinity capture-MS	Olma MH (2009)
BRCC36	HUWE1	-	-	Co-fractionation	Kristensen AR (2012)
BRCC36	WWP2	-	-	Affinity capture-MS	Chaudhary N (2014)
OTUB1	RNF128/GRAIL	T cell anergy	The two isoforms of OTUB1 have opposing epistatic functions in controlling the stability of GRAIL expression and the resultant anergy phenotype in T cell	Affinity capture-western, reconstituted complex, two-hybrid	Soares L (2004)
OTUB1	TRAF6	NFKB signaling	OTUB1 and OTUB2 negatively regulate virus-triggered type I IFN induction and cellular antiviral response by deubiquitinating TRAF3 and -6	Affinity capture-western, biochemical activity	Li S (2010)
OTUB1	RFFL	-	-	Biochemical activity	Loch CM (2012)
OTUB1	TRIM63	-	-	Biochemical activity	Loch CM (2012)
OTUB1	PJA1	-	-	Biochemical activity	Loch CM (2012)
OTUB1	STUB1	-	-	Affinity capture-MS	Scholz CC (2016)

REFERENCES

Ahmed, N., Zeng, M., Sinha, I., Polin, L., Wei, W.Z., Rathinam, C., Flavell, R., Massoumi, R., and Venuprasad, K. (2011). The E3 ligase Itch and deubiquitinase Cyld act together to regulate Tak1 and inflammation. Nat Immunol *12*, 1176-1183.

Akutsu, M., Dikic, I., and Bremm, A. (2016). Ubiquitin chain diversity at a glance. J Cell Sci *129*, 875-880.

Blount, J.R., Burr, A.A., Denuc, A., Marfany, G., and Todi, S.V. (2012). Ubiquitin-specific protease 25 functions in Endoplasmic Reticulum-associated degradation. PLoS One *7*, e36542.

Cadavid, A.L., Ginzel, A., and Fischer, J.A. (2000). The function of the Drosophila fat facets deubiquitinating enzyme in limiting photoreceptor cell number is intimately associated with endocytosis. Development *127*, 1727-1736.

Chen, B., Mariano, J., Tsai, Y.C., Chan, A.H., Cohen, M., and Weissman, A.M. (2006). The activity of a human endoplasmic reticulum-associated degradation E3, gp78, requires its Cue domain, RING finger, and an E2-binding site. Proc Natl Acad Sci U S A *103*, 341-346.

Chen, X., Zhang, B., and Fischer, J.A. (2002). A specific protein substrate for a deubiquitinating enzyme: Liquid facets is the substrate of Fat facets. Genes Dev *16*, 289-294.

Ciechanover, A., Heller, H., Elias, S., Haas, A.L., and Hershko, A. (1980). ATP-dependent conjugation of reticulocyte proteins with the polypeptide required for protein degradation. Proc Natl Acad Sci U S A *77*, 1365-1368.

Clague, M.J., Coulson, J.M., and Urbé, S. (2012). Cellular functions of the DUBs. J Cell Sci *125*, 277-286.

Clague, M.J., and Urbé, S. (2010). Ubiquitin: same molecule, different degradation pathways. Cell *143*, 682-685.

Clague, M.J., Urbé, S., and Komander, D. (2019). Breaking the chains: deubiquitylating enzyme specificity begets function. Nat Rev Mol Cell Biol *20*, 338-352.

Ding, Y., Zhang, Y., Xu, C., Tao, Q.H., and Chen, Y.G. (2013). HECT domain-containing E3 ubiquitin ligase NEDD4L negatively regulates Wnt signaling by targeting dishevelled for proteasomal degradation. J Biol Chem *288*, 8289-8298.

Ernst, R., Mueller, B., Ploegh, H.L., and Schlieker, C. (2009). The otubain YOD1 is a deubiquitinating enzyme that associates with p97 to facilitate protein dislocation from the ER. Mol Cell *36*, 28-38.

Fan, Y., Yu, Y., Mao, R., Zhang, H., and Yang, J. (2011). TAK1 Lys-158 but not Lys-209 is required for IL-1β-induced Lys63-linked TAK1 polyubiquitination and IKK/NF-κB activation. Cell Signal *23*, 660-665.

Fan, Y., Yu, Y., Shi, Y., Sun, W., Xie, M., Ge, N., Mao, R., Chang, A., Xu, G., Schneider, M.D.*, et al.* (2010). Lysine 63-linked polyubiquitination of TAK1 at lysine 158 is required for tumor necrosis factor alpha- and interleukin-1beta-induced IKK/NF-kappaB and JNK/AP-1 activation. J Biol Chem *285*, 5347-5360.

Felle, M., Joppien, S., Németh, A., Diermeier, S., Thalhammer, V., Dobner, T., Kremmer, E., Kappler, R., and Längst, G. (2011). The USP7/Dnmt1 complex stimulates the DNA methylation activity of Dnmt1 and regulates the stability of UHRF1. Nucleic

Acids Res *39*, 8355-8365.
Finley, D. (2009). Recognition and processing of ubiquitin-protein conjugates by the proteasome. Annu Rev Biochem *78*, 477-513.
Graner, E., Tang, D., Rossi, S., Baron, A., Migita, T., Weinstein, L.J., Lechpammer, M., Huesken, D., Zimmermann, J., Signoretti, S.*, et al.* (2004). The isopeptidase USP2a regulates the stability of fatty acid synthase in prostate cancer. Cancer Cell *5*, 253-261.
He, Y., Hryciw, D.H., Carroll, M.L., Myers, S.A., Whitbread, A.K., Kumar, S., Poronnik, P., and Hooper, J.D. (2008). The ubiquitin-protein ligase Nedd4-2 differentially interacts with and regulates members of the Tweety family of chloride ion channels. J Biol Chem *283*, 24000-24010.
Hershko, A., Ciechanover, A., Heller, H., Haas, A.L., and Rose, I.A. (1980). Proposed role of ATP in protein breakdown: conjugation of protein with multiple chains of the polypeptide of ATP-dependent proteolysis. Proc Natl Acad Sci U S A *77*, 1783-1786.
Hershko, A., Ciechanover, A., and Rose, I.A. (1979). Resolution of the ATP-dependent proteolytic system from reticulocytes: a component that interacts with ATP. Proc Natl Acad Sci U S A *76*, 3107-3110.
Hershko, A., Heller, H., Elias, S., and Ciechanover, A. (1983). Components of ubiquitin-protein ligase system. Resolution, affinity purification, and role in protein breakdown. J Biol Chem *258*, 8206-8214.
Hryciw, D.H., Ekberg, J., Lee, A., Lensink, I.L., Kumar, S., Guggino, W.B., Cook, D.I., Pollock, C.A., and Poronnik, P. (2004). Nedd4-2 functionally interacts with ClC-5: involvement in constitutive albumin endocytosis in proximal tubule cells. J Biol Chem *279*, 54996-55007.
Huang, X., and Dixit, V.M. (2016). Drugging the undruggables: exploring the ubiquitin system for drug development. Cell Res *26*, 484-498.
Huang, Y., Baker, R.T., and Fischer-Vize, J.A. (1995). Control of cell fate by a deubiquitinating enzyme encoded by the fat facets gene. Science *270*, 1828-1831.
Husnjak, K., and Dikic, I. (2012). Ubiquitin-binding proteins: decoders of ubiquitin-mediated cellular functions. Annu Rev Biochem *81*, 291-322.
Ingham, R.J., Gish, G., and Pawson, T. (2004). The Nedd4 family of E3 ubiquitin ligases: functional diversity within a common modular architecture. Oncogene *23*, 1972-1984.
Jana, N.R. (2012). Protein homeostasis and aging: role of ubiquitin protein ligases. Neurochem Int *60*, 443-447.
Kim, H.C., and Huibregtse, J.M. (2009). Polyubiquitination by HECT E3s and the determinants of chain type specificity. Mol Cell Biol *29*, 3307-3318.
Kim, R.Q., and Sixma, T.K. (2017). Regulation of USP7: A High Incidence of E3 Complexes. J Mol Biol *429*, 3395-3408.
Komander, D., Clague, M.J., and Urbé, S. (2009). Breaking the chains: structure and function of the deubiquitinases. Nat Rev Mol Cell Biol *10*, 550-563.
Komander, D., and Rape, M. (2012). The ubiquitin code. Annu Rev Biochem *81*, 203-229.
Koyano, F., Okatsu, K., Kosako, H., Tamura, Y., Go, E., Kimura, M., Kimura, Y., Tsuchiya, H., Yoshihara, H., Hirokawa, T.*, et al.* (2014). Ubiquitin is phosphorylated by PINK1 to activate parkin. Nature *510*, 162-166.
Kushwaha, D., O'Leary, C., Cron, K.R., Deraska, P., Zhu, K., D'Andrea, A.D., and

Kozono, D. (2015). USP9X inhibition promotes radiation-induced apoptosis in non-small cell lung cancer cells expressing mid-to-high MCL1. Cancer Biol Ther *16*, 392-401.
Lee, S., Tumolo, J.M., Ehlinger, A.C., Jernigan, K.K., Qualls-Histed, S.J., Hsu, P.C., McDonald, W.H., Chazin, W.J., and MacGurn, J.A. (2017). Ubiquitin turnover and endocytic trafficking in yeast are regulated by Ser57 phosphorylation of ubiquitin. Elife *6*.
Li, W., and Ye, Y. (2008). Polyubiquitin chains: functions, structures, and mechanisms. Cell Mol Life Sci *65*, 2397-2406.
Lin, A., Hou, Q., Jarzylo, L., Amato, S., Gilbert, J., Shang, F., and Man, H.Y. (2011). Nedd4-mediated AMPA receptor ubiquitination regulates receptor turnover and trafficking. J Neurochem *119*, 27-39.
Liu, Y., Soetandyo, N., Lee, J.G., Liu, L., Xu, Y., Clemons, W.M., and Ye, Y. (2014). USP13 antagonizes gp78 to maintain functionality of a chaperone in ER-associated degradation. Elife *3*, e01369.
MacGurn, J.A., Hsu, P.C., and Emr, S.D. (2012). Ubiquitin and membrane protein turnover: from cradle to grave. Annu Rev Biochem *81*, 231-259.
Mouchantaf, R., Azakir, B.A., McPherson, P.S., Millard, S.M., Wood, S.A., and Angers, A. (2006). The ubiquitin ligase itch is auto-ubiquitylated in vivo and in vitro but is protected from degradation by interacting with the deubiquitylating enzyme FAM/USP9X. J Biol Chem *281*, 38738-38747.
Murtaza, M., Jolly, L.A., Gecz, J., and Wood, S.A. (2015). La FAM fatale: USP9X in development and disease. Cell Mol Life Sci *72*, 2075-2089.
Overstreet, E., Fitch, E., and Fischer, J.A. (2004). Fat facets and Liquid facets promote Delta endocytosis and Delta signaling in the signaling cells. Development *131*, 5355-5366.
Paudel, P., Zhang, Q., Leung, C., Greenberg, H.C., Guo, Y., Chern, Y.H., Dong, A., Li, Y., Vedadi, M., Zhuang, Z.*, et al.* (2019). Crystal structure and activity-based labeling reveal the mechanisms for linkage-specific substrate recognition by deubiquitinase USP9X. Proc Natl Acad Sci U S A *116*, 7288-7297.
Paul, S. (2008). Dysfunction of the ubiquitin-proteasome system in multiple disease conditions: therapeutic approaches. Bioessays *30*, 1172-1184.
Potu, H., Peterson, L.F., Kandarpa, M., Pal, A., Sun, H., Durham, A., Harms, P.W., Hollenhorst, P.C., Eskiocak, U., Talpaz, M.*, et al.* (2017). Usp9x regulates Ets-1 ubiquitination and stability to control NRAS expression and tumorigenicity in melanoma. Nat Commun *8*, 14449.
Prives, C. (1998). Signaling to p53: breaking the MDM2-p53 circuit. Cell *95*, 5-8.
Pérez-Mancera, P.A., Rust, A.G., van der Weyden, L., Kristiansen, G., Li, A., Sarver, A.L., Silverstein, K.A., Grützmann, R., Aust, D., Rümmele, P.*, et al.* (2012). The deubiquitinase USP9X suppresses pancreatic ductal adenocarcinoma. Nature *486*, 266-270.
Reinstein, E., and Ciechanover, A. (2006). Narrative review: protein degradation and human diseases: the ubiquitin connection. Ann Intern Med *145*, 676-684.
Ritorto, M.S., Ewan, R., Perez-Oliva, A.B., Knebel, A., Buhrlage, S.J., Wightman, M., Kelly, S.M., Wood, N.T., Virdee, S., Gray, N.S.*, et al.* (2014). Screening of DUB activity and specificity by MALDI-TOF mass spectrometry. Nat Commun *5*, 4763.
Rotin, D., and Kumar, S. (2009). Physiological functions of the HECT family of ubiquitin

ligases. Nat Rev Mol Cell Biol *10*, 398-409.
Schwickart, M., Huang, X., Lill, J.R., Liu, J., Ferrando, R., French, D.M., Maecker, H., O'Rourke, K., Bazan, F., Eastham-Anderson, J.*, et al.* (2010). Deubiquitinase USP9X stabilizes MCL1 and promotes tumour cell survival. Nature *463*, 103-107.
Stevenson, L.F., Sparks, A., Allende-Vega, N., Xirodimas, D.P., Lane, D.P., and Saville, M.K. (2007). The deubiquitinating enzyme USP2a regulates the p53 pathway by targeting Mdm2. EMBO J *26*, 976-986.
Tavana, O., and Gu, W. (2017). Modulation of the p53/MDM2 interplay by HAUSP inhibitors. J Mol Cell Biol *9*, 45-52.
Vucic, D., Dixit, V.M., and Wertz, I.E. (2011). Ubiquitylation in apoptosis: a post-translational modification at the edge of life and death. Nat Rev Mol Cell Biol *12*, 439-452.
Wang, Q., Li, L., and Ye, Y. (2006). Regulation of retrotranslocation by p97-associated deubiquitinating enzyme ataxin-3. J Cell Biol *174*, 963-971.
Wertz, I.E., O'Rourke, K.M., Zhou, H., Eby, M., Aravind, L., Seshagiri, S., Wu, P., Wiesmann, C., Baker, R., Boone, D.L.*, et al.* (2004). De-ubiquitination and ubiquitin ligase domains of A20 downregulate NF-kappaB signalling. Nature *430*, 694-699.
Wu, H.T., Kuo, Y.C., Hung, J.J., Huang, C.H., Chen, W.Y., Chou, T.Y., Chen, Y., Chen, Y.J., Cheng, W.C., Teng, S.C.*, et al.* (2016). K63-polyubiquitinated HAUSP deubiquitinates HIF-1α and dictates H3K56 acetylation promoting hypoxia-induced tumour progression. Nat Commun *7*, 13644.
Xie, Y., Avello, M., Schirle, M., McWhinnie, E., Feng, Y., Bric-Furlong, E., Wilson, C., Nathans, R., Zhang, J., Kirschner, M.W.*, et al.* (2013). Deubiquitinase FAM/USP9X interacts with the E3 ubiquitin ligase SMURF1 protein and protects it from ligase activity-dependent self-degradation. J Biol Chem *288*, 2976-2985.
Zhong, X., and Pittman, R.N. (2006). Ataxin-3 binds VCP/p97 and regulates retrotranslocation of ERAD substrates. Hum Mol Genet *15*, 2409-2420.

Abdul Rehman, S.A., Kristariyanto, Y.A., Choi, S.Y., Nkosi, P.J., Weidlich, S., Labib, K., Hofmann, K., and Kulathu, Y. (2016). MINDY-1 Is a Member of an Evolutionarily Conserved and Structurally Distinct New Family of Deubiquitinating Enzymes. Mol Cell *63*, 146-155.
Abriel, H., Loffing, J., Rebhun, J.F., Pratt, J.H., Schild, L., Horisberger, J.D., Rotin, D., and Staub, O. (1999). Defective regulation of the epithelial Na+ channel by Nedd4 in Liddle's syndrome. J Clin Invest *103*, 667-673.
Ahmed, N., Zeng, M., Sinha, I., Polin, L., Wei, W.Z., Rathinam, C., Flavell, R., Massoumi, R., and Venuprasad, K. (2011). The E3 ligase Itch and deubiquitinase Cyld act together to regulate Tak1 and inflammation. Nat Immunol *12*, 1176-1183.
Akutsu, M., Dikic, I., and Bremm, A. (2016). Ubiquitin chain diversity at a glance. J Cell Sci *129*, 875-880.
Allache, R., Wang, M., De Marco, P., Merello, E., Capra, V., and Kibar, Z. (2015). Genetic studies of ANKRD6 as a molecular switch between Wnt signaling pathways in human neural tube defects. Birth Defects Res A Clin Mol Teratol *103*, 20-26.
Amerik, A.Y., Li, S.J., and Hochstrasser, M. (2000). Analysis of the deubiquitinating enzymes of the yeast Saccharomyces cerevisiae. Biol Chem *381*, 981-992.
Angers, S., Thorpe, C.J., Biechele, T.L., Goldenberg, S.J., Zheng, N., MacCoss, M.J., and Moon, R.T. (2006). The KLHL12-Cullin-3 ubiquitin ligase negatively regulates the Wnt-beta-catenin pathway by targeting Dishevelled for degradation. Nat Cell Biol *8*, 348-357.
Bakowska, J.C., Jenkins, R., Pendleton, J., and Blackstone, C. (2005). The Troyer syndrome (SPG20) protein spartin interacts with Eps15. Biochem Biophys Res Commun *334*, 1042-1048.
Barnwal, R.P., Loh, E., Godin, K.S., Yip, J., Lavender, H., Tang, C.M., and Varani, G. (2016). Structure and mechanism of a molecular rheostat, an RNA thermometer that modulates immune evasion by Neisseria meningitidis. Nucleic Acids Res *44*, 9426-9437.
Bernassola, F., Karin, M., Ciechanover, A., and Melino, G. (2008). The HECT family of E3 ubiquitin ligases: multiple players in cancer development. Cancer Cell *14*, 10-21.
Blount, J.R., Burr, A.A., Denuc, A., Marfany, G., and Todi, S.V. (2012). Ubiquitin-specific protease 25 functions in Endoplasmic Reticulum-associated degradation. PLoS One *7*, e36542.
Botero-Velez, M., Curtis, J.J., and Warnock, D.G. (1994). Brief report: Liddle's syndrome revisited--a disorder of sodium reabsorption in the distal tubule. N Engl J Med *330*, 178-181.
Cadavid, A.L., Ginzel, A., and Fischer, J.A. (2000). The function of the Drosophila fat facets deubiquitinating enzyme in limiting photoreceptor cell number is intimately associated with endocytosis. Development *127*, 1727-1736.
Cao, L.G., Babcock, G.G., Rubenstein, P.A., and Wang, Y.L. (1992). Effects of profilin and profilactin on actin structure and function in living cells. J Cell Biol *117*, 1023-1029.
Castella, M., Jacquemont, C., Thompson, E.L., Yeo, J.E., Cheung, R.S., Huang, J.W., Sobeck, A., Hendrickson, E.A., and Taniguchi, T. (2015). FANCI Regulates Recruitment of the FA Core Complex at Sites of DNA Damage Independently of FANCD2. PLoS

Genet *11*, e1005563.
Chau, V., Tobias, J.W., Bachmair, A., Marriott, D., Ecker, D.J., Gonda, D.K., and Varshavsky, A. (1989). A multiubiquitin chain is confined to specific lysine in a targeted short-lived protein. Science *243*, 1576-1583.
Chen, B., Mariano, J., Tsai, Y.C., Chan, A.H., Cohen, M., and Weissman, A.M. (2006). The activity of a human endoplasmic reticulum-associated degradation E3, gp78, requires its Cue domain, RING finger, and an E2-binding site. Proc Natl Acad Sci U S A *103*, 341-346.
Chen, C., and Matesic, L.E. (2007). The Nedd4-like family of E3 ubiquitin ligases and cancer. Cancer Metastasis Rev *26*, 587-604.
Chen, H.I., Einbond, A., Kwak, S.J., Linn, H., Koepf, E., Peterson, S., Kelly, J.W., and Sudol, M. (1997). Characterization of the WW domain of human yes-associated protein and its polyproline-containing ligands. J Biol Chem *272*, 17070-17077.
Chen, X., Zhang, B., and Fischer, J.A. (2002). A specific protein substrate for a deubiquitinating enzyme: Liquid facets is the substrate of Fat facets. Genes Dev *16*, 289-294.
Ciechanover, A., Elias, S., Heller, H., Ferber, S., and Hershko, A. (1980a). Characterization of the heat-stable polypeptide of the ATP-dependent proteolytic system from reticulocytes. J Biol Chem *255*, 7525-7528.
Ciechanover, A., Heller, H., Elias, S., Haas, A.L., and Hershko, A. (1980b). ATP-dependent conjugation of reticulocyte proteins with the polypeptide required for protein degradation. Proc Natl Acad Sci U S A *77*, 1365-1368.
Ciechanover, A., Hod, Y., and Hershko, A. (2012). A heat-stable polypeptide component of an ATP-dependent proteolytic system from reticulocytes. 1978. Biochem Biophys Res Commun *425*, 565-570.
Clague, M.J., and Urbé, S. (2010). Ubiquitin: same molecule, different degradation pathways. Cell *143*, 682-685.
Clague, M.J., Urbé, S., and Komander, D. (2019). Breaking the chains: deubiquitylating enzyme specificity begets function. Nat Rev Mol Cell Biol *20*, 338-352.
Cohen, P., and Tcherpakov, M. (2010). Will the ubiquitin system furnish as many drug targets as protein kinases? Cell *143*, 686-693.
Colland, F., Formstecher, E., Jacq, X., Reverdy, C., Planquette, C., Conrath, S., Trouplin, V., Bianchi, J., Aushev, V.N., Camonis, J.*, et al.* (2009). Small-molecule inhibitor of USP7/HAUSP ubiquitin protease stabilizes and activates p53 in cells. Mol Cancer Ther *8*, 2286-2295.
Cooper, E.M., Cutcliffe, C., Kristiansen, T.Z., Pandey, A., Pickart, C.M., and Cohen, R.E. (2009). K63-specific deubiquitination by two JAMM/MPN+ complexes: BRISC-associated Brcc36 and proteasomal Poh1. EMBO J *28*, 621-631.
D'Arcy, P., Brnjic, S., Olofsson, M.H., Fryknäs, M., Lindsten, K., De Cesare, M., Perego, P., Sadeghi, B., Hassan, M., Larsson, R.*, et al.* (2011). Inhibition of proteasome deubiquitinating activity as a new cancer therapy. Nat Med *17*, 1636-1640.
David, D., Nair, S.A., and Pillai, M.R. (2013). Smurf E3 ubiquitin ligases at the cross roads of oncogenesis and tumor suppression. Biochim Biophys Acta *1835*, 119-128.
de Las Pozas, A., Reiner, T., De Cesare, V., Trost, M., and Perez-Stable, C. (2018). Inhibiting Multiple Deubiquitinases to Reduce Androgen Receptor Expression in Prostate Cancer Cells. Sci Rep *8*, 13146.

Debonneville, C., Flores, S.Y., Kamynina, E., Plant, P.J., Tauxe, C., Thomas, M.A., Münster, C., Chraïbi, A., Pratt, J.H., Horisberger, J.D.*, et al.* (2001). Phosphorylation of Nedd4-2 by Sgk1 regulates epithelial Na(+) channel cell surface expression. EMBO J *20*, 7052-7059.
Dexheimer, T.S., Rosenthal, A.S., Luci, D.K., Liang, Q., Villamil, M.A., Chen, J., Sun, H., Kerns, E.H., Simeonov, A., Jadhav, A.*, et al.* (2014). Synthesis and structure-activity relationship studies of N-benzyl-2-phenylpyrimidin-4-amine derivatives as potent USP1/UAF1 deubiquitinase inhibitors with anticancer activity against nonsmall cell lung cancer. J Med Chem *57*, 8099-8110.
Dikic, I., Wakatsuki, S., and Walters, K.J. (2009). Ubiquitin-binding domains - from structures to functions. Nat Rev Mol Cell Biol *10*, 659-671.
Ding, Y., Zhang, Y., Xu, C., Tao, Q.H., and Chen, Y.G. (2013). HECT domain-containing E3 ubiquitin ligase NEDD4L negatively regulates Wnt signaling by targeting dishevelled for proteasomal degradation. J Biol Chem *288*, 8289-8298.
Dong, Y., Hakimi, M.A., Chen, X., Kumaraswamy, E., Cooch, N.S., Godwin, A.K., and Shiekhattar, R. (2003). Regulation of BRCC, a holoenzyme complex containing BRCA1 and BRCA2, by a signalosome-like subunit and its role in DNA repair. Mol Cell *12*, 1087-1099.
Dunn, R., and Hicke, L. (2001). Domains of the Rsp5 ubiquitin-protein ligase required for receptor-mediated and fluid-phase endocytosis. Mol Biol Cell *12*, 421-435.
Eide, P.W., Cekaite, L., Danielsen, S.A., Eilertsen, I.A., Kjenseth, A., Fykerud, T.A., Ågesen, T.H., Bruun, J., Rivedal, E., Lothe, R.A.*, et al.* (2013). NEDD4 is overexpressed in colorectal cancer and promotes colonic cell growth independently of the PI3K/PTEN/AKT pathway. Cell Signal *25*, 12-18.
Ermekova, K.S., Zambrano, N., Linn, H., Minopoli, G., Gertler, F., Russo, T., and Sudol, M. (1997). The WW domain of neural protein FE65 interacts with proline-rich motifs in Mena, the mammalian homolog of Drosophila enabled. J Biol Chem *272*, 32869-32877.
Ernst, R., Mueller, B., Ploegh, H.L., and Schlieker, C. (2009). The otubain YOD1 is a deubiquitinating enzyme that associates with p97 to facilitate protein dislocation from the ER. Mol Cell *36*, 28-38.
Fan, Y., Yu, Y., Mao, R., Zhang, H., and Yang, J. (2011). TAK1 Lys-158 but not Lys-209 is required for IL-1β-induced Lys63-linked TAK1 polyubiquitination and IKK/NF-κB activation. Cell Signal *23*, 660-665.
Fan, Y., Yu, Y., Shi, Y., Sun, W., Xie, M., Ge, N., Mao, R., Chang, A., Xu, G., Schneider, M.D.*, et al.* (2010). Lysine 63-linked polyubiquitination of TAK1 at lysine 158 is required for tumor necrosis factor alpha- and interleukin-1beta-induced IKK/NF-kappaB and JNK/AP-1 activation. J Biol Chem *285*, 5347-5360.
Fei, C., He, X., Xie, S., Miao, H., Zhou, Z., and Li, L. (2014). Smurf1-mediated axin ubiquitination requires Smurf1 C2 domain and is cell cycle-dependent. J Biol Chem *289*, 14170-14177.
Fei, C., Li, Z., Li, C., Chen, Y., Chen, Z., He, X., Mao, L., Wang, X., Zeng, R., and Li, L. (2013). Smurf1-mediated Lys29-linked nonproteolytic polyubiquitination of axin negatively regulates Wnt/β-catenin signaling. Mol Cell Biol *33*, 4095-4105.
Felle, M., Joppien, S., Németh, A., Diermeier, S., Thalhammer, V., Dobner, T., Kremmer, E., Kappler, R., and Längst, G. (2011). The USP7/Dnmt1 complex stimulates the DNA methylation activity of Dnmt1 and regulates the stability of UHRF1. Nucleic

Acids Res *39*, 8355-8365.
Finley, D. (2009). Recognition and processing of ubiquitin-protein conjugates by the proteasome. Annu Rev Biochem *78*, 477-513.
Fu, P., Du, F., Liu, Y., Yao, M., Zhang, S., Zheng, X., and Zheng, S. (2017). WP1130 increases cisplatin sensitivity through inhibition of. Am J Transl Res *9*, 1783-1791.
Fulzele, A., and Bennett, E.J. (2018). Ubiquitin diGLY Proteomics as an Approach to Identify and Quantify the Ubiquitin-Modified Proteome. Methods Mol Biol *1844*, 363-384.
Gajewska, B., Kamińska, J., Jesionowska, A., Martin, N.C., Hopper, A.K., and Zoładek, T. (2001). WW domains of Rsp5p define different functions: determination of roles in fluid phase and uracil permease endocytosis in Saccharomyces cerevisiae. Genetics *157*, 91-101.
Galan, J.M., Moreau, V., Andre, B., Volland, C., and Haguenauer-Tsapis, R. (1996). Ubiquitination mediated by the Npi1p/Rsp5p ubiquitin-protein ligase is required for endocytosis of the yeast uracil permease. J Biol Chem *271*, 10946-10952.
Garty, H., and Palmer, L.G. (1997). Epithelial sodium channels: function, structure, and regulation. Physiol Rev *77*, 359-396.
Gatti, M., Pinato, S., Maiolica, A., Rocchio, F., Prato, M.G., Aebersold, R., and Penengo, L. (2015). RNF168 promotes noncanonical K27 ubiquitination to signal DNA damage. Cell Rep *10*, 226-238.
Gavory, G., O'Dowd, C.R., Helm, M.D., Flasz, J., Arkoudis, E., Dossang, A., Hughes, C., Cassidy, E., McClelland, K., Odrzywol, E.*, et al.* (2018). Discovery and characterization of highly potent and selective allosteric USP7 inhibitors. Nat Chem Biol *14*, 118-125.
Glinka, A., Dolde, C., Kirsch, N., Huang, Y.L., Kazanskaya, O., Ingelfinger, D., Boutros, M., Cruciat, C.M., and Niehrs, C. (2011). LGR4 and LGR5 are R-spondin receptors mediating Wnt/β-catenin and Wnt/PCP signalling. EMBO Rep *12*, 1055-1061.
Goulet, C.C., Volk, K.A., Adams, C.M., Prince, L.S., Stokes, J.B., and Snyder, P.M. (1998). Inhibition of the epithelial Na+ channel by interaction of Nedd4 with a PY motif deleted in Liddle's syndrome. J Biol Chem *273*, 30012-30017.
Greenblatt, M.B., Shin, D.Y., Oh, H., Lee, K.Y., Zhai, B., Gygi, S.P., Lotinun, S., Baron, R., Liu, D., Su, B.*, et al.* (2016). MEKK2 mediates an alternative β-catenin pathway that promotes bone formation. Proc Natl Acad Sci U S A *113*, E1226-1235.
Grice, G.L., and Nathan, J.A. (2016). The recognition of ubiquitinated proteins by the proteasome. Cell Mol Life Sci *73*, 3497-3506.
Han, K.J., Foster, D.G., Zhang, N.Y., Kanisha, K., Dzieciatkowska, M., Sclafani, R.A., Hansen, K.C., Peng, J., and Liu, C.W. (2012). Ubiquitin-specific protease 9x deubiquitinates and stabilizes the spinal muscular atrophy protein-survival motor neuron. J Biol Chem *287*, 43741-43752.
Hao, Y.H., Doyle, J.M., Ramanathan, S., Gomez, T.S., Jia, D., Xu, M., Chen, Z.J., Billadeau, D.D., Rosen, M.K., and Potts, P.R. (2013). Regulation of WASH-dependent actin polymerization and protein trafficking by ubiquitination. Cell *152*, 1051-1064.
Hao, Y.H., Fountain, M.D., Fon Tacer, K., Xia, F., Bi, W., Kang, S.H., Patel, A., Rosenfeld, J.A., Le Caignec, C., Isidor, B.*, et al.* (2015). USP7 Acts as a Molecular Rheostat to Promote WASH-Dependent Endosomal Protein Recycling and Is Mutated in a Human Neurodevelopmental Disorder. Mol Cell *59*, 956-969.
Harvey, K.F., Dinudom, A., Cook, D.I., and Kumar, S. (2001). The Nedd4-like protein

KIAA0439 is a potential regulator of the epithelial sodium channel. J Biol Chem *276*, 8597-8601.
Hatakeyama, J., Wald, J.H., Printsev, I., Ho, H.Y., and Carraway, K.L. (2014). Vangl1 and Vangl2: planar cell polarity components with a developing role in cancer. Endocr Relat Cancer *21*, R345-356.
He, Y., Hryciw, D.H., Carroll, M.L., Myers, S.A., Whitbread, A.K., Kumar, S., Poronnik, P., and Hooper, J.D. (2008). The ubiquitin-protein ligase Nedd4-2 differentially interacts with and regulates members of the Tweety family of chloride ion channels. J Biol Chem *283*, 24000-24010.
Hein, C., Springael, J.Y., Volland, C., Haguenauer-Tsapis, R., and André, B. (1995). NPl1, an essential yeast gene involved in induced degradation of Gap1 and Fur4 permeases, encodes the Rsp5 ubiquitin-protein ligase. Mol Microbiol *18*, 77-87.
Herhaus, L., and Dikic, I. (2015). Expanding the ubiquitin code through post-translational modification. EMBO Rep *16*, 1071-1083.
Heride, C., Urbé, S., and Clague, M.J. (2014). Ubiquitin code assembly and disassembly. Curr Biol *24*, R215-220.
Hermanns, T., Pichlo, C., Woiwode, I., Klopffleisch, K., Witting, K.F., Ovaa, H., Baumann, U., and Hofmann, K. (2018). A family of unconventional deubiquitinases with modular chain specificity determinants. Nat Commun *9*, 799.
Hershko, A., Ciechanover, A., Heller, H., Haas, A.L., and Rose, I.A. (1980). Proposed role of ATP in protein breakdown: conjugation of protein with multiple chains of the polypeptide of ATP-dependent proteolysis. Proc Natl Acad Sci U S A *77*, 1783-1786.
Hershko, A., Ciechanover, A., and Rose, I.A. (1979). Resolution of the ATP-dependent proteolytic system from reticulocytes: a component that interacts with ATP. Proc Natl Acad Sci U S A *76*, 3107-3110.
Hershko, A., Heller, H., Elias, S., and Ciechanover, A. (1983). Components of ubiquitin-protein ligase system. Resolution, affinity purification, and role in protein breakdown. J Biol Chem *258*, 8206-8214.
Hryciw, D.H., Ekberg, J., Lee, A., Lensink, I.L., Kumar, S., Guggino, W.B., Cook, D.I., Pollock, C.A., and Poronnik, P. (2004). Nedd4-2 functionally interacts with ClC-5: involvement in constitutive albumin endocytosis in proximal tubule cells. J Biol Chem *279*, 54996-55007.
Hu, M., Li, P., Li, M., Li, W., Yao, T., Wu, J.W., Gu, W., Cohen, R.E., and Shi, Y. (2002). Crystal structure of a UBP-family deubiquitinating enzyme in isolation and in complex with ubiquitin aldehyde. Cell *111*, 1041-1054.
Huang, X., and Dixit, V.M. (2016). Drugging the undruggables: exploring the ubiquitin system for drug development. Cell Res *26*, 484-498.
Husnjak, K., and Dikic, I. (2012). Ubiquitin-binding proteins: decoders of ubiquitin-mediated cellular functions. Annu Rev Biochem *81*, 291-322.
Ichimura, T., Yamamura, H., Sasamoto, K., Tominaga, Y., Taoka, M., Kakiuchi, K., Shinkawa, T., Takahashi, N., Shimada, S., and Isobe, T. (2005). 14-3-3 proteins modulate the expression of epithelial Na+ channels by phosphorylation-dependent interaction with Nedd4-2 ubiquitin ligase. J Biol Chem *280*, 13187-13194.
Iglesias-Bexiga, M., Castillo, F., Cobos, E.S., Oka, T., Sudol, M., and Luque, I. (2015). WW domains of the yes-kinase-associated-protein (YAP) transcriptional regulator behave as independent units with different binding preferences for PPxY motif-

containing ligands. PLoS One *10*, e0113828.
Ikeda, F., and Dikic, I. (2008). Atypical ubiquitin chains: new molecular signals. 'Protein Modifications: Beyond the Usual Suspects' review series. EMBO Rep *9*, 536-542.
Imajo, M., Miyatake, K., Iimura, A., Miyamoto, A., and Nishida, E. (2012). A molecular mechanism that links Hippo signalling to the inhibition of Wnt/β-catenin signalling. EMBO J *31*, 1109-1122.
Ingham, R.J., Gish, G., and Pawson, T. (2004). The Nedd4 family of E3 ubiquitin ligases: functional diversity within a common modular architecture. Oncogene *23*, 1972-1984.
Jones, C., Qian, D., Kim, S.M., Li, S., Ren, D., Knapp, L., Sprinzak, D., Avraham, K.B., Matsuzaki, F., Chi, F.*, et al.* (2014). Ankrd6 is a mammalian functional homolog of Drosophila planar cell polarity gene diego and regulates coordinated cellular orientation in the mouse inner ear. Dev Biol *395*, 62-72.
Kapuria, V., Peterson, L.F., Fang, D., Bornmann, W.G., Talpaz, M., and Donato, N.J. (2010). Deubiquitinase inhibition by small-molecule WP1130 triggers aggresome formation and tumor cell apoptosis. Cancer Res *70*, 9265-9276.
Katoh, M. (2005). WNT/PCP signaling pathway and human cancer (review). Oncol Rep *14*, 1583-1588.
Kavsak, P., Rasmussen, R.K., Causing, C.G., Bonni, S., Zhu, H., Thomsen, G.H., and Wrana, J.L. (2000). Smad7 binds to Smurf2 to form an E3 ubiquitin ligase that targets the TGF beta receptor for degradation. Mol Cell *6*, 1365-1375.
Keusekotten, K., Elliott, P.R., Glockner, L., Fiil, B.K., Damgaard, R.B., Kulathu, Y., Wauer, T., Hospenthal, M.K., Gyrd-Hansen, M., Krappmann, D.*, et al.* (2013). OTULIN antagonizes LUBAC signaling by specifically hydrolyzing Met1-linked polyubiquitin. Cell *153*, 1312-1326.
Khan, O.M., Carvalho, J., Spencer-Dene, B., Mitter, R., Frith, D., Snijders, A.P., Wood, S.A., and Behrens, A. (2018). The deubiquitinase USP9X regulates FBW7 stability and suppresses colorectal cancer. J Clin Invest.
Kim, H.C., and Huibregtse, J.M. (2009). Polyubiquitination by HECT E3s and the determinants of chain type specificity. Mol Cell Biol *29*, 3307-3318.
Kim, H.T., Kim, K.P., Lledias, F., Kisselev, A.F., Scaglione, K.M., Skowyra, D., Gygi, S.P., and Goldberg, A.L. (2007). Certain pairs of ubiquitin-conjugating enzymes (E2s) and ubiquitin-protein ligases (E3s) synthesize nondegradable forked ubiquitin chains containing all possible isopeptide linkages. J Biol Chem *282*, 17375-17386.
Kim, M., and Jho, E.H. (2014). Cross-talk between Wnt/β-catenin and Hippo signaling pathways: a brief review. BMB Rep *47*, 540-545.
Kim, R.Q., and Sixma, T.K. (2017). Regulation of USP7: A High Incidence of E3 Complexes. J Mol Biol *429*, 3395-3408.
Kim, W., Bennett, E.J., Huttlin, E.L., Guo, A., Li, J., Possemato, A., Sowa, M.E., Rad, R., Rush, J., Comb, M.J.*, et al.* (2011). Systematic and quantitative assessment of the ubiquitin-modified proteome. Mol Cell *44*, 325-340.
Komander, D., and Barford, D. (2008). Structure of the A20 OTU domain and mechanistic insights into deubiquitination. Biochem J *409*, 77-85.
Komander, D., Clague, M.J., and Urbé, S. (2009). Breaking the chains: structure and function of the deubiquitinases. Nat Rev Mol Cell Biol *10*, 550-563.
Komander, D., and Rape, M. (2012). The ubiquitin code. Annu Rev Biochem *81*, 203-

229.
Koyano, F., Okatsu, K., Kosako, H., Tamura, Y., Go, E., Kimura, M., Kimura, Y., Tsuchiya, H., Yoshihara, H., Hirokawa, T.*, et al.* (2014). Ubiquitin is phosphorylated by PINK1 to activate parkin. Nature *510*, 162-166.
Kuratomi, G., Komuro, A., Goto, K., Shinozaki, M., Miyazawa, K., Miyazono, K., and Imamura, T. (2005). NEDD4-2 (neural precursor cell expressed, developmentally down-regulated 4-2) negatively regulates TGF-beta (transforming growth factor-beta) signalling by inducing ubiquitin-mediated degradation of Smad2 and TGF-beta type I receptor. Biochem J *386*, 461-470.
Kushwaha, D., O'Leary, C., Cron, K.R., Deraska, P., Zhu, K., D'Andrea, A.D., and Kozono, D. (2015). USP9X inhibition promotes radiation-induced apoptosis in non-small cell lung cancer cells expressing mid-to-high MCL1. Cancer Biol Ther *16*, 392-401.
Lee, S., Tumolo, J.M., Ehlinger, A.C., Jernigan, K.K., Qualls-Histed, S.J., Hsu, P.C., McDonald, W.H., Chazin, W.J., and MacGurn, J.A. (2017). Ubiquitin turnover and endocytic trafficking in yeast are regulated by Ser57 phosphorylation of ubiquitin. Elife *6*.
Lee, Y.S., Park, J.S., Kim, J.H., Jung, S.M., Lee, J.Y., Kim, S.J., and Park, S.H. (2011). Smad6-specific recruitment of Smurf E3 ligases mediates TGF-β1-induced degradation of MyD88 in TLR4 signalling. Nat Commun *2*, 460.
Li, L., Liu, T., Li, Y., Wu, C., Luo, K., Yin, Y., Chen, Y., Nowsheen, S., Wu, J., Lou, Z.*, et al.* (2018). The deubiquitinase USP9X promotes tumor cell survival and confers chemoresistance through YAP1 stabilization. Oncogene *37*, 2422-2431.
Li, X., Song, N., Liu, L., Liu, X., Ding, X., Song, X., Yang, S., Shan, L., Zhou, X., Su, D.*, et al.* (2017). USP9X regulates centrosome duplication and promotes breast carcinogenesis. Nat Commun *8*, 14866.
Lin, A., Hou, Q., Jarzylo, L., Amato, S., Gilbert, J., Shang, F., and Man, H.Y. (2011). Nedd4-mediated AMPA receptor ubiquitination regulates receptor turnover and trafficking. J Neurochem *119*, 27-39.
Lin, X., Liang, M., and Feng, X.H. (2000). Smurf2 is a ubiquitin E3 ligase mediating proteasome-dependent degradation of Smad2 in transforming growth factor-beta signaling. J Biol Chem *275*, 36818-36822.
Liu, C.C., Kanekiyo, T., Roth, B., and Bu, G. (2014a). Tyrosine-based signal mediates LRP6 receptor endocytosis and desensitization of Wnt/β-catenin pathway signaling. J Biol Chem *289*, 27562-27570.
Liu, Y., Soetandyo, N., Lee, J.G., Liu, L., Xu, Y., Clemons, W.M., and Ye, Y. (2014b). USP13 antagonizes gp78 to maintain functionality of a chaperone in ER-associated degradation. Elife *3*, e01369.
Lu, Y., Adegoke, O.A., Nepveu, A., Nakayama, K.I., Bedard, N., Cheng, D., Peng, J., and Wing, S.S. (2009). USP19 deubiquitinating enzyme supports cell proliferation by stabilizing KPC1, a ubiquitin ligase for p27Kip1. Mol Cell Biol *29*, 547-558.
Luga, V., Zhang, L., Viloria-Petit, A.M., Ogunjimi, A.A., Inanlou, M.R., Chiu, E., Buchanan, M., Hosein, A.N., Basik, M., and Wrana, J.L. (2012). Exosomes mediate stromal mobilization of autocrine Wnt-PCP signaling in breast cancer cell migration. Cell *151*, 1542-1556.
Lui, T.T., Lacroix, C., Ahmed, S.M., Goldenberg, S.J., Leach, C.A., Daulat, A.M., and Angers, S. (2011). The ubiquitin-specific protease USP34 regulates axin stability and

Wnt/β-catenin signaling. Mol Cell Biol *31*, 2053-2065.
MacDonald, B.T., Tamai, K., and He, X. (2009). Wnt/beta-catenin signaling: components, mechanisms, and diseases. Dev Cell *17*, 9-26.
MacGurn, J.A., Hsu, P.C., and Emr, S.D. (2012). Ubiquitin and membrane protein turnover: from cradle to grave. Annu Rev Biochem *81*, 231-259.
Madrzak, J., Fiedler, M., Johnson, C.M., Ewan, R., Knebel, A., Bienz, M., and Chin, J.W. (2015). Ubiquitination of the Dishevelled DIX domain blocks its head-to-tail polymerization. Nat Commun *6*, 6718.
Malik, R., Soh, U.J., Trejo, J., and Marchese, A. (2012). Novel roles for the E3 ubiquitin ligase atrophin-interacting protein 4 and signal transduction adaptor molecule 1 in G protein-coupled receptor signaling. J Biol Chem *287*, 9013-9027.
Marikawa, Y., and Elinson, R.P. (1998). beta-TrCP is a negative regulator of Wnt/beta-catenin signaling pathway and dorsal axis formation in Xenopus embryos. Mech Dev *77*, 75-80.
Matsumoto, M.L., Wickliffe, K.E., Dong, K.C., Yu, C., Bosanac, I., Bustos, D., Phu, L., Kirkpatrick, D.S., Hymowitz, S.G., Rape, M.*, et al.* (2010). K11-linked polyubiquitination in cell cycle control revealed by a K11 linkage-specific antibody. Mol Cell *39*, 477-484.
Matus, S., Lisbona, F., Torres, M., León, C., Thielen, P., and Hetz, C. (2008). The stress rheostat: an interplay between the unfolded protein response (UPR) and autophagy in neurodegeneration. Curr Mol Med *8*, 157-172.
McDonald, F.J., Western, A.H., McNeil, J.D., Thomas, B.C., Olson, D.R., and Snyder, P.M. (2002). Ubiquitin-protein ligase WWP2 binds to and downregulates the epithelial Na(+) channel. Am J Physiol Renal Physiol *283*, F431-436.
McIntosh, D.J., Walters, T.S., Arinze, I.J., and Davis, J. (2018). Arkadia (RING Finger Protein 111) Mediates Sumoylation-Dependent Stabilization of Nrf2 Through K48-Linked Ubiquitination. Cell Physiol Biochem *46*, 418-430.
Meyer, H.J., and Rape, M. (2014). Enhanced protein degradation by branched ubiquitin chains. Cell *157*, 910-921.
Miyazaki, K., Fujita, T., Ozaki, T., Kato, C., Kurose, Y., Sakamoto, M., Kato, S., Goto, T., Itoyama, Y., Aoki, M.*, et al.* (2004). NEDL1, a novel ubiquitin-protein isopeptide ligase for dishevelled-1, targets mutant superoxide dismutase-1. J Biol Chem *279*, 11327-11335.
Mizuno, E., Kobayashi, K., Yamamoto, A., Kitamura, N., and Komada, M. (2006). A deubiquitinating enzyme UBPY regulates the level of protein ubiquitination on endosomes. Traffic *7*, 1017-1031.
Mouchantaf, R., Azakir, B.A., McPherson, P.S., Millard, S.M., Wood, S.A., and Angers, A. (2006). The ubiquitin ligase itch is auto-ubiquitylated in vivo and in vitro but is protected from degradation by interacting with the deubiquitylating enzyme FAM/USP9X. J Biol Chem *281*, 38738-38747.
Mukai, A., Yamamoto-Hino, M., Awano, W., Watanabe, W., Komada, M., and Goto, S. (2010). Balanced ubiquitylation and deubiquitylation of Frizzled regulate cellular responsiveness to Wg/Wnt. EMBO J *29*, 2114-2125.
Mund, T., Graeb, M., Mieszczanek, J., Gammons, M., Pelham, H.R., and Bienz, M. (2015). Disinhibition of the HECT E3 ubiquitin ligase WWP2 by polymerized Dishevelled. Open Biol *5*, 150185.
Murtaza, M., Jolly, L.A., Gecz, J., and Wood, S.A. (2015). La FAM fatale: USP9X in

development and disease. Cell Mol Life Sci *72*, 2075-2089.
Nakagawa, T., and Nakayama, K. (2015). Protein monoubiquitylation: targets and diverse functions. Genes Cells *20*, 543-562.
Narimatsu, M., Bose, R., Pye, M., Zhang, L., Miller, B., Ching, P., Sakuma, R., Luga, V., Roncari, L., Attisano, L.*, et al.* (2009). Regulation of planar cell polarity by Smurf ubiquitin ligases. Cell *137*, 295-307.
Nathan, J.A., Sengupta, S., Wood, S.A., Admon, A., Markson, G., Sanderson, C., and Lehner, P.J. (2008). The ubiquitin E3 ligase MARCH7 is differentially regulated by the deubiquitylating enzymes USP7 and USP9X. Traffic *9*, 1130-1145.
Nethe, M., de Kreuk, B.J., Tauriello, D.V., Anthony, E.C., Snoek, B., Stumpel, T., Salinas, P.C., Maurice, M.M., Geerts, D., Deelder, A.M.*, et al.* (2012). Rac1 acts in conjunction with Nedd4 and dishevelled-1 to promote maturation of cell-cell contacts. J Cell Sci *125*, 3430-3442.
Nijman, S.M., Huang, T.T., Dirac, A.M., Brummelkamp, T.R., Kerkhoven, R.M., D'Andrea, A.D., and Bernards, R. (2005). The deubiquitinating enzyme USP1 regulates the Fanconi anemia pathway. Mol Cell *17*, 331-339.
Overstreet, E., Fitch, E., and Fischer, J.A. (2004). Fat facets and Liquid facets promote Delta endocytosis and Delta signaling in the signaling cells. Development *131*, 5355-5366.
Paudel, P., Zhang, Q., Leung, C., Greenberg, H.C., Guo, Y., Chern, Y.H., Dong, A., Li, Y., Vedadi, M., Zhuang, Z.*, et al.* (2019). Crystal structure and activity-based labeling reveal the mechanisms for linkage-specific substrate recognition by deubiquitinase USP9X. Proc Natl Acad Sci U S A *116*, 7288-7297.
Peterson, L.F., Sun, H., Liu, Y., Potu, H., Kandarpa, M., Ermann, M., Courtney, S.M., Young, M., Showalter, H.D., Sun, D.*, et al.* (2015). Targeting deubiquitinase activity with a novel small-molecule inhibitor as therapy for B-cell malignancies. Blood *125*, 3588-3597.
Peth, A., Uchiki, T., and Goldberg, A.L. (2010). ATP-dependent steps in the binding of ubiquitin conjugates to the 26S proteasome that commit to degradation. Mol Cell *40*, 671-681.
Pickart, C.M. (2001). Mechanisms underlying ubiquitination. Annu Rev Biochem *70*, 503-533.
Potu, H., Peterson, L.F., Kandarpa, M., Pal, A., Sun, H., Durham, A., Harms, P.W., Hollenhorst, P.C., Eskiocak, U., Talpaz, M.*, et al.* (2017). Usp9x regulates Ets-1 ubiquitination and stability to control NRAS expression and tumorigenicity in melanoma. Nat Commun *8*, 14449.
Premarathne, S., Murtaza, M., Matigian, N., Jolly, L.A., and Wood, S.A. (2017). Loss of Usp9x disrupts cell adhesion, and components of the Wnt and Notch signaling pathways in neural progenitors. Sci Rep *7*, 8109.
Prives, C. (1998). Signaling to p53: breaking the MDM2-p53 circuit. Cell *95*, 5-8.
Pérez-Mancera, P.A., Rust, A.G., van der Weyden, L., Kristiansen, G., Li, A., Sarver, A.L., Silverstein, K.A., Grützmann, R., Aust, D., Rümmele, P.*, et al.* (2012). The deubiquitinase USP9X suppresses pancreatic ductal adenocarcinoma. Nature *486*, 266-270.
Qian, G., Ren, Y., Zuo, Y., Yuan, Y., Zhao, P., Wang, X., Cheng, Q., Liu, J., Zhang, L., Guo, T.*, et al.* (2016). Smurf1 represses TNF-α production through ubiquitination and

destabilization of USP5. Biochem Biophys Res Commun *474*, 491-496.
Reinstein, E., and Ciechanover, A. (2006). Narrative review: protein degradation and human diseases: the ubiquitin connection. Ann Intern Med *145*, 676-684.
Reverdy, C., Conrath, S., Lopez, R., Planquette, C., Atmanene, C., Collura, V., Harpon, J., Battaglia, V., Vivat, V., Sippl, W.*, et al.* (2012). Discovery of specific inhibitors of human USP7/HAUSP deubiquitinating enzyme. Chem Biol *19*, 467-477.
Rossier, B.C., Pradervand, S., Schild, L., and Hummler, E. (2002). Epithelial sodium channel and the control of sodium balance: interaction between genetic and environmental factors. Annu Rev Physiol *64*, 877-897.
Rotin, D., and Kumar, S. (2009). Physiological functions of the HECT family of ubiquitin ligases. Nat Rev Mol Cell Biol *10*, 398-409.
Row, P.E., Prior, I.A., McCullough, J., Clague, M.J., and Urbé, S. (2006). The ubiquitin isopeptidase UBPY regulates endosomal ubiquitin dynamics and is essential for receptor down-regulation. J Biol Chem *281*, 12618-12624.
Saito-Diaz, K., Chen, T.W., Wang, X., Thorne, C.A., Wallace, H.A., Page-McCaw, A., and Lee, E. (2013). The way Wnt works: components and mechanism. Growth Factors *31*, 1-31.
Santos, S.D., and Ferrell, J.E. (2008). Systems biology: On the cell cycle and its switches. Nature *454*, 288-289.
Savio, M.G., Wollscheid, N., Cavallaro, E., Algisi, V., Di Fiore, P.P., Sigismund, S., Maspero, E., and Polo, S. (2016). USP9X Controls EGFR Fate by Deubiquitinating the Endocytic Adaptor Eps15. Curr Biol *26*, 173-183.
Schild, L., Lu, Y., Gautschi, I., Schneeberger, E., Lifton, R.P., and Rossier, B.C. (1996). Identification of a PY motif in the epithelial Na channel subunits as a target sequence for mutations causing channel activation found in Liddle syndrome. EMBO J *15*, 2381-2387.
Schwarz-Romond, T., Fiedler, M., Shibata, N., Butler, P.J., Kikuchi, A., Higuchi, Y., and Bienz, M. (2007). The DIX domain of Dishevelled confers Wnt signaling by dynamic polymerization. Nat Struct Mol Biol *14*, 484-492.
Schwarz-Romond, T., Merrifield, C., Nichols, B.J., and Bienz, M. (2005). The Wnt signalling effector Dishevelled forms dynamic protein assemblies rather than stable associations with cytoplasmic vesicles. J Cell Sci *118*, 5269-5277.
Schwickart, M., Huang, X., Lill, J.R., Liu, J., Ferrando, R., French, D.M., Maecker, H., O'Rourke, K., Bazan, F., Eastham-Anderson, J.*, et al.* (2010). Deubiquitinase USP9X stabilizes MCL1 and promotes tumour cell survival. Nature *463*, 103-107.
Shao, G., Lilli, D.R., Patterson-Fortin, J., Coleman, K.A., Morrissey, D.E., and Greenberg, R.A. (2009). The Rap80-BRCC36 de-ubiquitinating enzyme complex antagonizes RNF8-Ubc13-dependent ubiquitination events at DNA double strand breaks. Proc Natl Acad Sci U S A *106*, 3166-3171.
Sherk, A.B., Frigo, D.E., Schnackenberg, C.G., Bray, J.D., Laping, N.J., Trizna, W., Hammond, M., Patterson, J.R., Thompson, S.K., Kazmin, D.*, et al.* (2008). Development of a small-molecule serum- and glucocorticoid-regulated kinase-1 antagonist and its evaluation as a prostate cancer therapeutic. Cancer Res *68*, 7475-7483.
Sierra, M.I., Wright, M.H., and Nash, P.D. (2010). AMSH interacts with ESCRT-0 to regulate the stability and trafficking of CXCR4. J Biol Chem *285*, 13990-14004.
SIMPSON, M.V. (1953). The release of labeled amino acids from the proteins of rat liver

slices. J Biol Chem *201*, 143-154.
Snyder, P.M., Price, M.P., McDonald, F.J., Adams, C.M., Volk, K.A., Zeiher, B.G., Stokes, J.B., and Welsh, M.J. (1995). Mechanism by which Liddle's syndrome mutations increase activity of a human epithelial Na+ channel. Cell *83*, 969-978.
Staub, O., Dho, S., Henry, P., Correa, J., Ishikawa, T., McGlade, J., and Rotin, D. (1996). WW domains of Nedd4 bind to the proline-rich PY motifs in the epithelial Na+ channel deleted in Liddle's syndrome. EMBO J *15*, 2371-2380.
Stevenson, L.F., Sparks, A., Allende-Vega, N., Xirodimas, D.P., Lane, D.P., and Saville, M.K. (2007). The deubiquitinating enzyme USP2a regulates the p53 pathway by targeting Mdm2. EMBO J *26*, 976-986.
Sun, H., Kapuria, V., Peterson, L.F., Fang, D., Bornmann, W.G., Bartholomeusz, G., Talpaz, M., and Donato, N.J. (2011). Bcr-Abl ubiquitination and Usp9x inhibition block kinase signaling and promote CML cell apoptosis. Blood *117*, 3151-3162.
Tanksley, J.P., Chen, X., and Coffey, R.J. (2013). NEDD4L is downregulated in colorectal cancer and inhibits canonical WNT signaling. PLoS One *8*, e81514.
Tauriello, D.V., Haegebarth, A., Kuper, I., Edelmann, M.J., Henraat, M., Canninga-van Dijk, M.R., Kessler, B.M., Clevers, H., and Maurice, M.M. (2010). Loss of the tumor suppressor CYLD enhances Wnt/beta-catenin signaling through K63-linked ubiquitination of Dvl. Mol Cell *37*, 607-619.
Tavana, O., and Gu, W. (2017). Modulation of the p53/MDM2 interplay by HAUSP inhibitors. J Mol Cell Biol *9*, 45-52.
Thrower, J.S., Hoffman, L., Rechsteiner, M., and Pickart, C.M. (2000). Recognition of the polyubiquitin proteolytic signal. EMBO J *19*, 94-102.
Théard, D., Labarrade, F., Partisani, M., Milanini, J., Sakagami, H., Fon, E.A., Wood, S.A., Franco, M., and Luton, F. (2010). USP9x-mediated deubiquitination of EFA6 regulates de novo tight junction assembly. EMBO J *29*, 1499-1509.
Toloczko, A., Guo, F., Yuen, H.F., Wen, Q., Wood, S.A., Ong, Y.S., Chan, P.Y., Shaik, A.A., Gunaratne, J., Dunne, M.J.*, et al.* (2017). Deubiquitinating Enzyme USP9X Suppresses Tumor Growth via LATS Kinase and Core Components of the Hippo Pathway. Cancer Res *77*, 4921-4933.
Troyanovsky, B., Levchenko, T., Månsson, G., Matvijenko, O., and Holmgren, L. (2001). Angiomotin: an angiostatin binding protein that regulates endothelial cell migration and tube formation. J Cell Biol *152*, 1247-1254.
Varelas, X., Miller, B.W., Sopko, R., Song, S., Gregorieff, A., Fellouse, F.A., Sakuma, R., Pawson, T., Hunziker, W., McNeill, H.*, et al.* (2010). The Hippo pathway regulates Wnt/beta-catenin signaling. Dev Cell *18*, 579-591.
Vucic, D., Dixit, V.M., and Wertz, I.E. (2011). Ubiquitylation in apoptosis: a post-translational modification at the edge of life and death. Nat Rev Mol Cell Biol *12*, 439-452.
Wang, B., and Elledge, S.J. (2007). Ubc13/Rnf8 ubiquitin ligases control foci formation of the Rap80/Abraxas/Brca1/Brcc36 complex in response to DNA damage. Proc Natl Acad Sci U S A *104*, 20759-20763.
Wang, C., An, J., Zhang, P., Xu, C., Gao, K., Wu, D., Wang, D., Yu, H., Liu, J.O., and Yu, L. (2012). The Nedd4-like ubiquitin E3 ligases target angiomotin/p130 to ubiquitin-dependent degradation. Biochem J *444*, 279-289.
Wang, Q., Li, L., and Ye, Y. (2006). Regulation of retrotranslocation by p97-associated

deubiquitinating enzyme ataxin-3. J Cell Biol *174*, 963-971.
Wang, Q., Liu, X., Cui, Y., Tang, Y., Chen, W., Li, S., Yu, H., Pan, Y., and Wang, C. (2014a). The E3 ubiquitin ligase AMFR and INSIG1 bridge the activation of TBK1 kinase by modifying the adaptor STING. Immunity *41*, 919-933.
Wang, S., Kollipara, R.K., Srivastava, N., Li, R., Ravindranathan, P., Hernandez, E., Freeman, E., Humphries, C.G., Kapur, P., Lotan, Y.*, et al.* (2014b). Ablation of the oncogenic transcription factor ERG by deubiquitinase inhibition in prostate cancer. Proc Natl Acad Sci U S A *111*, 4251-4256.
Wang, X., D'Arcy, P., Caulfield, T.R., Paulus, A., Chitta, K., Mohanty, C., Gullbo, J., Chanan-Khan, A., and Linder, S. (2015). Synthesis and evaluation of derivatives of the proteasome deubiquitinase inhibitor b-AP15. Chem Biol Drug Des *86*, 1036-1048.
Wang, X., Mazurkiewicz, M., Hillert, E.K., Olofsson, M.H., Pierrou, S., Hillertz, P., Gullbo, J., Selvaraju, K., Paulus, A., Akhtar, S.*, et al.* (2016). The proteasome deubiquitinase inhibitor VLX1570 shows selectivity for ubiquitin-specific protease-14 and induces apoptosis of multiple myeloma cells. Sci Rep *6*, 26979.
Wang, Y. (2009). Wnt/Planar cell polarity signaling: a new paradigm for cancer therapy. Mol Cancer Ther *8*, 2103-2109.
Wauer, T., Swatek, K.N., Wagstaff, J.L., Gladkova, C., Pruneda, J.N., Michel, M.A., Gersch, M., Johnson, C.M., Freund, S.M., and Komander, D. (2015). Ubiquitin Ser65 phosphorylation affects ubiquitin structure, chain assembly and hydrolysis. EMBO J *34*, 307-325.
Wei, W., Li, M., Wang, J., Nie, F., and Li, L. (2012). The E3 ubiquitin ligase ITCH negatively regulates canonical Wnt signaling by targeting dishevelled protein. Mol Cell Biol *32*, 3903-3912.
Weinstock, J., Wu, J., Cao, P., Kingsbury, W.D., McDermott, J.L., Kodrasov, M.P., McKelvey, D.M., Suresh Kumar, K.G., Goldenberg, S.J., Mattern, M.R.*, et al.* (2012). Selective Dual Inhibitors of the Cancer-Related Deubiquitylating Proteases USP7 and USP47. ACS Med Chem Lett *3*, 789-792.
Wertz, I.E., O'Rourke, K.M., Zhou, H., Eby, M., Aravind, L., Seshagiri, S., Wu, P., Wiesmann, C., Baker, R., Boone, D.L.*, et al.* (2004). De-ubiquitination and ubiquitin ligase domains of A20 downregulate NF-kappaB signalling. Nature *430*, 694-699.
Wilkinson, K.D. (2005). The discovery of ubiquitin-dependent proteolysis. Proc Natl Acad Sci U S A *102*, 15280-15282.
Wu, X., Fukushima, H., North, B.J., Nagaoka, Y., Nagashima, K., Deng, F., Okabe, K., Inuzuka, H., and Wei, W. (2014). SCFβ-TRCP regulates osteoclastogenesis via promoting CYLD ubiquitination. Oncotarget *5*, 4211-4221.
Xie, Y., Avello, M., Schirle, M., McWhinnie, E., Feng, Y., Bric-Furlong, E., Wilson, C., Nathans, R., Zhang, J., Kirschner, M.W.*, et al.* (2013). Deubiquitinase FAM/USP9X interacts with the E3 ubiquitin ligase SMURF1 protein and protects it from ligase activity-dependent self-degradation. J Biol Chem *288*, 2976-2985.
Yang, B., Zhang, S., Wang, Z., Yang, C., Ouyang, W., Zhou, F., Zhou, Y., and Xie, C. (2016). Deubiquitinase USP9X deubiquitinates β-catenin and promotes high grade glioma cell growth. Oncotarget *7*, 79515-79525.
Yang, Y., and Mlodzik, M. (2015). Wnt-Frizzled/planar cell polarity signaling: cellular orientation by facing the wind (Wnt). Annu Rev Cell Dev Biol *31*, 623-646.
Yoshioka, Y., Ye, Y.Q., Okada, K., Taniguchi, K., Yoshida, A., Sugaya, K., Onose, J.,

Koshino, H., Takahashi, S., Yajima, A.*, et al.* (2013). Ubiquitin-specific peptidase 5, a target molecule of vialinin A, is a key molecule of TNF-α production in RBL-2H3 cells. PLoS One *8*, e80931.
Yu, A., Rual, J.F., Tamai, K., Harada, Y., Vidal, M., He, X., and Kirchhausen, T. (2007). Association of Dishevelled with the clathrin AP-2 adaptor is required for Frizzled endocytosis and planar cell polarity signaling. Dev Cell *12*, 129-141.
Yu, A., Xing, Y., Harrison, S.C., and Kirchhausen, T. (2010). Structural analysis of the interaction between Dishevelled2 and clathrin AP-2 adaptor, a critical step in noncanonical Wnt signaling. Structure *18*, 1311-1320.
Yu, X., Wang, M., Dong, Q., and Jin, F. (2014). Diversin is overexpressed in breast cancer and accelerates cell proliferation and invasion. PLoS One *9*, e98591.
Yuan, W.C., Lee, Y.R., Lin, S.Y., Chang, L.Y., Tan, Y.P., Hung, C.C., Kuo, J.C., Liu, C.H., Lin, M.Y., Xu, M.*, et al.* (2014). K33-Linked Polyubiquitination of Coronin 7 by Cul3-KLHL20 Ubiquitin E3 Ligase Regulates Protein Trafficking. Mol Cell *54*, 586-600.
Zhang, Y., Chang, C., Gehling, D.J., Hemmati-Brivanlou, A., and Derynck, R. (2001). Regulation of Smad degradation and activity by Smurf2, an E3 ubiquitin ligase. Proc Natl Acad Sci U S A *98*, 974-979.
Zhang, Z.R., Bonifacino, J.S., and Hegde, R.S. (2013). Deubiquitinases sharpen substrate discrimination during membrane protein degradation from the ER. Cell *154*, 609-622.
Zheng, H., Gupta, V., Patterson-Fortin, J., Bhattacharya, S., Katlinski, K., Wu, J., Varghese, B., Carbone, C.J., Aressy, B., Fuchs, S.Y.*, et al.* (2013). A BRISC-SHMT complex deubiquitinates IFNAR1 and regulates interferon responses. Cell Rep *5*, 180-193.
Zheng, N., and Shabek, N. (2017). Ubiquitin Ligases: Structure, Function, and Regulation. Annu Rev Biochem *86*, 129-157.
Zhong, X., and Pittman, R.N. (2006). Ataxin-3 binds VCP/p97 and regulates retrotranslocation of ERAD substrates. Hum Mol Genet *15*, 2409-2420.
Zhu, H., Kavsak, P., Abdollah, S., Wrana, J.L., and Thomsen, G.H. (1999). A SMAD ubiquitin ligase targets the BMP pathway and affects embryonic pattern formation. Nature *400*, 687-693.
Zhu, Y., Tian, Y., Du, J., Hu, Z., Yang, L., Liu, J., and Gu, L. (2012). Dvl2-dependent activation of Daam1 and RhoA regulates Wnt5a-induced breast cancer cell migration. PLoS One *7*, e37823.